RSC Chemical Biology

ROYAL SOCIETY OF CHEMISTRY

REVIEW

View Article Online
View Journal | View Issue

Check for updates

Cite this: *RSC Chem. Biol.*, 2022, 3, 648

Perspectives on conformationally constrained peptide nucleic acid (PNA): insights into the structural design, properties and applications

Chaturong Suparpprom [ab] and Tirayut Vilaivan [*ab]

Peptide nucleic acid or PNA is a synthetic DNA mimic that contains a sequence of nucleobases attached to a peptide-like backbone derived from *N*-2-aminoethylglycine. The semi-rigid PNA backbone acts as a scaffold that arranges the nucleobases in a proper orientation and spacing so that they can pair with their complementary bases on another DNA, RNA, or even PNA strand perfectly well through the standard Watson–Crick base-pairing. The electrostatically neutral backbone of PNA contributes to its many unique properties that make PNA an outstanding member of the xeno-nucleic acid family. Not only PNA can recognize its complementary nucleic acid strand with high affinity, but it does so with excellent specificity that surpasses the specificity of natural nucleic acids and their analogs. Nevertheless, there is still room for further improvements of the original PNA in terms of stability and specificity of base-pairing, direction of binding, and selectivity for different types of nucleic acids, among others. This review focuses on attempts towards the rational design of new generation PNAs with superior performance by introducing conformational constraints such as a ring or a chiral substituent in the PNA backbone. A large collection of conformationally rigid PNAs developed during the past three decades are analyzed and compared in terms of molecular design and properties in relation to structural data if available. Applications of selected modified PNA in various areas such as targeting of structured nucleic acid targets, supramolecular scaffold, biosensing and bioimaging, and gene regulation will be highlighted to demonstrate how the conformation constraint can improve the performance of the PNA. Challenges and future of the research in the area of constrained PNA will also be discussed.

Received 18th January 2022,
Accepted 17th March 2022

DOI: 10.1039/d2cb00017b

rsc.li/rsc-chembio

[a] *Department of Chemistry and Center of Excellence for Innovation in Chemistry, Faculty of Science, Naresuan University, Tah-Poe District, Muang, Phitsanulok 65000, Thailand. E-mail: vtirayut@chula.ac.th*

[b] *Organic Synthesis Research Unit, Department of Chemistry, Faculty of Science, Chulalongkorn University, Phayathai Road, Pathumwan, Bangkok 10330, Thailand*

Chaturong Suparpprom

Chaturong Suparpprom received his PhD degree in Chemistry from Chulalongkorn University (Thailand) in 2006. Under the supervision of Prof. Tirayut Vilaivan, he developed interest in the fields of peptide nucleic acid (PNA) and organic synthesis. His PhD work contributes to the development of a new family of conformationally constrained pyrrolidinyl PNA. In 2006, he started his independent career at Naresuan University, where he is currently holding an assistant professorship. He continued to develop and expand the applications of pyrrolidinyl PNA in diagnostics and biomolecular fields. His other research interests apart from PNA encompass natural fatty acid and bioactive compounds from Thai herbs.

Tirayut Vilaivan

Tirayut Vilaivan received his DPhil from Oxford in 1996 under the supervision of the late Professor Gordon Lowe, FRS. He started his independent career at the Department of Chemistry, Chulalongkorn University in Bangkok in 1996. He is currently a professor of chemistry at Chulalongkorn University. His research interests include (1) design, synthesis, properties, and applications of conformationally constrained peptide nucleic acid (PNA), (2) development of novel synthetic methodologies (focusing on catalysis and green processes) and (3) development of novel antimalarials based on dihydrofolate reductase inhibitors.

Open Access Article. Published on 18 Nyenyankulu 2022. Downloaded on 2026-01-28 04:18:10.
This article is licensed under a Creative Commons Attribution-NonCommercial 3.0 Unported Licence.

© 2022 The Author(s). Published by the Royal Society of Chemistry

Open Access Article. Published on 18 Nyenyankulu 2022. Downloaded on 2026-01-28 04:18:10.
This article is licensed under a Creative Commons Attribution-NonCommercial 3.0 Unported Licence.

Introduction

In all organisms, nucleic acids play important roles in the storage, transmission, and expression of genetic information in a precisely controlled fashion. Central to this is the unique pairing ability of the two complementary strands of nucleic acids *via* the highly specific Watson–Crick base-pairing scheme. The high fidelity of the base-pairing scheme suggests potential uses of nucleic acids for regulating gene expression which is indeed one of the mechanisms used by nature.[1] This can have tremendous implications in the areas of therapeutics. One example that highlights the importance of nucleic acid-based therapeutics is the recent success of the mRNA vaccine accelerated by the emergence of COVID-19.[2] However, due to their susceptibility to degradation by the ubiquitous endogenous nucleases, natural nucleic acids are not suitable for therapeutic purposes. Modifications are generally required to improve the stability of nucleic acids so that they can last long enough to bind to the target nucleic acids and exert the biological effects that they were designed for.[3,4] Thus, the research in the area of modified nucleic acids or xeno-nucleic acids is an important field that supports the fast-growing trends of nucleic acid-based therapy. Moreover, they can be used in other areas of applications including diagnostics, biosensors, and materials science. In addition, these xeno-nucleic acids are interesting in their own right as a model for prebiotic systems chemistry.[5,6]

Peptide nucleic acid (PNA) is one of the most fascinating members of the xeno-nucleic acid family. While modified nucleic acids generally retain the original negatively charged sugar-phosphate backbone of natural nucleic acids (or at least part of it),[7] PNA carries a drastically different electrostatically neutral peptide-like backbone which makes it a unique kind of nucleic acid mimic. The first PNA reported in 1991 consisting of an *N*-2-aminoethylglycyl backbone (now being referred to as aegPNA) was originally designed to be a triplex-forming agent.[8] However, homothymine aegPNA showed an unexpectedly strong affinity towards the DNA target and bound to it sequence-specifically in a novel triplex invasion mode. Subsequently, the ability of PNA to recognize single-stranded DNA/RNA targets following the standard Watson–Crick base-pairing rules was demonstrated.[9] In addition, PNA can pair with itself to form highly stable PNA·PNA duplexes. Thus, PNA is among the first testimonies to the fact that the (deoxy)ribose-phosphate was not a requirement for base–base recognition. The electrostatically neutral backbone of PNA contributes to its exceptionally strong binding without compromising specificity. In fact, PNAs show even better mismatch discrimination than natural nucleic acids. These properties together with the complete stability towards nucleases make PNA a potential tool for nucleic-acid-based therapeutics and other applications that rely on specific base-pairing.[10,11]

Even though the original aegPNA system already possesses many desirable characteristics and has been widely employed in various applications, there are still great demands for further improvement. During the three decades after the discovery of PNA, numerous modifications of the original aegPNA structure have been explored with the aim of improving the base-pairing efficiency and solubility, and introducing other functions in the PNA molecules such as cellular uptake or reporter groups. Chemistry-wise, the modifications of PNA can be divided into three categories: acyclic backbone modification, cyclic backbone modification, and modification that does not follow the aegPNA template. Although some earlier reviews on modified PNA exist,[12–16] this review is complementary to the existing ones as it will focus mainly on the backbone modification to introduce conformational constraint in the PNA molecules. Such modification, even a minor one, will result in altering and restriction of one or more torsional angle values that will ultimately affect the global structure and binding properties of the modified PNA oligomers (Fig. 1). A broad landscape will be provided in addition to a more detailed comparison and evaluation of the impact of different structural modifications of the original aegPNA backbone on the stability and specificity of the duplex formation in a systematic way. The properties and applications of selected modified PNA are discussed in more detail. Thus, this review should be useful for specialists in the PNA area seeking a comprehensive source of information on this topic. It should also help those who are new to the PNA field to learn what modified PNA can offer and may inspire the adoption of PNA that might well suit their required applications or thinking for novel and imaginative uses of PNA.

Modified PNA with acyclic backbones

This section will cover modified PNA with an acyclic backbone that follows the generic aegPNA template (as well as its homolog) with one or more substituents on the *N*-aminoethylglycine backbone. There are four possible sites for substitution including α-, β-, γ-, and the secondary amide nitrogen atom (N) (Fig. 2). More than one substituent may be present on the same or different backbone carbon or nitrogen atoms, but this section will cover only the cases where the substituents are not joined to form a cyclic structure.

Modified PNA with α-substituents (αPNA)

Due to its synthetic accessibility from standard amino acids, αPNA is one of the earliest PNA modifications that has been

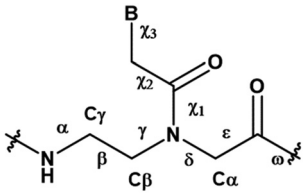

α: C(O)(NH)-N(H)-Cγ-Cβ	ω: Cα-C(O)(NH)-N(H)-Cγ
β: N(H)-Cγ-Cβ-N(CO)	χ_1: Cβ-N(CO)-C(O)(CH_2B)-CH_2(B)
γ: Cγ-Cβ-N(CO)-Cα	χ_2: N(CO)-C(O)(CH_2B)-CH_2(B)-N^1/N^9
δ: Cβ-N(CO)-Cα-CO(NH)	χ_3: C(O)(CH_2B)-CH_2(B)-N^1/N^9-C^2/C^4
ε: N(CO)-Cα-C(O)(NH)-O	

Fig. 1 The structure of aegPNA with definition of backbone atom positions and torsional angles.

Open Access Article. Published on 18 Nyenyankulu 2022. Downloaded on 2026-01-28 04:18:10.
This article is licensed under a Creative Commons Attribution-NonCommercial 3.0 Unported Licence.

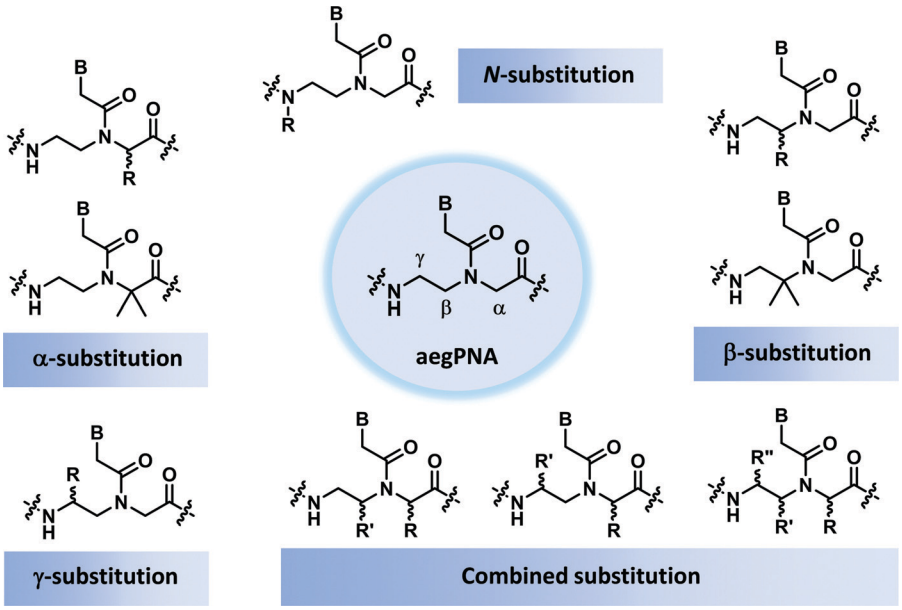

Fig. 2 Possible sites for modification of aegPNA without forming a cyclic structure as part of the backbone.

introduced as early as 1994 by the same group that developed aegPNA.[17] According to the thermal denaturation study on a chimeric α/aegPNA system, the introduction of a small methyl substituent at the α-position of the aegPNA backbone slightly destabilizes the PNA·DNA duplex in a stereochemically dependent fashion. The ^{D}Ala αPNA modification was less destabilizing than the ^{L}Ala modification. Bulky or negatively charged substituents are more destabilizing than smaller ones.[18,19] The D-Lys modification showed the most promising DNA binding characteristics whereby the duplex stability was slightly enhanced due to the combination of correct stereochemistry and positively charged side chain.[18,20] CD studies indicated a preferential right-handedness pre-organization of the single-stranded PNA carrying even only one D-Lys modification in the middle of the strand.[20] The matching chirality of the D-Lys modified αPNA and native DNA explained the higher stability of the αPNA·DNA duplexes of the D- over the L-series. A molecular dynamics (MD) simulation of Leu-modified αPNA·DNA duplexes suggested that the amino acid side chain in the D-series is directed away from the minor groove.[21] The blockage of the minor groove in the L-series was responsible for the decrease in the binding of groove binding dyes compared to the D-series or unmodified PNA. Importantly, the mismatch specificity and antiparallel selectivity of ^{D}Lys αPNA were enhanced when compared to unmodified aegPNA. A stretch of three consecutive D-Lys "chiral box" modifications was sufficient to drive the binding mode to exclusively antiparallel.[22] T_m data of αPNA hybrids are summarized in Table 1.

The crystal structure of such chiral box αPNA was successfully determined at 1.66 Å resolution (Fig. 3).[23] It revealed an antiparallel right-handed double helix that is grossly similar to the P-helix with a diameter of 22 Å, a helical twist of 23.2°, a rise of 3.5 Å, an *x*-displacement of 3.8 Å, and 15.5 base pairs per turn. The DNA sugar rings adopt both C3′-*endo* and C2′-*endo*

Table 1 T_m data of αPNA with DNA

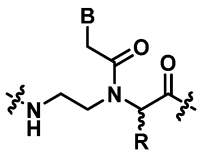

Sequence[a] (N–H/C–NH_2)	Substituent (R) derived from	T_m DNA (°C)	ΔT_m[b] (°C)	Ref.
GTAGATCACT	None (aegPNA)	49	—	20
GTAGAtCACT	L-Leu	47	−2	20
GTAGAtCACT	L-Lys	47	−2	20
GTAGAtCACT	D-Lys	51	+2	20
GtAGAtCACt	D-Lys	53	+4	20
GTAGatcACT	D-Lys	43	−6	22

[a] The modification site is denoted by a small letter. [b] ΔT_m refers to T_m difference between the modified PNA and aegPNA duplexes.

conformations (6 *vs.* 4). This is in sharp contrast to the PNA_2·DNA triplexes[24] and PNA·DNA duplexes[25], in which the DNA sugar rings adopted the C3′-*endo* and predominantly C2′-*endo*, respectively. Thus, the P-helix can accommodate both types of sugar ring puckering well. All amide bonds in the PNA backbone are in the *trans*-conformation without the intramolecular hydrogen bonding earlier proposed based on a molecular mechanics calculation.[26] The C=O group of the methylenecarbonyl linker pointed towards the C-terminus of the PNA strand to maximize the stabilizing n → π* interaction with the backbone carbonyl of the glycine unit. The lysine side chain did not electrostatically interact with the phosphate backbone of the DNA counter strand. However, it formed an ion pair with the DNA phosphate backbone of the adjacent PNA·DNA duplex in the crystal lattice to provide additional stabilization, but this interaction would likely be absent in the solution phase. The right-handed helicity was determined primarily by the steric

© 2022 The Author(s). Published by the Royal Society of Chemistry

Open Access Article. Published on 18 Nyenyankulu 2022. Downloaded on 2026-01-28 04:18:10.
This article is licensed under a Creative Commons Attribution-NonCommercial 3.0 Unported Licence.

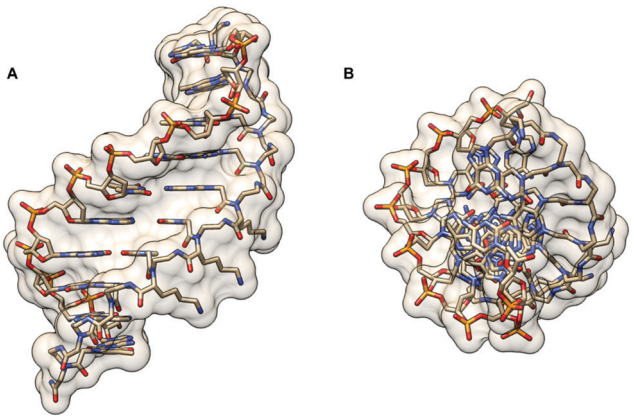

Fig. 3 X-Ray structure of the αPNA·DNA duplex (1NR8): (A) side view from the minor groove side and (B) top view from the 3′/*N*-side along the helix axis.[23]

interaction between the D-Lys side chain and the N-terminal aminoethyl group. The improved directional and mismatch specificity was probably benefitted from the conformational restriction imparted by the D-Lys substituent.

Modified PNA with two α-substituents

In contrast to the marginal change in the DNA/RNA duplex stability of mono-substituted αPNA, the introduction of a gem-dimethyl substituent at the α-position of the aegPNA backbone (aedmgPNA) was reported to substantially increase the stability of both DNA and RNA duplexes.[27] This is true for both PNAs with chimeric and homogeneous backbones, although the data for the latter were available only for the homothymine sequence. The stability of the PNA·DNA hybrids was increased much more than that of the corresponding RNA hybrids, resulting in the reversal of DNA/RNA binding selectivity when compared to aegPNA. In addition, the antiparallel duplexes were also selectively stabilized over the parallel duplexes, making the antiparallel selectivity much better than in the case of aegPNA. The backbone-extended homolog of aegPNA with similar α-*gem*-dimethyl substituents (apdmgPNA) also exhibited improved stability albeit to a lesser extent. In the absence of the *gem*-dimethyl substituent, the backbone-extended PNA exhibited very poor binding affinity towards the DNA target. The stability against mismatched DNA was evaluated only with the homothymine sequence and was found to be more discriminating than the corresponding aegPNA hybrids (Table 2).

Table 2 T_m data of α-*gem*-dimethylated PNA with DNA and RNA[27]

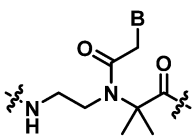

aedmgPNA

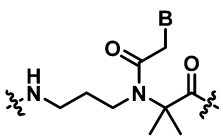

apdmgPNA

Sequence[a] (N–H/C–NH_2)	Modification	T_m DNA[b] (°C)	T_m RNA[b] (°C)
TTTTTTT-Lys	None (aegPNA)	43	54
TtTtTtTt-Lys	aedmgPNA	80	73
ttttttttt-Lys	aedmgPNA	>85	>85
TtTtTtTt-Lys	apdmgPNA	59	57
ttttttttt-Lys	apdmgPNA	77	61
GTAGATCACT	None (aegPNA)	50 (38)	50 (40)
GtAGAtCACt	aedmgPNA	81 (56)	72 (32)
GtAGAtCACt	apdmgPNA	73 (50)	65 (33)

[a] The modification site is denoted by a small letter. [b] Antiparallel duplexes; T_m values for parallel duplexes are shown in parentheses.

A recent structural study of the α-gem-dimethylated PNA monomer was performed by NMR and computational calculation which revealed the exclusive *Z*-rotamer preference of the tertiary amide bond in the PNA backbone (Fig. 4).[28] On the other hand, previous studies indicate that a mixture of *Z*/*E* rotamers are formed in the case of aegPNA monomers and dimers,[29–31] while only the *Z*-rotamers were observed in the NMR and crystal structures of PNA duplexes.[32] The steric repulsion between the α-*gem*-dimethyl substituent and the CH_2B on the tertiary amide group favored the formation of the *Z*-rotamer, which was also further stabilized by the n → π* interaction. This suggests that the tertiary amide bond in the α-*gem*-dimethylated PNA monomer is pre-organized in the correct *Z*-rotamer required for the duplex formation. The smaller entropy loss in the hybridization process nicely explains the higher stability of the aedmgPNA over aegPNA hybrids. At present, only the T-monomer is available; thus it is not yet known whether the conclusion will be general for mixed-sequence PNA with a fully α-gem-dimethylated backbone. In addition, the mismatch specificity has not yet been reported. Nevertheless, the preliminary results look promising. Other α-gem-disubstituted PNA monomers have been synthesized,[33–35] although the incorporation into PNA oligomers and their DNA binding properties have not been reported.

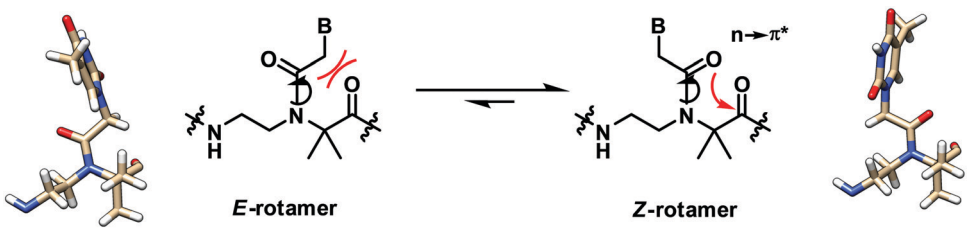

Fig. 4 Interconversion of the *E*- and *Z*-rotamers in the α-*gem*-dimethylated PNA monomer.[28]

© 2022 The Author(s). Published by the Royal Society of Chemistry

Open Access Article. Published on 18 Nyenyankulu 2022. Downloaded on 2026-01-28 04:18:10.
This article is licensed under a Creative Commons Attribution-NonCommercial 3.0 Unported Licence.

Table 3 T_m data of βPNA with DNA[36]

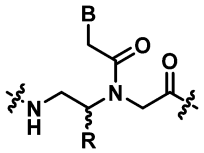

Sequence (N–H/C–NH_2)[a]	Substituent (R)	T_m DNA (°C)	ΔT_m[b] (°C)
GTAGATCACT-^{L}Lys	None	51.4	—
GtAGAtCACt-^{L}Lys	β-(*S*)-Me	51.0	−0.4
GtAGAtCACt-^{D}Lys	β-(*R*)-Me	No melting	Large

[a] The modification site is denoted by a small letter. [b] ΔT_m refers to T_m difference between the modified PNA and aegPNA.

Modified PNA with β-substituents (βPNA)

While PNA systems with the β-carbon atom as part of a cyclic structure have been extensively studied (see Modified PNA with cyclic structure as part of the backbones), only one β-substituted PNA system with simple methyl substituents has been reported so far.[36] This could be attributed to the less availability of the chiral diamine building blocks required for the synthesis of βPNA compared to the amino acid-derived αPNA and γPNA. The chimeric mixed-sequence PNA carrying three β-methyl substituents in the (*S*)-configuration when hybridized to DNA provided a duplex with comparable stability to unmodified aegPNA (Table 3). Similar to the case of αPNA, the stereochemistry of the substituent significantly affects the PNA·DNA duplex stability. However, the effect is more pronounced as shown by the complete absence of DNA binding of the corresponding β-methyl-substituted PNA with the (*R*)-configuration. Molecular modeling of the PNA·DNA duplexes indicated a steric clash between the (*R*)-β-methyl substituent and the CH_2 group of the BCH_2CO substituent on the PNA backbone (Fig. 5). In the case of αPNA, the steric clash between the less hindered C═O group and the α-methyl substituent is expected to be smaller, which is consistent with the observed experimental results. In addition, CD spectra of the single-stranded βPNA suggested pre-organization into a helical conformation with opposite helical senses for the two different configurations. The (*S*)-β-methyl-substituted PNA adopted a right-handed helical conformation that matched the natural handedness of native DNA duplexes (Fig. 6). However, after hybridization, the CD signal changed significantly indicating a substantial conformational change which might counterbalance the effect of conformational pre-organization, resulting in the observed lack of stabilization relative to the unmodified aegPNA.

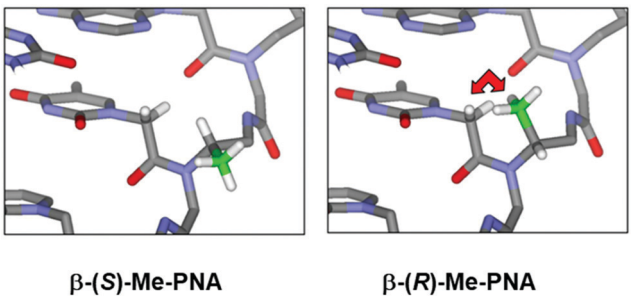

Fig. 5 A model of the βPNA structure showing a different degree of steric clash between the β-(*S*)- or β-(*R*)-methyl groups and the nucleobase side arm (reprinted from ref. 36, Copyright (2011), with permission from Elsevier).

Modified PNA with two β-substituents

In contrast to the α-gem-dimethylated PNA, the analogous NMR and theoretical study on the β-gem-dimethylated PNA monomer indicated that the *E*-rotamer was preferred over the *Z*-rotamer.[28] In fact, only the *E*-rotamer was observed by NMR in the monomer. According to the simulation of the mono-β-methyl-substituted PNA above, the *Z*-rotamer would result in a severe steric clash with the pro-*R* methyl group, thus necessitating the adoption of the *E*-rotamer despite the loss of the stabilizing n → π* interaction (Fig. 7). Since the *Z*-rotamer was exclusively observed in the structures of all PNA duplexes and triplexes reported in the literature,[32] it is unlikely that the β-*gem*-dimethylated PNA will interact strongly with the DNA

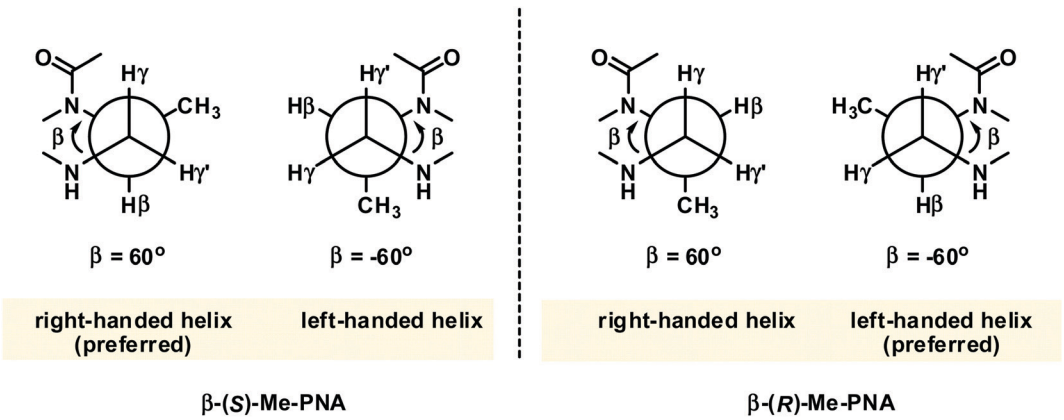

Fig. 6 The gauche conformation of the N(H)–Cγ–Cβ–N(CO) groups necessitates pre-organization into the right-handed helix in β-(*S*)-methyl PNA.[36] The structure is viewed along the Cγ–Cβ axis.

© 2022 The Author(s). Published by the Royal Society of Chemistry

Open Access Article. Published on 18 Nyenyankulu 2022. Downloaded on 2026-01-28 04:18:10.
This article is licensed under a Creative Commons Attribution-NonCommercial 3.0 Unported Licence.

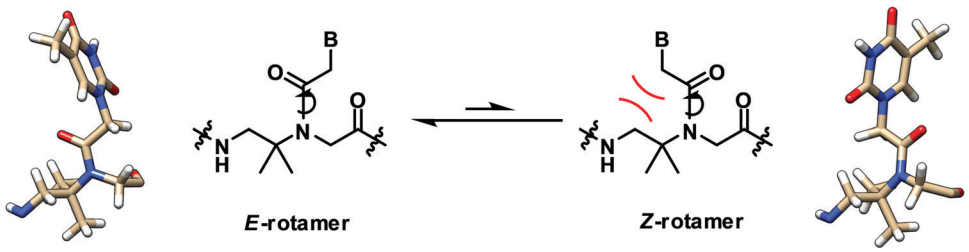

Fig. 7 Interconversion of the *E*- and *Z*-rotamers in the β-*gem*-dimethylated PNA monomer.[28]

counterpart. However, this remains to be experimentally verified.

Modified PNA with γ-substituents (γPNA)

The γ-modified PNA monomers are conveniently obtained from standard amino acids *via* the corresponding N-protected α-amino aldehydes. They were first reported as early as 1994,[37] but it was not until more than a decade later that the full potential of γPNA was recognized. Early studies focused on the use of γ-substituents as a handle for subsequent modification with dyes or other functional entities to create functional PNA probes[38,39] or for creating long PNA strands by native chemical ligation.[40,41] These reports suggest that the partial γ-substitution by the lysine or cysteine side chain does not much affect the PNA·DNA duplex stability provided that the chirality of the γ-carbon was derived from the natural L-amino acids. The remarkable stabilizing effect of the γ-substituent was revealed for the partially and fully modified γPNA derived from L-serine in the seminal paper by Ly's group in 2006.[42] A single γ-hydroxymethyl modification (^{L}Ser γPNA) in a 10mer aegPNA increased the T_m of the PNA·DNA and PNA·RNA duplexes by +4 and +3 °C, respectively. In the fully γ-modified PNA, the T_m values for the PNA·DNA and PNA·RNA duplexes were increased by +19 and +10 °C with improved mismatch specificity (ΔT_m = 16–19 and 12–18 °C) (Table 4). The CD spectra of single-stranded γPNA suggested the formation of helical structures – the helicity of which was determined by the configuration of the Cγ. The signal became more intense and changed from PNA·PNA- to PNA·DNA-like helices when more γPNA units were incorporated into the aegPNA strand. The observed CD signal in the single-stranded γPNA was much more pronounced than the corresponding αPNA. The degree of pre-organization is temperature-dependent – being diminished at higher temperatures – but is not sensitive to the concentration, thus indicating the intramolecular nature of the pre-organization. By varying the position of the γPNA unit in the PNA strand, it was revealed that the helical induction was unidirectional from the C-to-N termini. Even the small methyl substituent could effectively induce the pre-organization.

Conformational studies of a γPNA dimer C(^{L}Ala)T in solution by NMR indicated that it exists as a mixture of tertiary amide rotamers similar to aegPNA. However, the γPNA backbone adopted a well-defined conformation while the aegPNA dimer with the same sequence adopted a random coil structure. Detailed analysis of coupling constants revealed that the backbone of all four rotamers of γPNA adopted a right-handed helical structure with a torsional angle β [N(H)–Cγ–Cβ–N(CO)] in the range of +50 to +60° to avoid the steric clash between the γ-substituent and the C-terminal backbone tertiary amide nitrogen atom (Fig. 8). Theoretical calculation suggested that the right-handed conformation was more stable than the left-handed conformation by 3.5 kcal mol^{-1}, *i.e.* >99% population excess. A solution NMR structure of a γPNA·γPNA duplex[43] and an X-ray structure of a γPNA·DNA duplex are available.[44] The conformation of the single-stranded γPNA dimer[42] closely resembles the conformation of the γPNA·γPNA duplex,[43] the γPNA·DNA duplex,[44] as well as the aeg/αPNA unit from an X-ray structure of a PNA·DNA duplex (Fig. 9).[23] This indicates that the γ-substituent forces the single-stranded PNA to adopt the appropriate helical conformation that is similar to those found in the duplexes thus explaining its strong binding properties. The three-dimensional structures also revealed that the γ-substituent resided at the edge of the grooves of the γPNA·γPNA and γPNA·DNA duplexes and should not significantly interfere with the duplex formation. Indeed, several other substituents in addition to CH_3 including $HOCH_2$-,[42] $HOCH_2CH_2OCH_2$-,[45] guanidinoethyl,[46] guanidinobutyl-,[47] $H_2NCH_2CH_2$-,[46] $H_2NCH_2CH_2CH_2$-,[48] $H_2NCH_2CH_2CH_2CH_2$-,[38,39] and $HO_2CCH_2CH_2$-[49] have been placed at the γ-position without significantly altering the binding properties as long as the L-configuration is preserved. Charged groups showed relatively

Table 4 T_m data of ^{L}Ser γPNA with DNA and RNA[42]

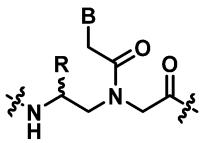

Sequence (N–H/C–LysNH$_2$)[a]	Substituent (R-)	T_m DNA (°C)	T_m RNA (°C)	T_m mmDNA[b] (°C)	T_m mmRNA[b] (°C)
GCATGTTTGA	None (aegPNA)	44	54	30–34	36–43
GCATGtTTGA	(*R*)-$HOCH_2$-	48	57	—	—
GCAtGtTtGA	(*R*)-$HOCH_2$-	53	60	—	—
GCATGtttGA	(*R*)-$HOCH_2$-	53	59	—	—
gcatgtttga	(*R*)-$HOCH_2$-	63	64	44–47	46–52

[a] The modification site is denoted by a small letter. [b] T_m values for mismatched targets, expressed as a range for different mismatched bases.

Open Access Article. Published on 18 Nyenyankulu 2022. Downloaded on 2026-01-28 04:18:10.
This article is licensed under a Creative Commons Attribution-NonCommercial 3.0 Unported Licence.

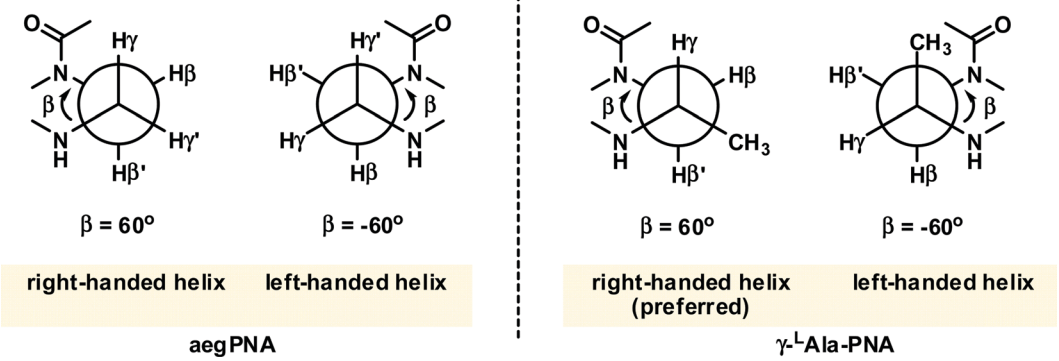

Fig. 8 The gauche conformation of the N(H)–Cγγ–Cβ–N(CO) groups necessitates pre-organization into the right-handed helix in γ-(*S*)-methyl PNA. The structure is viewed along the Cγ–Cβ axis (adapted with permission from ref. 42. Copyright 2006 American Chemical Society).

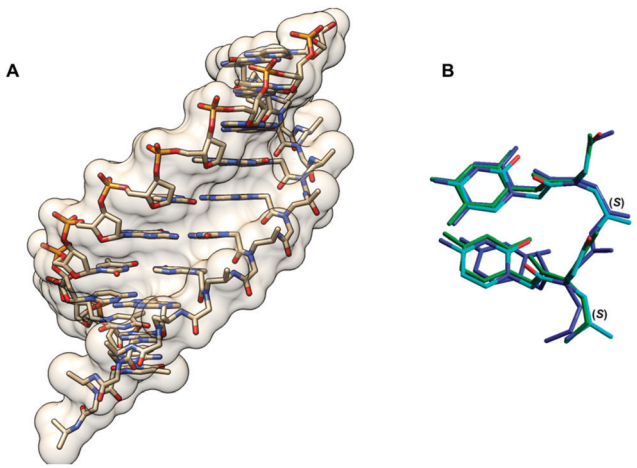

Fig. 9 (A) X-Ray structure of the γPNA·DNA duplex (3PA0) viewed from the minor groove side.[44] (B) Superposition of the PNA strand from the γPNA·DNA duplex (cyan), aegPNA·DNA duplex (green), and single-stranded γPNA dimer (blue) (reprinted with permission from ref. 44. Copyright 2010 American Chemical Society).

Table 5 T_m data of αPNA and γPNA bearing charged aminoalkyl side chains with DNA and RNA

Sequence (N–H/C–LysNH$_2$)[a]	Substituent	T_m DNA (°C)	T_m RNA (°C)	Ref.
TTACCTCAGT	None (aegPNA)	49	62	48
TtACCtCAGT	H_2NCH_2-, α-(*S*)	54	—	50
TtACCtCAGT	H_2NCH_2-, α-(*R*)	58	—	50
TtACCtCAGT	H_2NCH_2-, γ-(*S*)	62	—	50
TtACCtCAGT	$H_2N(CH_2)_2$-, γ-(*S*)	50	59	46
TtACCtCAGT	$H_2N(CH_2)_3$-, γ-(*S*)	53	63	48

[a] The modification site is denoted by a small letter.

little effects on the binding affinity and specificity. However, the electrostatic effect may be significant if the linker was short as in the case of H_2NCH_2-γ-PNA whereby the duplex stability was higher than in the case of the amino-modified γPNA with longer linkers (Table 5).[48,50,51] Interestingly, γPNA with the negatively charged $-CH_2SO_3^-$ substituent adopted a more extended conformation in the single-stranded form as shown by NMR and CD analyses which could be due to the intra-strand electrostatic and steric interactions among the sulfate groups. Accordingly, the PNA_2·DNA triplexes formed from γ-sulfated PNA were less stable than the corresponding unmodified PNA.[52] On the other hand, the corresponding carboxyethyl-modified γ-PNA formed a highly stable triplex with oligo(dA).[49] Under physiological ionic strength, γPNA with negatively charged side chain bound more strongly to RNA than DNA, and the reverse was true for γPNA with positively charged side chain.[53] However, the selectivity was rather small.

Modified PNA with two γ-substituents

The solution structure of a γ-gem-dimethylated PNA monomer was also studied by NMR, which indicated that both *Z*- and *E*-rotamers exist in almost equal amounts (Fig. 10).[28] Theoretical calculation confirmed the similar stability and indicated the absence of significant stabilization interactions including the n → π* interaction in both rotamers. In contrast to mono-γ-substituted PNA, the helicity induction by the chirality of the γ-substituent will be absent. This, together with the significant steric clash of the CH_2B with one of the γ-methyl groups in the *Z*-rotamer which could not be relieved by adopting the alternative helicity, suggests that the γ-gem-dimethylated PNA may not interact strongly with the DNA counterpart. This, however, remains to be verified experimentally.

N-Methylated PNA: modified PNA with *N*-substituents

Only one example of *N*-substituted PNA has been reported whereby the *N*-substituent was the methyl group.[54] The T_m values of the duplexes of the fully *N*-methylated PNA decamer with both DNA and RNA were decreased compared to those of the unmethylated PNA by 12–18 °C, although partial substitution was more tolerated (Table 6). CD spectra indicated that the incorporation of up to 30% of *N*-methylation does not change the overall conformation of the PNA·DNA duplexes, but a distinct conformation was observed in the fully methylated PNA·DNA duplexes. The crystal structure of a 50% methylated

© 2022 The Author(s). Published by the Royal Society of Chemistry

Open Access Article. Published on 18 Nyenyankulu 2022. Downloaded on 2026-01-28 04:18:10.
This article is licensed under a Creative Commons Attribution-NonCommercial 3.0 Unported Licence.

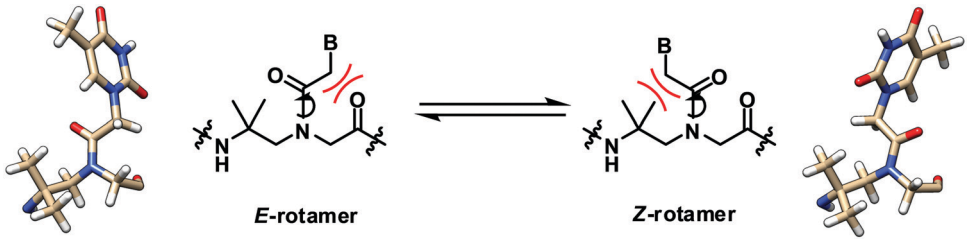

Fig. 10 Interconversion of the *E*- and *Z*-rotamers in the γ-gem-dimethylated PNA monomer.[28]

Table 6 T_m data of *N*-Me PNA with DNA and RNA[54]

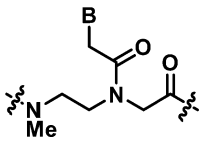

Sequence (N–H/C–NH_2)[a]	T_m DNA (°C)	T_m RNA (°C)
GTAGATCACT	50	54
GTAGATCACT-Lys	51	56
GtAGAtCACt	42	49
gcatgtttga-Lys	33	44

[a] The modification site is denoted by a small letter.

PNA·PNA hexamer duplex was determined at 2.2 Å resolution (Fig. 11). Since the PNA·PNA duplex is achiral, both left-handed and right-handed antiparallel duplexes were observed in the asymmetric unit. The helical parameters include a diameter of 28 Å, a helical twist of 19–20°, a rise of 3.5/3.8 Å, an *x*-displacement of 4.8/7.2 Å, and 18 base pairs per turn which are consistent with the P-helix. Although the overall structures of the *N*-methylated and unmethylated PNA·PNA duplexes are similar, the major difference is the orientation of the backbone carbonyl groups. In the case of the *N*-methylated monomer, the amide carbonyl group turned inward to form a water-mediated hydrogen bonding with the nucleobase. For the unmethylated monomer, this amide carbonyl pointed away towards the solution and the NH group formed a water-mediated hydrogen bonding with the nucleobase instead. No other examples or applications of *N*-substituted PNAs have been reported so far. In view of the minimal impact on the overall conformation and the ease of modification of the nitrogen atom without the problem of introduction of additional chirality, this system offers a potential platform for the introduction of additional functions to the PNA molecules.

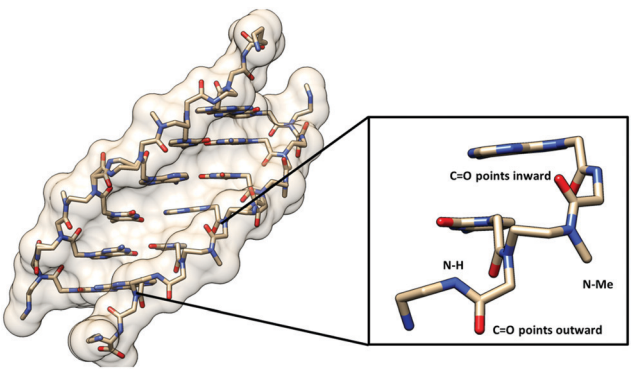

Fig. 11 X-Ray structure of the *N*-Me PNA·PNA duplex (1QPY) viewed from the minor groove side with the different orientation of the backbone carbonyl groups of the *N*-Me and normal aegPNA monomers shown.[54]

Backbone-modified PNA with multiple modifications

In most PNAs with multiple modifications, the substituents are generally tied to form a ring. Such PNAs with a cyclic structure will be covered under the topic "Modified PNA with cyclic structure as part of the backbones". This section will cover only when the substituents were not connected to form a ring. In 2005, Marchelli *et al.* reported a modified PNA system bearing two substituents at the α- and γ-positions – one at each position.[55,56] The substituent at both positions was the same aminobutyl group derived from lysine with different stereochemistries. All four combinations (αD/γD, αD/γL, αL/γD, αL/γL), as well as the individually modified (αD, αL, γD, γL) PNAs, were synthesized and the stability of the corresponding complementary PNA·DNA hybrids was compared (Table 7). According to thermal stability measurements, the L-configuration at the γ-position is strongly preferred over the D-configuration. The chirality at the α-position showed much smaller effects on the PNA·DNA duplex stability, with the D-configuration being more preferred than the L-configuration. The results are consistent with the PNA individually modified at either the α- or γ-positions, suggesting that the two sites are independent, and the stabilization effects are additive/synergistic. Thus, the αD/γL showed the highest thermal stability, and no DNA binding was observed in the αL/γD isomer. According to CD spectroscopic studies, the helicity in α/γPNA·aegPNA and α/γPNA·DNA duplexes is primarily controlled by the configuration of the γ-position, and when the helicity induced by both positions matched that of the DNA, strong binding was observed. The preference for right- or left-handed helicities arose from the attempt to minimize the intrastrand steric clashes due to the amino acid side chains. Steric disturbances are less tolerated in the γ-position than in the α-position, and consequently, the helical induction is dominated by the stereogenic center at the γ-position. Thermodynamic parameters extracted from the melting curve data suggested that the contribution of the α-position is dominated by the enthalpic term (*i.e.*, more negative enthalpy change), while the contribution of the γ-position is

Open Access Article. Published on 18 Nyenyankulu 2022. Downloaded on 2026-01-28 04:18:10.
This article is licensed under a Creative Commons Attribution-NonCommercial 3.0 Unported Licence.

Table 7 T_m data of backbone-modified PNA with α- and γ-substitution[56]

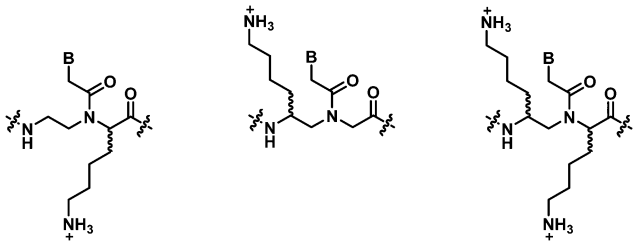

System	Helical induction induced by Cα	Helical induction induced by Cγ	Overall helical preference	T_m DNA[a] (°C)
α_D,γ_L	Right-handed	Right-handed	Right-handed	57
γ_L	—	Right-handed	Right-handed	56
α_L,γ_L	Left-handed	Right-handed	Right-handed	52
α_D	Right-handed	—	Right-handed	52
Unmodified	—	—	—	50
α_L	Left-handed	—	Left-handed	47
α_D,γ_D	Right-handed	Left-handed	Left-handed	33
γ_D	—	Left-handed	Left-handed	32
α_L,γ_D	Left-handed	Left-handed	Left-handed	<20

[a] T_m was determined from CD melting curves at 260 nm; PNA sequence = H-GTAGAtCACT-NH_2; DNA sequence = dAGTGATCTAC. The modification sites are denoted by a small letter.

dominated by the entropic term (*i.e.*, less negative entropy change).

In a more recent example, Kumar *et al.* reported the only example of acyclic β,γ-disubstituted PNA.[57] The substituents studied were methoxymethyl and hydroxymethyl in the (*R*,*R*) and (*S*,*S*)-configurations (Fig. 12A). Thermal denaturation studies on chimeric aeg/β,γ-bis(methoxymethyl)-substituted PNA with DNA/RNA showed comparable or slightly improved stability over aegPNA for the (*R*,*R*) isomer (Table 8). The duplex with parallel DNA was more destabilized than the antiparallel DNA, leading to a higher directional specificity when compared to aegPNA. Much lower stability was observed for the (*S*,*S*)-isomer, with the ΔT_m in the range of −20 °C for a single modification, and the introduction of another modification completely diminished the binding. The preferred stereochemistry is in accordance with other β- or γ-substituted PNA as well as

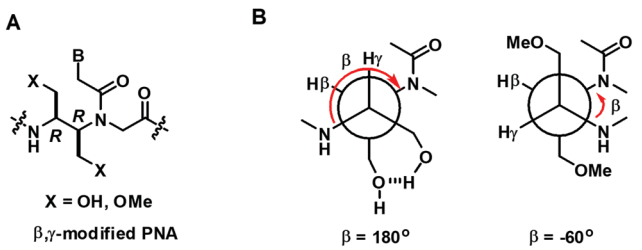

Fig. 12 (A) Structure of β,γ-modified PNA. (B) The proposed different conformation of the OH and OMe substituted PNA (reproduced from ref. 57 with permission from the Royal Society of Chemistry).

Table 8 T_m data of backbone-modified PNA with β- and γ-substitution[57]

Sequence (N–H/C–$LysNH_2$)[a]	Modification	T_m apDNA[bcd] (°C)	T_m pDNA[bcd] (°C)	T_m apRNA[bcd] (°C)
AACCGATTTCAG	None (aegPNA)	58	46	63
AACCGAtTTCAG	X = HO-	n.t.	n.t.	n.t.
AACCGAtTTCAG	X = MeO-	59 (44)	38	65 (52)
AACCGaTTTCAG	X = HO-	n.t.	n.t.	n.t.
AACCGaTTTCAG	X = MeO-	58 (38)	39	62 (49)
AACCGAtTtCAG	X = MeO-	60 (n.t.)	n.t.	66 (n.t.)

[a] The modification site is denoted by a small letter. [b] ap = antiparallel; p = parallel. [c] (*R*,*R*)-isomer; values for the (*S*,*S*)-isomer are shown in parentheses. [d] No melting transition is denoted by n.t.

β,γ-linked PNA with cyclic structures, but the configuration notations were different due to the change in priority of the groups involved. Interestingly, the presence of two hydroxymethyl substituents was detrimental to both DNA and RNA binding as the introduction of only one modification as either (*R*,*R*) or (*S*,*S*)-isomers resulted in a complete inability to form stable hybrids with both DNA and RNA targets. It was proposed that the intramolecular hydrogen bonding between the two adjacent hydroxymethyl groups changes the torsional angle *β* from 60° to 180° making the conformation unsuitable for DNA/RNA binding (Fig. 12B).

Modified PNA with cyclic structure as part of the backbones

This section will discuss how conformation constraint can be introduced in the aegPNA structure by introducing a bond, an atom or a group of atoms (denoted by X) to form a bridge between different positions in the core backbone. Such bridging would create a carbocyclic or heterocyclic ring within the

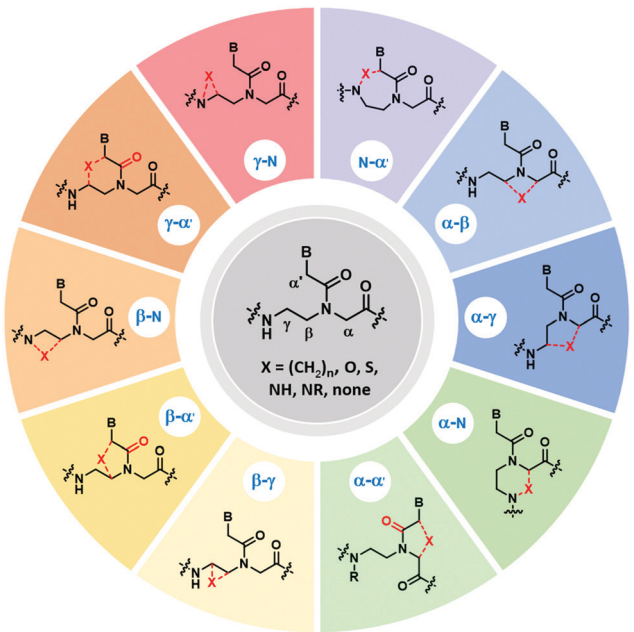

Fig. 13 Possible sites for modification of aegPNA by forming a cyclic structure as part of the backbone.

© 2022 The Author(s). Published by the Royal Society of Chemistry

Open Access Article. Published on 18 Nyenyankulu 2022. Downloaded on 2026-01-28 04:18:10.
This article is licensed under a Creative Commons Attribution-NonCommercial 3.0 Unported Licence.

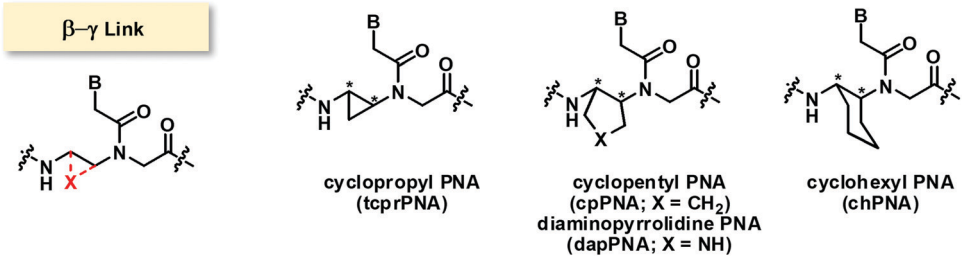

Fig. 14 Structures of modified PNA with (β–γ)-linkage.

PNA backbone leading to new conformationally constrained PNA analogs. Possible sites for the introduction of bridging include α, β, γ, N and α′ as illustrated in Fig. 13, although not all possibilities of such bridging may have been realized as these modified PNAs are more synthetically challenging when compared to the simple backbone-substituted αPNA or γPNA. The carbonyl group on the nucleobase side arm may optionally be removed. In addition, the backbone may be extended, or some atoms swapped. The modified PNA systems will be discussed according to the bridging positions.

Modified PNA with (β-γ)-linkage

The bridging between the β- and γ- positions within the aegPNA backbone by a $-(CH_2)_n-$ linkage introduces a carbocyclic ring within the aegPNA structure. Such carbocyclic bridging will increase rigidity in the structure by the limited conformations that the ring can adopt. The introduction of the ring also generates chirality that can affect pre-organization of the PNA chain, although not all possible combinations may have been investigated. Only the 3-, 5- and 6-membered carbocyclic ring (n = 1, 3 and 4) modifications have been reported in the literature (Fig. 14). The *trans*-cyclohexyl PNA (chPNA) was the first example of such carbocyclic PNA systems that were reported since early dates (Fig. 15).[58] The DNA binding of chPNA is stereochemically dependent. The partial introduction of the (*S*,*S*)-cyclohexyl PNA monomer into the aegPNA strand resulted in a small effect on the stability of the PNA·DNA and PNA·RNA hybrids, with $\Delta T_m = \pm 1$ °C per (*S*,*S*)-cyclohexyl PNA unit. On the other hand, the (*R*,*R*)-cyclohexyl PNA significantly reduced the stability of the PNA·DNA and PNA·RNA hybrids. Molecular dynamics simulations based on the NMR structure of an aegPNA·DNA duplex[25] suggested that the two amino groups in the diaminocyclohexane unit assumed an anti-periplanar relationship with a torsional angle β close to 180° and only minimal conformation adjustment was required for the (*S*,*S*)-chPNA binding to DNA, whereas more pronounced structural perturbation was observed in the (*R*,*R*)-chPNA. In the former case, the cyclohexane bridge was located outside the helix, while in the latter case the cyclohexane bridge resided within the major groove. However, the fully modified mixed-sequence (*S*,*S*)-chPNA decamer formed less stable duplexes with DNA and RNA when compared to aegPNA (T_m = 41 °C and 37 °C for PNA·DNA and PNA·RNA, respectively). Thermodynamic data indicated that the introduction of the (*S*,*S*)-chPNA indeed reduces the entropy loss as proposed, but it also lowers enthalpic gain resulting in lowering of the overall stability than aegPNA.

In a series of subsequent studies by Kumar and Ganesh, the *cis*-chPNA systems with the (1*S*,2*R*) and (1*R*,2*S*) configurations on the diaminocyclohexane ring were reported.[59–61] The major difference between the *trans*- and *cis*-diaminocyclohexane system is the torsional angle (β; NH–CH–CH–NHCO) which should be in the range of 60°–90° for the *cis*-isomer (+60° in the case of (1*R*,2*S*)-chPNA and −60° in the case of (1*S*,2*R*)-chPNA[62]) and 180° for the *trans*-isomer if the two amino substituents adopt the diaxial conformation or close to 60° if they assume the diequatorial conformation (Fig. 15). This indicates that *cis*-(1*S*,2*R*/1*R*,2*S*)-chPNA has a torsion angle more closely similar to that of the PNA·RNA duplex than the PNA·DNA duplex based on the torsional angle β of 60–70° and 140° obtained from NMR studies of PNA·RNA[63] and PNA·DNA duplexes,[25] respectively.

Thermal stability data of aegPNA and chimeric ch/aegPNA with DNA and RNA are summarized in Table 9. The results suggest the importance of the stereochemistry of the cyclohexane ring that leads to the proper arrangement and specific torsion angle which could provide a basis for the selective

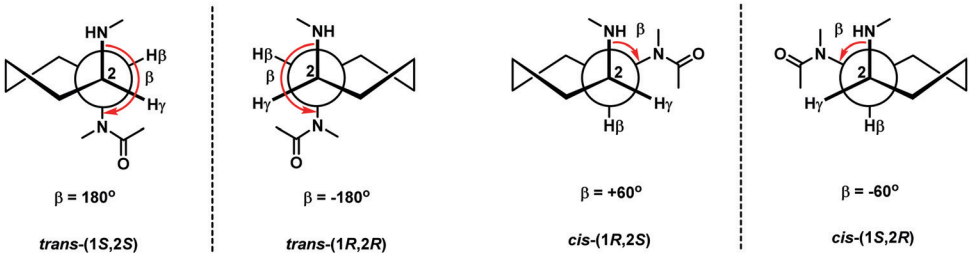

Fig. 15 Structures of cyclohexane-modified PNA with (β–γ)-linkage.

Open Access Article. Published on 18 Nyenyankulu 2022. Downloaded on 2026-01-28 04:18:10.
This article is licensed under a Creative Commons Attribution-NonCommercial 3.0 Unported Licence.

Table 9 T_m data of aegPNA and stereoisomeric chPNAs with DNA and RNA

PNA sequences[a] (N–H/C–LysNH$_2$)	Modification	β[b]	T_m (°C) DNA	T_m (°C) RNA	Ref.
TTTTTTTTTT	None (aegPNA)	141	72	81	58
TTTTtTTTTT	(1*S*,2*S*)-cHex		70	76	58
TTTTtTTTTT	(1*R*,2*R*)-cHex		52	56	58
TTTTtTTTTT	(1*S*,2*R*)-cHex	−63	62	77	59
TTTTtTTTTT	(1*R*,2*S*)-cHex	66	64	71	59
GTAGATCACT	None (aegPNA)	141	55	55	64
GtAGAtCACt	(1*S*,2*S*)-cHex		51	54	58
GtAGAtCACt	(1*R*,2*R*)-cHex		34	33	58
GtAGAtCACt	(1*S*,2*R*)-cHex	−63	25	58	64
GtAGAtCACt	(1*R*,2*S*)-cHex	66	35	>85	64
gtagatcact	(1*S*,2*S*)-cHex		41	37	58

[a] The modification site is denoted by a small letter. [b] Torsional angle value of aegPNA was taken from ref. 25, and others were based on X-ray structures of monomers.

Table 10 T_m data of aegPNA and stereoisomeric cpPNAs with DNA and RNA

PNA sequences[a] (N–H/C–LysNH$_2$)	Modification	β[b]	T_m (°C) DNA	T_m (°C) RNA	Ref.
TTTTTTTT	None (aegPNA)	141	45	62	60
TTTtTTTT	(1*S*,2*R*)-cPen	−24	22	76	60
TTTtTTTT	(1*R*,2*S*)-cPen	25	62	61	60
tttttttt	(1*S*,2*R*)-cPen	−24	67	>85	60
tttttttt	(1*R*,2*S*)-cPen	25	72	>85	60
GTAGATCACT	None (aegPNA)	141	55 (49)[c]	55	64 and 65
GTAGAtCACT	(1*S*,2*S*)-cPen	86	55	—	65
GTAGAtCACT	(1*R*,2*R*)-cPen	70–90	n.t.[d]	—	65
GTAGAtCACT	(1*R*,2*R*)-Pyrrolidine	103	58	—	66
GtAGAtCACt	(1*S*,2*S*)-cPen	86	60	—	67
GtAGAtCACt	(1*S*,2*R*)-cPen	−24	77	84	64
GtAGAtCACt	(1*R*,2*S*)-cPen	25	79	>85	64

[a] The modification site is denoted by a small letter. [b] Torsional angle value of aegPNA was taken from ref. 25, and others were based on X-ray structures of monomers. [c] Two different values are obtained from different sources. [d] n.t. = no melting transition.

binding of RNA over DNA targets. Given the substantial destabilization of the (1*R*,2*R*)-chPNA when compared to the (1*S*,2*S*)-chPNA systems, the relatively high stability for the PNA·RNA duplexes observed for both *cis*-(1*S*,2*R*)- and (1*R*,2*S*)- chPNA is quite remarkable. Nevertheless, these results are only from chimeric systems and care should be taken in interpreting the results as already noted in the case of *trans*-chPNA.[58] At present, no T_m data for the fully modified *cis*-chPNA systems are available.

When the (β–γ)-linkage in the cyclohexyl PNA backbone was changed from –$(CH_2)_4$– to –$(CH_2)_3$–, a cyclopentane ring was formed in cyclopentyl PNA (cpPNA). The cyclopentane ring exhibits characteristic pseudoaxial/pseudoequatorial puckering properties which relaxed the torsional strain compared to the cyclohexane ring system. In addition, the five-membered ring should provide more flexibility compared to the rigid cyclohexane ring system. Such cyclopentyl PNA was introduced almost simultaneously by Kumar and Ganesh's group[60,68] for the *cis*-(1*S*,2*R*/1*R*,2*S*)-cpPNA and Appella's group for the *trans*-(1*S*,2*S*/1*R*,2*R*)-cyclopentyl PNA (cpPNA).[65,69–71] According to the X-ray data, the *cis*-diaminocyclopentane rings show $\beta = -24^\circ$ for (1*S*,2*R*)-cpPNA and +25° for (1*R*,2*S*)-cpPNA monomers.[60] Hybridization studies with complementary DNA/RNA sequences by UV-T_m measurements indicate that the cp/aegPNA chimera forms thermally stable hybrids with both DNA and RNA (Table 10). While stereochemistry-dependent selective binding to RNA over DNA was observed in the chimeric homothymine sequences,[60] subsequent studies in the mixed-sequence context did not show the same effect.[64] Thus, both stereoisomers of *cis*-cpPNA appeared to strongly stabilize both DNA and RNA hybrids which is in sharp contrast to the chPNA. Again, these results are only from chimeric systems and care should be taken in generalizing the results.

The cyclopentyl PNAs with the *trans*-(1*S*,2*S*) and (1*R*,2*R*)-configurations were investigated by Appella *et al.* The studies were more focused on DNA binding, and thus no data for RNA were available. The effect of stereochemistry on the binding properties of *trans*-cpPNA was remarkable as an increase in T_m of around +5 °C per (1*S*,2*S*)-cpPNA unit added to the aegPNA structure whereas no melting was observed when a single unit of (1*R*,2*R*)-cpPNA was introduced (Table 10). Thermodynamic parameters show that replacing the cyclopentyl ring in aegPNA reduces conformational flexibility and entropic cost of the hybridization, resulting in the higher thermal stability of the cpPNA·DNA hybrids.[65] The T_m was increased progressively and CD spectra indicated an increasing level of pre-organization upon the introduction of more (1*S*,2*S*)-cpPNA units. Subsequent studies in a fully modified cpPNA nonamer revealed a very high T_m of 94 °C which is 52 °C higher compared to the corresponding unmodified aegPNA.[71] The crystal structure of the (1*S*,2*S*)-cpPNA·DNA hybrid at 1.3 Å resolution revealed an antiparallel right-handed helix with a helical twist of 27.1 Å, a rise of 3.4 Å, and a pitch of 13.2 base-pairs per turn as shown in Fig. 16. The average torsional angle β of the *trans*-diaminocyclopentane unit was 86 ± 8°. This value was quite different from the aegPNA·DNA structure obtained by an earlier NMR study.[25] However, it is compatible with the torsional angle β obtained from other X-ray structures of PNA·DNA duplexes.[23,44] This indicates that the PNA structure in the PNA·DNA duplex may be able to adopt a broad range of conformations. Thus, from the hindsight, the apparent correlation of the torsional angle of the PNA monomer and the DNA/RNA selectivity in earlier studies of cpPNA and chPNA might be considered as over-simplification.[12,64]

An aza analog of cpPNA in which the –$(CH_2)_3$– bridge that was part of the cyclopentane ring was replaced by a –CH_2NHCH_2– bridge to create a 5-membered heterocyclic ring called dapPNA was also recently reported.[66] Despite carrying the wrong (*R*,*R*)-configuration, the chimeric dap/aegPNA with a single modification showed decent DNA binding (T_m = 57.2 °C, which is +6.3 °C higher than that in the case of the corresponding aegPNA). This is in sharp contrast to the corresponding carbocyclic analog reported in the literature.[65] The stabilization effect was explained by the favorable electrostatic interaction due to the presence of the protonatable nitrogen

© 2022 The Author(s). Published by the Royal Society of Chemistry

Open Access Article. Published on 18 Nyenyankulu 2022. Downloaded on 2026-01-28 04:18:10.
This article is licensed under a Creative Commons Attribution-NonCommercial 3.0 Unported Licence.

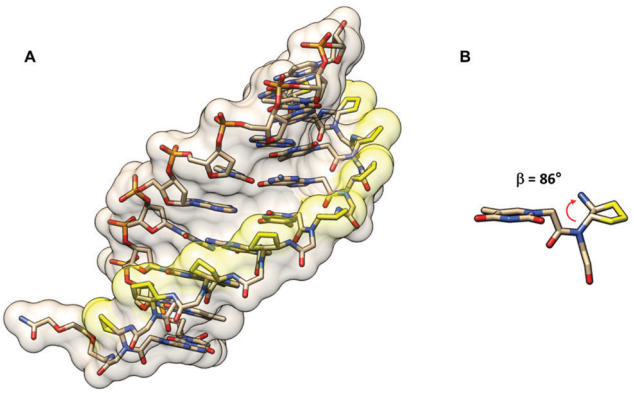

Fig. 16 (A) X-Ray structure of the *trans*-(*S*,*S*)-cpPNA·DNA duplex (7KZL)[71] viewed from the minor groove side. (B) Torsional angle β of the diaminocyclopentane unit from the X-ray structure of the cpPNA·DNA duplex. The cyclopentyl modification of the PNA backbone is shown in yellow.

atom in the dapPNA backbone. Despite the non-specific nature of such electrostatic interaction, the mismatch specificity was reported to be better than in the case of aegPNA (ΔT_m for mismatched PNA·DNA duplexes: aegPNA = −6.6 °C; dapPNA = −9.2 °C).[66]

Only one example of PNA with *trans*-(*S*,*S*)-cyclopropane (tcprPNA) bridging the β–γ positions was reported in the literature.[72] The extreme rigidity of the 3-membered ring was expected to make an impact on the pre-organization of the PNA. Mono-substituting the tcprPNA unit in the aegPNA results in a large decrease in thermal stability in both PNA·DNA and PNA·RNA. The torsional angle β of *trans*-diaminocyclopropane was not reported but it can be presumed to be more open than the *trans*-diaminocyclopentane analogs. The PNA_2·DNA triplex showed a two-step melting indicative of different structural compatibility of tcprPNA as a Hoogsteen and Watson–Crick strand. Significant hysteresis was observed especially in the case of PNA_2·RNA triplex melting, which suggested the slow kinetics of PNA·RNA binding.

Modified PNA with (α–γ)-linkage

In early attempts to constrain the conformation of aegPNA, the α- and γ-positions were linked to form 4-aminoproline isomers which generated four possible configurations (L-*trans*, L-*cis*, D-*trans*, D-*cis*) (Fig. 17).[73,74] The chimeric PNA with alternating L-*trans*-4-aminoproline and aegPNA monomers showed marginally higher DNA·PNA duplex stability than the unmodified aegPNA in the context of the homothymine sequence. Other stereoisomers formed DNA hybrids with lower stability. Reports from another group on a similar system focused on the synthesis of the monomers and small homothymine oligomers derived from these monomers.[75,76] CD studies of the single-stranded oligomers indicated well-ordered structures that are stereochemically dependent. The study on chimeric mixed-sequence PNA incorporating a single L-*trans* or D-*trans* diastereomer indicated that both isomers slightly stabilized the PNA·DNA duplexes. The parallel/antiparallel selectivity was also improved in a stereochemically dependent fashion (L-*trans*: antiparallel; D-*trans*: parallel).

Modified PNA with (β–α′)-linkage

Another common bridging strategy involves the linkage of the β- and α′-positions to form a 5-membered ring (Fig. 18). The tertiary amide carbonyl group of the nucleobase side-arm may be present or reduced to a CH_2 group. In the latter situation, the backbone nitrogen atom became positively charged due to protonation under physiological pH which could provide additional electrostatic interaction with the negatively charged phosphate backbone of DNA.

A conformationally constrained pyrrolidinone PNA with (β–α′)-linkage was reported in 2001.[77] All possible stereoisomers [(3*S*,5*S*), (3*R*,5*S*), (3*S*,5*R*), (3*S*,5*S*)] of the adenine pyrrolidinone PNA monomer were synthesized and incorporated in the middle of a mixed-sequence aegPNA strand to form chimeric pyrrolidinone/aegPNA. None of the four stereoisomers of pyrrolidinone PNA showed improvement in DNA and RNA binding

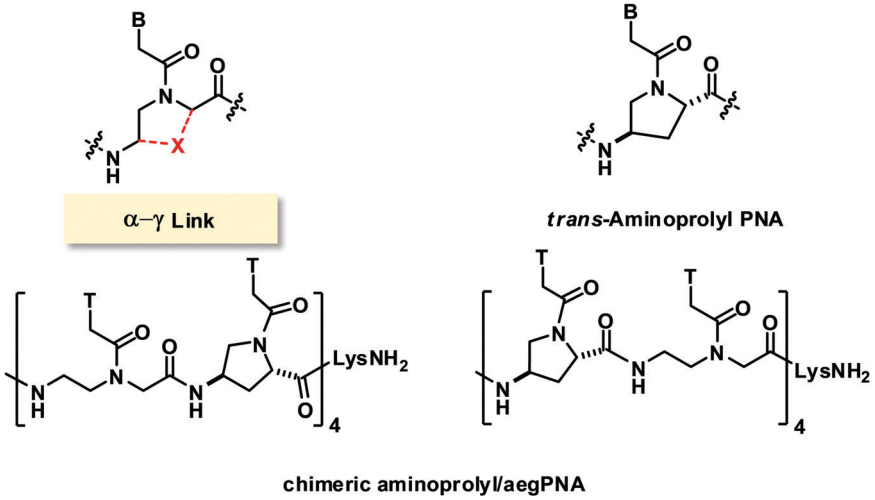

Fig. 17 Structures of modified PNA with (α–γ)-linkage.

Open Access Article. Published on 18 Nyenyankulu 2022. Downloaded on 2026-01-28 04:18:10.
This article is licensed under a Creative Commons Attribution-NonCommercial 3.0 Unported Licence.

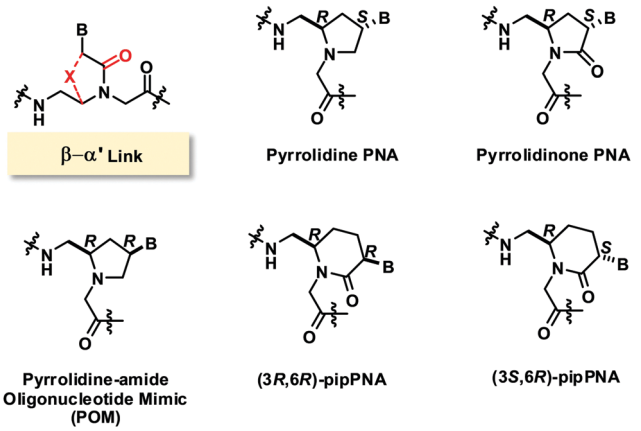

Fig. 18 Structures of modified PNA with (β–α′)-linkage.

when compared to unmodified aegPNA. However, the chimeric PNA carrying the (3*S*,5*R*) pyrrolidinone PNA monomer showed the highest preference for binding to RNA over DNA. A homoadenine sequence with the fully modified (3*S*,5*R*) pyrrolidinone PNA monomer was also synthesized, but its RNA hybrid was less stable than the corresponding aegPNA·RNA hybrid. This indicates that the conformational lock may not be in the optimal conformation to mimic the aegPNA structures in the DNA/RNA-bound forms. The six-membered ring homolog piperidinone PNA (pipPNA) was also reported.[78] The incorporation of either the (3*R*,6*R*) or (3*S*,6*R*)-pipPNA monomer into a mixed-sequence chimeric pip/aegPNA resulted in significant destabilization of DNA, RNA, and aegPNA hybrids. Furthermore, two transitions were observed in most cases suggesting that the six-membered structure is less compatible with the aegPNA duplexes.

The same group also reported a similar constrained PNA design, but with the carbonyl group reduced to the CH_2 group.[79] Only the (2*R*,4*S*) diastereomer of the pyrrolidine PNA with the same stereochemistry as the (3*S*,5*R*) pyrrolidinone PNA was reported. The single incorporation of the pyrrolidine PNA monomer in a mixed-sequence aegPNA resulted in dramatic destabilization for both DNA (ΔT_m −21 °C) and RNA hybrids (ΔT_m −15 °C) which is much more than the destabilization induced by the corresponding pyrrolidinone PNA monomer under the same circumstance (ΔT_m −8.5 °C for DNA and −5.5 °C for RNA). This indicates that the conformation of the pyrrolidine PNA may not be compatible with the aegPNA, and the presence of the protonatable nitrogen atom did not increase the binding affinity. On the other hand, the fully modified pyrrolidine PNA with a homoadenine sequence formed very stable DNA_2·PNA triplexes with DNA (ΔT_m = +23.5 °C) and RNA (ΔT_m = +25.5 °C) whereas the homoadenine pyrrolidinone PNA did not show appreciable binding to both DNA and RNA (Table 11). In addition, significant hysteresis was observed in the case of pyrrolidine PNA which suggested a slow rate of hybridization. Such discrepancy between T_m data from the chimeric and fully modified PNAs emphasizes the danger of drawing general conclusions from the chimeric sequences.

Similar pyrrolidine PNA (POM, pyrrolidine-amide oligonucleotide mimics) with the (2*R*,4*R*)-configuration that was supposed to mimic the configuration of natural nucleosides was reported by Micklefield.[80,81] From a semi-empirical quantum mechanics calculation and the X-ray crystal structure,[82] the conformation of the protonated pyrrolidine ring was proposed to be similar to that of the C3′ endo-conformation of the ribose ring in native RNA (Fig. 19). Therefore, these PNA systems were proposed to preferentially bind to RNA over DNA. However, it should be noted that the nature of the substituent on the pyrrolidine ring can affect the ring puckering significantly.[83,84] The non-chimeric homothymine POM binds to DNA and RNA with slightly less affinity than the corresponding aegPNA (Table 11). It appeared that the selectivity was due to kinetics rather than thermodynamics at least for the context.[80] Less pronounced kinetics selectivity was observed in the homoadenine and mixed-sequence POM, and in this case, they formed more stable hybrids than aegPNA.[81,85] However,

Table 11 T_m data of selected modified PNA with (β–α′)-linkage with DNA and RNA

DNA or PNA sequences (N–H/C–NH_2)[a]	Modification	T_m (°C) apDNA	pDNA	apRNA	pRNA	Ref.
AAAAAAAAAA	None (aegPNA)	56	—	35	—	79
aaaaaaaaaa-Lys	Pyrrolidinone PNA (3*S*,5*R*)	n.t.	—	26	—	79
aaaaaaaaaa-Lys	Pyrrolidine PNA (2*R*,4*S*)	79[b]	—	60[b]	—	79
TACTCATACTCT-Lys	None (aegPNA)	50	—	60	—	79
TACTCaTACTCT-Lys	Pyrrolidinone PNA (3*S*,5*R*)	41	—	54	—	79
TACTCaTACTCT-Lys	Pyrrolidine PNA (2*R*,4*S*)	28	—	44	—	79
Lys-TTTTT-Lys	aegPNA	49[c]	—	54[c]	—	85
Lys-ttttt-Lys	POM (2*R*,4*R*)	54[bc]	—	45[c]	—	85
Lys-ttttt-Lys	POM (2*R*,4*R*) (pH 6)	—	—	49[c]	—	85
Lys-ttttt-Lys	POM (2*R*,4*R*) (pH 8)	—	—	40[c]	—	85
Lys-AAAAA	None (aegPNA)	48[c]	—	31[c]	—	85
Lys-aaaaa	POM (2*R*,4*R*)	50[bc]	—	70[bc]	—	85
TCACAACTT	DNA	32	n.t.	25	n.t.	82
Lys-TCACAACTT	None (aegPNA)	35	n.t.	38	24	82
Lys-tcacaactt	POM (2*R*,4*R*)	43[b]	45[b]	46[b]	44[b]	82

[a] The modification site is denoted by a small letter. [b] Significant hysteresis was observed. T_m values were taken from the heating curves. [c] T_m with either poly(dA), poly(rA), poly(dT), or poly(rU) as the complementary strand.

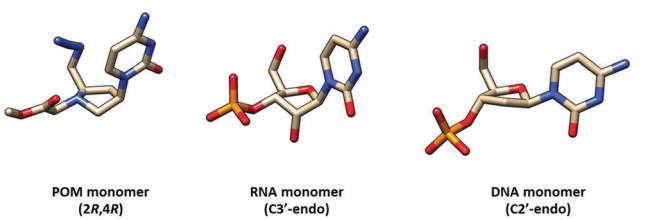

Fig. 19 Comparison of conformation of the pyrrolidine ring in the POM monomer[82] and sugar ring puckering in generic RNA and DNA structures.

© 2022 The Author(s). Published by the Royal Society of Chemistry

Open Access Article. Published on 18 Nyenyankulu 2022. Downloaded on 2026-01-28 04:18:10.
This article is licensed under a Creative Commons Attribution-NonCommercial 3.0 Unported Licence.

the rates of hybrid formation and dissociation are significantly slower than in the case of the corresponding aegPNA. The dependency of the hybrid stability and kinetics of its formation – being more stable and forming faster at lower pH – supports the role of electrostatic interaction due to the pyrrolidine ring protonation.

Modified PNA with (α–α′)-linkage

Modified PNAs with an (α–α′)-linkage were reported by several research groups under various names such as chiral PNA[86] and aepPNA[87–90] which are essentially the same systems but with different stereochemistry. In these PNA systems, the α and α′ positions were joined by a methylene bridge to form a five-membered pyrrolidine ring, and the tertiary amide C═O group linking the nucleobase to the backbone was removed. A six-membered ring homolog with a piperidine ring instead of the pyrrolidine ring was also reported.[91] In addition, a five-membered ring pyrrolidinone PNA bearing the tertiary amide C═O group was also reported under the name of aeponePNA (Fig. 20).[92]

The chiral PNA reported by Lui with a fully modified backbone with (2*S*,4*S*)-configuration showed a T_m of 46 °C for the pA_{12}-dT_{10} hybrid while the pT_{10}-dA_{10} and other mix-AT sequences showed no observable binding.[86] Other stereoisomers of aepPNA were studied by Kumar and Ganesh[87,88] and Vilaivan[89,90] and the T_m data are summarized in Table 12. Selective binding to RNA was observed in the non-chimeric aepPNA with a homothymine sequence when the stereochemistry was (2*R*,4*R*) and (2*S*,4*S*). The hybrids showed similar T_m but distinctive CD features that indicated opposite handedness. The other two stereoisomers showed no binding to both RNA and DNA. The hysteresis observed in the melting curves of the aepPNA·RNA hybrids and kinetics experiments suggested a slow association rate similar to that of pyrrolidine PNA/POM.[89,90] However, no binding was observed with both DNA and RNA targets in a mixed-sequence aepPNA with (2*R*,4*R*) stereochemistry in both parallel and antiparallel directions.

While Vilaivan and Liu did not observe DNA binding in the case of non-chimeric homothymine aepPNA, Kumar and Ganesh reported that the aepPNA homooligomer in both (2*S*,4*S*)- and (2*R*,4*S*)-configuration bound strongly to DNA with T_m values over 85 °C (Table 12).[88] They also reported a chimeric aep/aegPNA monomer with a mixed-sequence which showed varying degrees of stabilization/destabilization of the duplex

Table 12 T_m data of aepPNA and aeponePNA with RNA and DNA

PNA sequences[a]	Modification	T_m (°C) DNA	T_m (°C) RNA	Ref.
H-a_{12}-$LysNH_2$	aep-(2*S*,4*S*)	46[b]	—	86
H-t_{10}-$LysNH_2$	aep-(2*S*,4*S*)	n.t.[c]	—	86
H-tataaatt-$LysNH_2$	aep-(2*S*,4*S*)	n.t.[d]	—	86
Ac-t_{10}-$LysNH_2$	aep-(2*S*,4*S*)	n.t.[d]	42[e]	90
Ac-t_{10}-$LysNH_2$	aep-(2*R*,4*R*)	n.t.[d]	43[e]	90
Ac-t_{10}-$LysNH_2$	aep-(2*S*,4*R*)	n.t.[d]	n.t.[e]	90
Ac-t_{10}-$LysNH_2$	aep-(2*R*,4*S*)	24[d]	n.t.[e]	90
Ac-gtagatcact-$LysNH_2$	aep-(2*R*,4*R*)	n.t.	n.t.	90
H-t_8-β-AlaOH	aep-(2*R*,4*S*)	>80[f]	—	88
H-t_8-β-AlaOH	aep-(2*S*,4*S*)	>80[f]	35[e]	92
H-t_8-β-AlaOH	aepone-(2*S*,4*S*)	53[f]	46[e]	92
H-T_8-β-AlaOH	None (aegPNA)	35[f]	58[e]	92

[a] The modification site is denoted by a small letter. [b] With dT_{10}. [c] With dA_{10}. [d] With poly(dA). [e] With poly(rA). [f] With d(GCA_8CG).

that depend on the stereochemistry and type of nucleobase. The same group also reported that when the tertiary amide C═O group was present as in aeponePNA,[92] the stability of the DNA hybrid was decreased while that of the RNA hybrid was increased. However, the study was only performed on the homothymine sequence and no data for the mixed-sequence are available to allow a general conclusion to be drawn.

The reported T_m data in aepPNA from three different research groups showed some discrepancies. The comparison is complicated by the non-uniform base-pairing behavior of different aepPNA monomers. The data were interpreted, with the support from NMR and theoretical calculations, as aepPNA monomers with different nucleobases might adopt different conformations that could affect the pre-organization of the PNA (Fig. 21).[93] This principle could apply to other pyrrolidine-based PNAs as well, and thus the data derived from only homo-oligomers or chimeric systems with only one type of nucleobase modification should be interpreted with care.

The six-membered ring homolog aepipPNA was studied only for the (2*S*,5*R*)- and (2*R*,5*S*)-isomers.[91,94] Stabilization of the PNA·DNA duplexes and triplexes with some improvement in antiparallel selectivity over aegPNA was reported. However, the study was limited to chimeric aepip/aegPNA homopyrimidine sequences with terminal substitution, and thus general conclusion cannot be made.

Modified PNA with (γ–α′)-linkage

The only example of constrained PNA with (γ–α′)-linkage was linked by a methylene bridge to form a chiral piperidine ring.

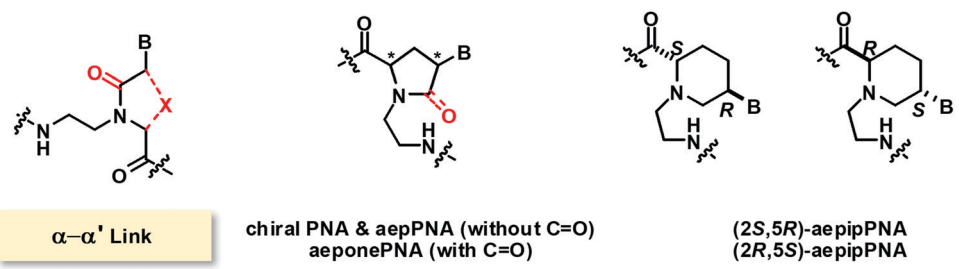

Fig. 20 Structures of modified PNA with (α–α′)-linkage.

Open Access Article. Published on 18 Nyenyankulu 2022. Downloaded on 2026-01-28 04:18:10.
This article is licensed under a Creative Commons Attribution-NonCommercial 3.0 Unported Licence.

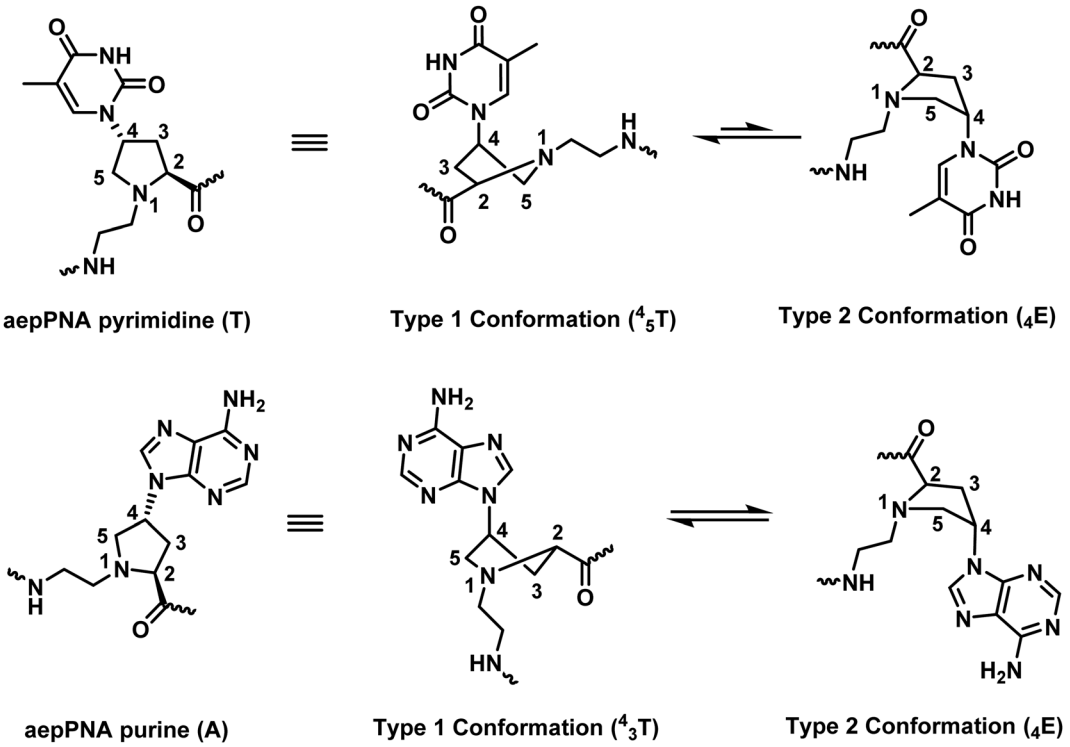

Fig. 21 The base-dependency of the conformation of the pyrrolidine ring in aepPNA (reprinted from ref. 93, Copyright (2010), with permission from Elsevier).

Two diastereomers [(3*S*,5*S*) and (3*R*,5*R*)] of the thymine monomer were synthesized (Fig. 22).[95] The molecule was designed to have the nucleobase oriented in the axial position to mimic the structure of hexitol nucleic acids. Stabilization of the PNA·DNA triplexes was reported, but again the study was limited to chimeric homothymine sequences, and thus general conclusion cannot be made.

Modified PNA with (α−β)-linkage

The only reported constrained PNA system with (α–β)-linkage consists of sulfur-containing linkages resulting in the incorporation of a thiazolidine ring[96] or a thiazane ring in the PNA structure (Fig. 23).[97] The two isomers of thiazolidine PNA [(2*S*,4*R*)-*anti* and (2*R*,4*R*)-*syn*] simultaneously obtained during the cyclization could be separated and the structures were confirmed by X-ray crystallography. The presence of the thiazolidine ring constrained the torsional angles γ and δ, and also limited β and χ^2 to the ranges that are compatible with the structures of aegPNA hybrids. However, it was found that the chimeric homothymine thiazolidine/aegPNA with a single thiazolidine monomer inserted in the middle showed a substantial decrease in the hybrid stability for both DNA and RNA when compared to unmodified aegPNA, although the specificity of base-pairing was still retained.[96] Subsequent studies on the dimethylthiazolidine (with opposite stereochemistry at Cα) and thiazane (as a racemate) constraints in the same sequence context also showed substantial destabilization of the PNA·DNA hybrids in all cases.[97]

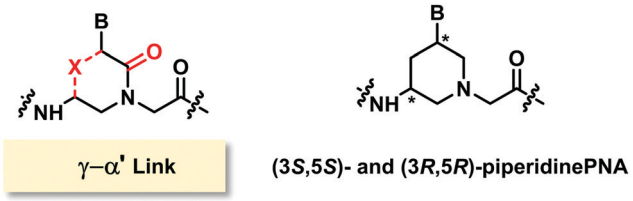

Fig. 22 Structures of modified PNA with (γ–α′)-linkage.

Modified PNA with (γ-N)- and (β-N)-linkages

Only one example of constrained PNA with (γ-N)-linkage has been reported.[98] In the *N*-(pyrrolidinyl-2-methyl)glycine PNA or pmgPNA, the presence of the pyrrolidine ring generates a new chiral center, and thus both (*S*)-pmgPNA and (*R*)-pmgPNA monomers as well as their chimeric and homooligomeric PNA have been prepared. Studies in chimeric PNA suggested that the insertion of a single pmgPNA monomer into a mixed-sequence aegPNA destabilized the PNA·DNA duplexes much more than the PNA·RNA duplexes. The (*R*)-pmgPNA monomer was less destabilizing than the (*S*)-pmgPNA monomer. Unfortunately, the fully modified mixed-sequence (*R*)-pmgPNA decamer showed no binding to both complementary DNA and RNA. The backbone-extended version of pmgPNA was also reported but the binding properties were not better than in the case of aegPNA.[99]

© 2022 The Author(s). Published by the Royal Society of Chemistry

Open Access Article. Published on 18 Nyenyankulu 2022. Downloaded on 2026-01-28 04:18:10.
This article is licensed under a Creative Commons Attribution-NonCommercial 3.0 Unported Licence.

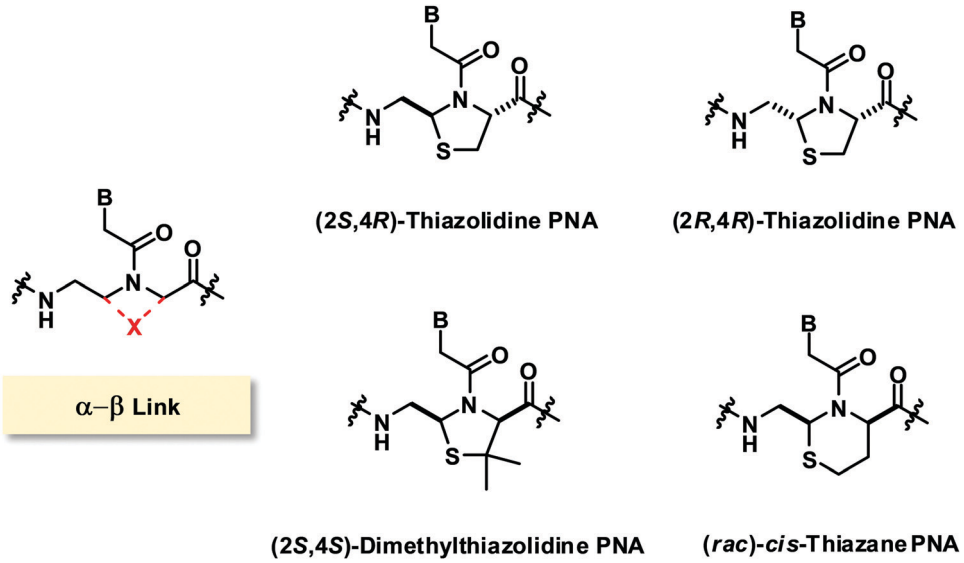

Fig. 23 Structures of modified PNA with (α–β)-linkage.

In an example of constrained PNA with (β-N)-linkage, 3-aminopyrrolidine ring was used to constrain the PNA backbone in ethano-PNA (Fig. 24).[100] The structure was designed based on the proposal that the amino substituent and the ring nitrogen should adopt the gauge conformation that would restrict the torsional angle β to 60–80° similar to the conformation of aegPNA·RNA duplexes. The use of 3-aminoproline as the starting material allowed a facile placement of various ring substituents such as aminomethyl and guanidinomethyl at the 5-position through the appropriate transformation of the carboxyl group. Incorporation of the ethano-PNA monomer into the aegPNA backbone destabilized both DNA and RNA duplexes, but the effect was smaller with RNA leading to an increase in RNA binding selectivity in a sequence-specific fashion (Table 13). The related secdapPNA with the same basic scaffold as ethano-PNA, but with an additional amino substituent showed substantial destabilization of PNA·DNA hybrids when incorporated into homothymine aegPNA, and no melting was observed in the case of the mixed-sequence.[66]

Constrained PNA designs with extended aegPNA backbones

In this section, the constrained PNA structure does not follow the generic aegPNA templates, but relates to it by backbone extension. The structures of such PNAs are included in Fig. 25.

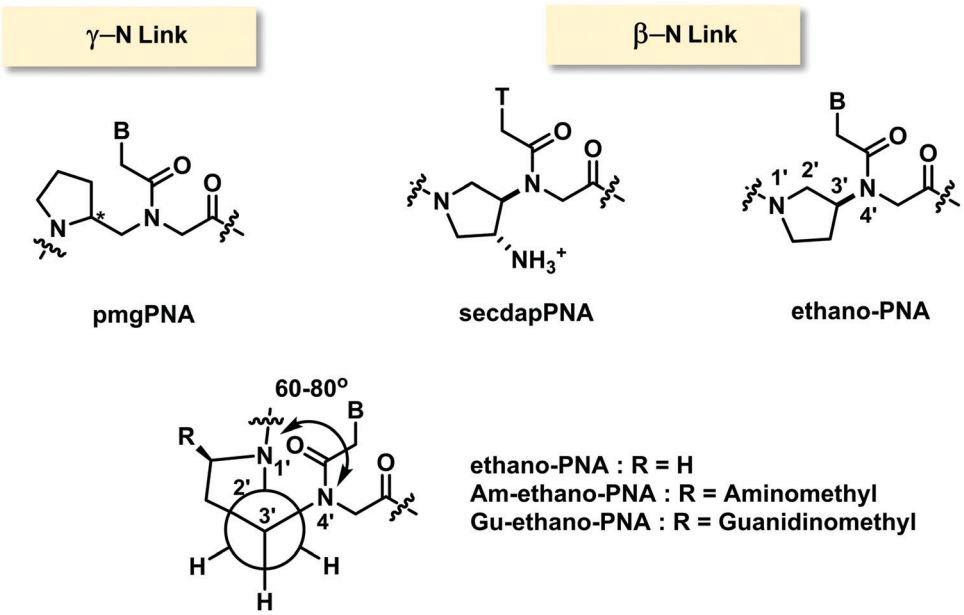

Fig. 24 Structures of modified PNA with (γ-N)- and (β-N)-linkages.

Open Access Article. Published on 18 Nyenyankulu 2022. Downloaded on 2026-01-28 04:18:10.
This article is licensed under a Creative Commons Attribution-NonCommercial 3.0 Unported Licence.

Table 13 T_m data of backbone-modified PNA with (β-N)-linkage[100]

PNA sequence[a] (N–H/C–LysNH$_2$)	Modification	T_m DNA (°C)	T_m RNA (°C)	T_m mmRNA (°C)
CATTGTCACACT	None (aegPNA)	65	66	55
CATTGtCACACT	Ethano- (R = H)	50	59	45
CATTGtCACACT	Am-ethano- (R = H_2NCH_2–)	52	60	47
CATTGtCACACT	Gu-ethano (R = guanidinomethyl–)	54	63	47

[a] The modification site is denoted by a small letter.

The backbone extended versions of POM reported by Mickelfield showed poorer binding when compared to the original POM. However, selective binding to RNA over DNA was observed when the extension was inserted in the right place, but the data were from the homothymine sequence only.[101] The same RNA selectivity was also reported by Kumar on the bepPNA system which is essentially the same as bePOM II but with opposite stereochemistry.[102] The six-membered ring constrained aminopipecolyl PNAs with the (2*S*,4*S*)-substitution and (2*S*,5*R*)-substitution patterns have been reported to show some stereochemistry- and sequence-dependent binding behavior. The chimeric aminopipecolyl/aegPNA with (2*S*,4*S*)-stereoisomer decreased the stability of the PNA$_2$·DNA triplex but increased the stability of the PNA·DNA duplex and the opposite is true for the (2*S*,5*R*)-stereoisomer.[103,104] Although technically the (2*S*,5*R*)-aminopipecolyl PNA should be regarded as an (α–γ)-linked system, it is more convenient to compare it with the (2*S*,4*R*)-aminopipecolyl PNA here.

Tsantrizos *et al.* reported another modified PNA with an aromatic ring incorporated in the extended backbone of aegPNA. This is perhaps the only constrained PNA with an achiral backbone. Incorporation of one aromatic PNA (APNA) monomer into the aegPNA backbone resulted in a small decrease in T_m for both DNA and RNA for both homothymine[105] and mixed-sequence.[106] However, the stability was not decreased further upon the incorporation of more APNA monomers up to 4 consecutive residues. Attempts to prepare the fully modified APNA failed due to insolubility. Replacement of the benzene ring with a more hydrophilic pyridine ring also resulted in further destabilization (Table 14).[107]

Alternative PNA designs that do not follow the generic aegPNA template

There are relatively few PNA systems that do not fit the aegPNA template that still show decent DNA/RNA binding (Fig. 26). In 1999, Sisido proposed a new PNA system called oxy-peptide nucleic acid or OPNA.[108,109] The glycine nitrogen atom in the aegPNA backbone was replaced by an oxygen atom in the OPNA and the nucleobase was attached to the Cγ *via* an ethylene linker. The system with the (*S*)-configuration derived from L-homoserine showed stronger binding than the (*R*)-configuration.[110] OPNA hybridizes with DNA to form duplexes with lower stability than the corresponding aegPNA·DNA

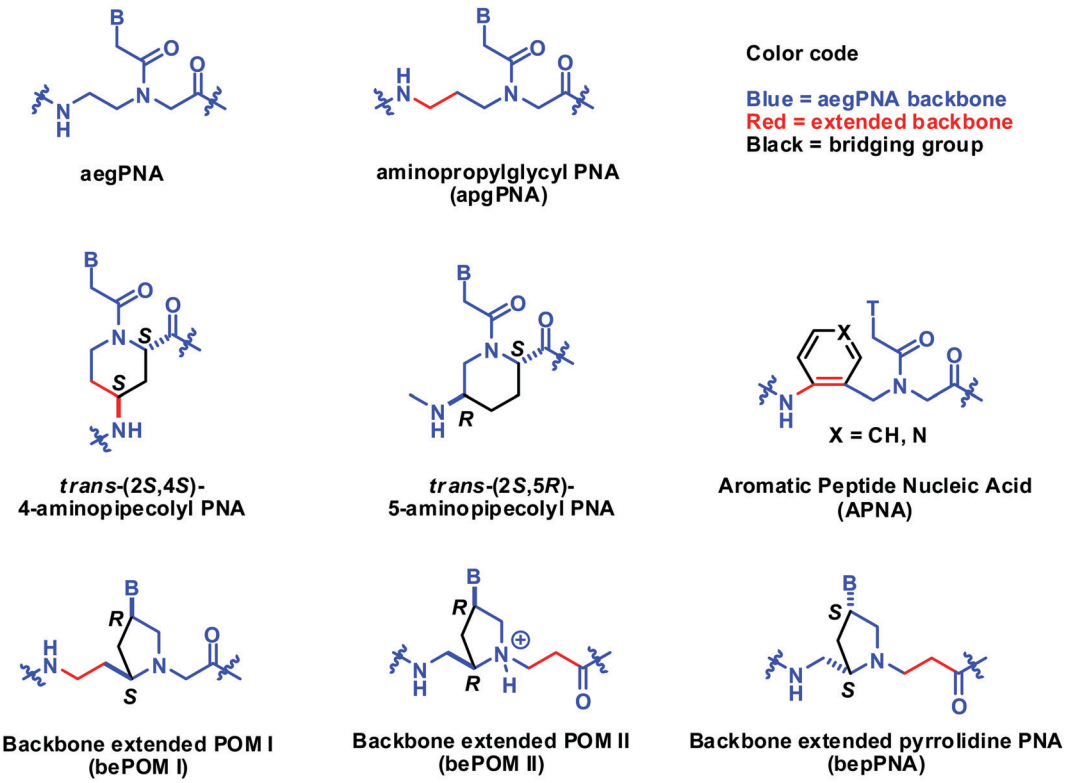

Fig. 25 Structures of constrained aegPNA with extended backbones.

© 2022 The Author(s). Published by the Royal Society of Chemistry

Open Access Article. Published on 18 Nyenyankulu 2022. Downloaded on 2026-01-28 04:18:10.
This article is licensed under a Creative Commons Attribution-NonCommercial 3.0 Unported Licence.

Table 14 T_m data of DNA and RNA hybrids of the constrained PNA with an extended backbone

Sequence[a] (N–H/C–NH_2)	System	T_m (°C) apDNA	pDNA[b]	apRNA[b]	pRNA[b]	Ref.
TTTTTTTT-Lys	aegPNA	52	—	66	—	102
Lys-tttttttt	POM (2*R*,4*R*)	53[b]	—	52[b]	—	101
Lys-tttttttt	bePOM I	n.t.	—	n.t.	—	101
Lys-tttttttt	bePOM II	n.t	—	44[b]	—	101
tttttttt-Lys	bepPNA	n.t.	—	59	—	102
GTAGATCACT-Lys	aegPNA	55	—	55	—	102
GtAGAtCACt-Lys	bepPNA	n.t.	—	81	—	102
TTTTTT-Lys	aegPNA	64	—	56	—	105
TTTtTT-Lys	APNA (X = CH)	44	—	50	—	105
TTTtTT-Lys	APNA (X = N)	39	—	47	—	107
TTTcTT-Lys	APNA (X = CH)	<5	—	17	—	105
GTAGATCACT-Lys	APNA (X = CH)	54	39	58	42	106
GTAGAtCACT-Lys	APNA (X = CH)	40	34	48	31	106
gtagATCACT-Lys	APNA (X = CH)	43	28	45	28	106

[a] The modification site is denoted by a small letter. [b] Significant hysteresis was observed.

duplex but showing a remarkably sharp melting transition. However, the system was quite flexible, and a read-through can happen, resulting in lowering of the specificity. A marginal preference for DNA over RNA and parallel selectivity were reported under a limited sequence context. The analysis of thermodynamic parameters indicated that the OPNA system showed a large entropy loss as expected from its rather flexible structure.[108] This entropy term decreases when the backbone of the OPNA was constrained by the incorporation of a pyrrolidine ring as in POPNA, at the expense of the decreased enthalpy term. Overall, the effect of the backbone constraint in terms of

Table 15 T_m data (°C) of DNA and RNA hybrids of the OPNA family with a homoadenine sequence and the corresponding data for DNA and aegPNA

System (A_9)	dT_9	dT_4CT_4	dT_4AT_4	dT_4GT_4	rU_9	Ref.
DNA	15	—	—	—	—	110
aegPNA	50	—	—	—	—	109
OPNA (*S*)	35	17	17	15	9	109 and 110
OPNA (*R*)	23	13	9	9	11	110
POPNA (*cis*-L)	34	19	13	15	12	110 and 111
POPNA (*cis*-D)	30	16	28	13	14	110 and 111
POPNA (*trans*-L)	23	20	20	21	22	110 and 111
POPNA (*trans*-D)	30	17	16	17	19	110 and 111

increasing binding affinity and specificity was relatively small.[110,111] Partial replacement of the backbone oxygen atom in OPNA by a protonatable N-Me group (PAPNA) did not affect the stability of the PNA·DNA duplex while improving the cell permeability.[112] The T_m data for the OPNA family are summarized in Table 15.

Kumar has reported yet another interesting PNA design derived from an alternating sequence of nucleoside β-amino acids and α-amino acid.[113,114] The nucleoside β-amino acids were obtained from the corresponding deoxyribosides. The homo-oligomer of a similar nucleoside β-amino acid derived from AZT has been independently shown to form well-defined folded helical structures but no DNA/RNA binding studies have been reported.[115] Various α-amino acids have been introduced as a spacer including glycine, proline, sarcosine, lysine, and methionine. Strong binding to both DNA and RNA with a preference for RNA over DNA binding was observed in a preliminary study with the homothymine PNA sequence for all α-amino acid spacers studied.[113] Subsequent report with

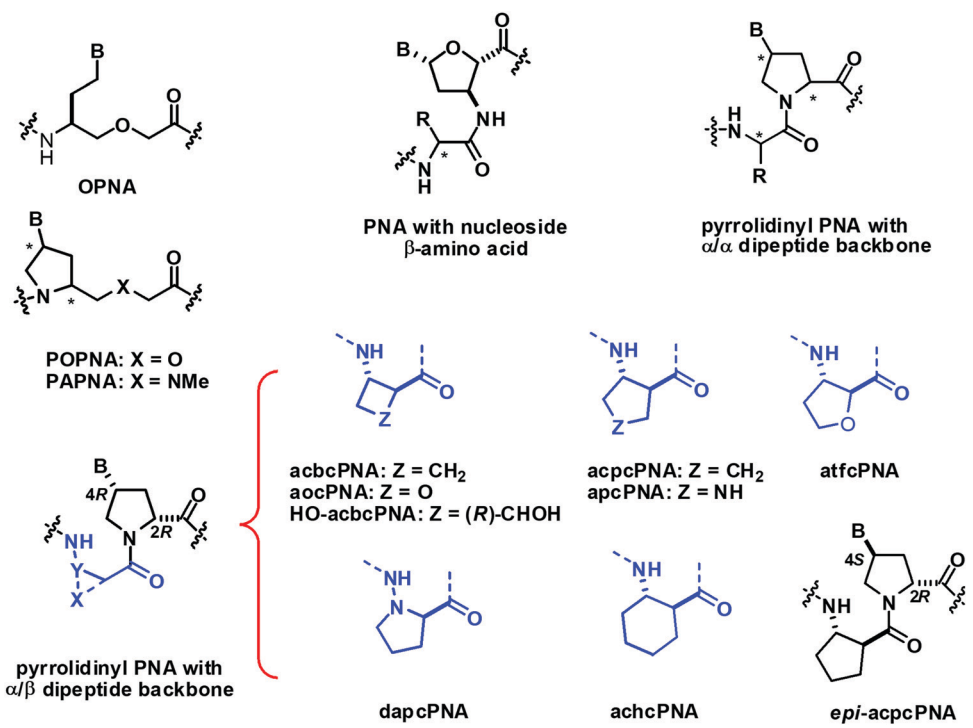

Fig. 26 Structures of conformationally constrained PNA that does not follow the generic aegPNA template.

Open Access Article. Published on 18 Nyenyankulu 2022. Downloaded on 2026-01-28 04:18:10.
This article is licensed under a Creative Commons Attribution-NonCommercial 3.0 Unported Licence.

Table 16 T_m data (°C) of the DNA and RNA hybrids of PNA with nucleoside β-amino acid and glycine as the spacer[114]

Sequence/system	apDNA	pDNA[a]	mmDNA	apRNA	pRNA[a]	mmRNA
CTTCTTCCTT						
DNA[b]	28	n.t.	19	36	n.t.	29
aegPNA	47	33	37	51	38	41
PNA[c]	40	n.t.	31	48	n.t.	38
CACTGATTTCAA						
DNA[b]	36	n.t.	29	45	n.t.	33
aegPNA	54	40	46	61	49	49
PNA[c]	45	n.t.	38	54	n.t.	43

[a] n.t. = no transition. [b] T_m of DNA was measured in the presence of 100 mM NaCl. [c] PNA with nucleoside β-amino acids and glycine linker.

Table 17 T_m data (°C) of the DNA and RNA hybrids of pyrrolidinyl PNA with α/β-dipeptide backbones

System[a]	apDNA	pDNA	mmDNA	apRNA	pRNA	mmRNA	Ref.
aegPNA[b]	43	32	33–36	47	31	29–37	53
acpcPNA	53	<20	24–29	42	<20	<20–24	125 and 132
epi-acpcPNA	51	<20	27–28	41	<20	—	130
atfcPNA	53	<20	23–25	36	<20	<20	132
aocPNA[c]	46	—	<20–28	30	—	—	136
acbcPNA	66	<20	36–47	58	32	—	137
achcPNA	n.t.	<20	<20	<20	<20	—	137

[a] Sequences: PNA: Ac-GTAGATCACT-LysNH$_2$; apDNA: dAGTGXTCTAC; pDNA: dCATCTAGATG; apRNA: rAGUGXUCUAC; pRNA: dCAUCUA GAUG. [b] Without C-terminal Lys. [c] Without the N-terminal Ac group.

mixed-sequence PNA with glycine spacer also confirmed the generality of this preference and allowed the determination of the directional selectivity as exclusively antiparallel.[114] Nevertheless, the stability difference between RNA and DNA was only marginally better than in the case of aegPNA (Table 16). In addition, the thermal stability was generally lower than that of the corresponding aegPNA duplexes with a similar level of mismatch discrimination. A single-stranded PNA dimer with a D-proline spacer showed a more pronounced CD signal than the same dimer with L-proline and glycine, which is indicative of stronger pre-organization due to the matching stereochemistry of the nucleoside β-amino acid and the spacer.[116]

Vilaivan *et al.* introduced an alternative design of conformationally constrained PNA featuring a dipeptide backbone derived from nucleobase-modified proline and an amino acid spacer.[117] The first generation of these pyrrolidinyl PNAs carried α-amino acid spacers including glycine and L-serine. They bound weakly to DNA in a stereochemically dependent fashion[118] Inspired by the ability of short oligomers of β-amino acids to form well-defined secondary structures,[119] the second generation pyrrolidinyl PNA was designed to incorporate a β-amino acid spacer instead of α-amino acid. The very first member of the second generation pyrrolidinyl PNAs that show strong DNA binding properties consists of thymine-modified proline in the (2*R*,4*R*) configuration and a cyclic hydrazino acid D-aminopyrrolidine carboxylic acid (DAPC) as the spacer.[120] This dapcPNA system also showed a strong preference for binding to DNA over RNA, at least in the polyT/U-polyA sequence context.[121] The same PNA sequence bearing acyclic spacers including β-alanine and *N*-amino-*N*-methylglycine,[122] as well as cyclic spacers with different stereochemistry including L-aminopyrrolidine carboxylic acid and (1*R*,2*S*)-2-aminocyclopentanecarboxylic acid,[120] failed to form stable hybrids with the complementary DNA target. This clearly indicated the crucial role of the spacer in determining the DNA binding ability of the pyrrolidinyl PNA. Subsequent studies on diastereomeric PNAs with a homogeneous backbone derived from (2*R*,4*R*)-thymine-modified proline and all possible stereoisomers of 2-aminocyclopentanecarboxylic acid (ACPC) spacers (1*R*,2*R*; 1*S*,2*S*; 1*R*,2*S*; and 1*S*,2*R*) led to the identification of acpcPNA with (2*R*,4*R*)-proline/(1*S*,2*S*)-ACPC backbone that showed exceptionally strong DNA binding ability and very high sequence specificity (Table 17).[123,124] Other unique features of acpcPNA include the exclusive antiparallel selectivity, the preference for binding to DNA over RNA, and the inability to form PNA·PNA self-duplexes.[124,125] Although experimental three-dimensional structures of acpcPNA and related pyrrolidinyl PNAs are not yet available, the structural bases of their unusual behaviors have been studied in detail by MD simulations.[126–129] When the stereochemistry of the ACPC spacer was fixed as (1*S*,2*S*) and the stereochemistry at the proline part was varied (2*R*,4*R*; 2*S*,4*S*; 2*R*,4*S*; and 2*S*,4*R*), only the acpcPNA stereoisomers with 2*R* configuration could bind to DNA whereby the configuration of the nucleobase can be either 4*R* or 4*S*. This led to the discovery of *epi*-acpcPNA with (2*R*,4*S*)-proline/(1*S*,2*S*)-ACPC backbone which exhibits very strong DNA binding affinity and specificity comparable to that of acpcPNA.[125,130] Heteroatoms such as N[131] and O[132] can be incorporated in the five-membered ring of the ACPC spacer in acpcPNA to improve water solubility without significantly interfering with the DNA binding ability. The nitrogen atom can be used as a convenient handle for subsequent modification to create functional PNA probes[133,134] or cell-permeable PNA.[135]

The effect of ring size of the cyclic β-amino acid in the (1*S*,2*S*)-configuration was explored in a series of pyrrolidinyl PNAs with (2*R*,4*R*)-proline stereochemistry (Fig. 27). This led to the discovery of acbcPNA with a four-membered cyclic β-amino acid spacer that exhibits even stronger DNA binding affinity than acpcPNA. On the other hand, the achcPNA with a six-membered cyclic β-amino acid spacer failed to bind to DNA/RNA. The difference in the DNA binding ability was explained in terms of the degree of similarity of the torsional angles N(H)-Cα-Cβ-C(O) of the cyclic β-amino acid oligomers from the literature (ACHC,[138] ACPC,[139] ACBC[140]) and of the PNA·DNA duplexes obtained from MD simulation – the closer the values the more stable the duplexes.[137] Attempts to increase the hydrophilicity of acbcPNA by incorporating an oxygen atom into the ring[136] or as a side chain in the form of a hydroxyl group[141] resulted in suboptimal DNA binding.

With regard to the backbone-modified PNA, it is worth mentioning the XNA systems developed by Asanuma *et al.*, namely serinol nucleic acid (SNA)[142] and acyclic threoninol

© 2022 The Author(s). Published by the Royal Society of Chemistry

Open Access Article. Published on 18 Nyenyankulu 2022. Downloaded on 2026-01-28 04:18:10.
This article is licensed under a Creative Commons Attribution-NonCommercial 3.0 Unported Licence.

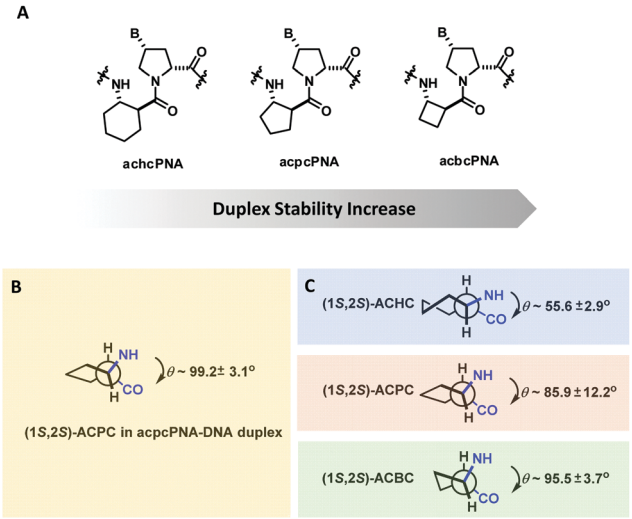

Fig. 27 (A) Structures of pyrrolidinyl PNA homologs. (B) Torsional angle N(H)–Cα–Cβ–C(O) of (1*S*,2*S*)-ACPC in ACPC PNA. C) Native torsional angles of cyclic β-amino acid oligomers are obtained from the literature (adapted with permission from ref. 137. Copyright 2012 American Chemical Society).

nucleic acid (aTNA)[143] (Fig. 28). Their backbones consist of phosphodiester-linked 2-amino-1,3-propanediols, and the nucleobases are attached to the backbone *via* the amide bond similar to the case of PNA. Despite the relatively flexible backbone, SNA and aTNA can form antiparallel self-pairing duplexes with comparable or even higher stability than that of PNA·PNA self-duplexes.[144] On the other hand, the SNA and aTNA duplexes with DNA/RNA are less stable than the corresponding PNA·DNA or PNA·RNA duplexes. The stereochemistry of the methyl group in aTNA showed pronounced effects on the hybrid stability, with L-aTNA forming more stable hybrids with both DNA and RNA than D-aTNA. Interestingly, the pseudosymmetric SNA paired to DNA only in the antiparallel direction and the L-aTNA must adopt parallel orientation to pair in the same way which was indeed observed experimentally.[145] Although the CD signal of single-stranded aTNA is weak, the self-duplex of L-aTNA is right-handed, suggesting the crucial role of the chiral methyl group in inducing the helicity by selectively stabilizing/destabilizing the helices. Overall, this suggests that the backbone rigidity is not a prerequisite for duplex formation but rather the delicate balance between flexibility and rigidity that should be taken into account for the design of new PNA systems.

Table 18 Summary of helical parameters of selected PNA hybrids

System	Method	Disp (Å)	Rise (Å)	Tilt (°)	Twist (°)	bp per turn	Ref.
PNA·PNA (1PUP)	X-ray	8.3	3.2	1.0	19.8	18	146
PNA·PNA[a] (2K4G)	NMR	7.9	3.7	−0.2	−17.3	21	32
γPNA·γPNA (2KVJ)	NMR	−9.0	2.9	2.1	16.3	22	43
PNA_2·DNA (1PNN)	X-ray	6.8	3.4	5.1	22.9	16	24
PNA·DNA (1PDT)	NMR	−2.9	3.5	−1.3	27.5	13	25 and 71
αPNA·DNA (1NR8)	X-ray	−3.8	3.5	0.2	23.2	16	23
γPNA·DNA[b] (3PA0)	X-ray	−5.5	3.2	0.3	23.9	16	44
		−6.3	2.9	2.3	23.3	16	
cpPNA·DNA (7KZL)	X-ray	−3.4	3.4	0.4	27.1	13	71
PNA·RNA (5EME/5EMF)	X-ray	−6	2.4	—	26	14	147
ADNA		−4.5	2.6	−4.5	32.7	11	44
BDNA		0	3.4	−0.1	36.0	10	44

[a] Left-handed helix. [b] Values for two different duplexes in the same asymmetric unit.

Structural aspects of the design of conformationally constrained PNA

In order to minimize the entropy loss as a result of conformational re-organization upon duplex (or higher-order structures) formation, the structure of the single-stranded PNA should closely mimic the DNA/RNA-target bound conformation. The information from three-dimensional structures of PNA·DNA, PNA·RNA, and PNA·PNA hybrids will be useful for the design of new PNA systems that can not only bind strongly but can also exhibit selectivity among different types of nucleic acid targets. The key helix parameters and torsional angle data are summarized in Tables 18 and 19, respectively. The three-dimensional structures of standard DNA and RNA duplexes as well as those of selected unmodified and modified aegPNA duplexes are shown in Fig. 29–31.

X-Ray structures of native aegPNA duplexes suggested that the PNA itself exhibits an inherent propensity to form helical structures. Since the aegPNA molecule is achiral, both right-handed and left-handed are observed in equal amounts. The PNA·PNA duplex showed distinct structural features from conventional A- or B-type DNA helices. It is characterized by a more open and elongated helix (18–21 bp per turn) with a narrow and shallow minor groove and a wide, deep major groove which was described as a novel "P" type helix.[146] The base pairs are more or less perpendicular to the helix axis. NMR structures of other PNA·PNA duplexes revealed the same general helix feature at the global level.[32,43] In the case of γPNA·γPNA, the base pair rise

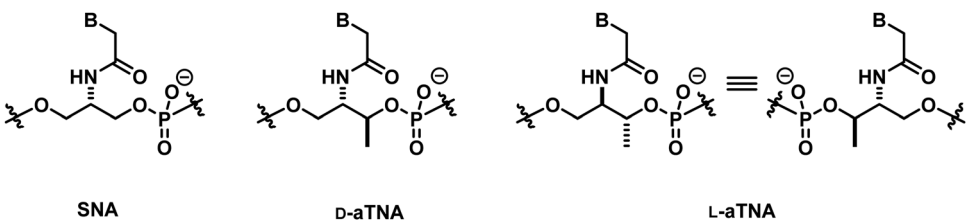

Fig. 28 Structures of SNA, D-aTNA and L-aTNA.

Open Access Article. Published on 18 Nyenyankulu 2022. Downloaded on 2026-01-28 04:18:10.
This article is licensed under a Creative Commons Attribution-NonCommercial 3.0 Unported Licence.

Table 19 Summary of torsional angle values of the PNA monomer in selected PNA hybrids[a]

System	Method	α	β	γ	δ	ε	χ_1	χ_2	χ_3	ω	Ref.
PNA·PNA (1PUP)	X-ray	−120(6) 83(11)	66(5)	74(9)	91(11)	174(11) −19(3)	6(6)	−175(4)	83(3)	−170(14)	146
PNA·PNA (2K4G)	NMR	−93(24) 123(16)	−66(5)	−75(4)	−88(10)	−155(17) −3(12)	2(4)	169(10)	−82(8)	175(10)	32
γPNA·γPNA (2KVJ)	NMR	−110 to −130	60	75	90	175/−175	10 to −10	175/−175	90 to 110		43
PNA_2·DNA[b] (1PNN)	X-ray	−103(W) −108(H)	73(W) 69(H)	70(W) 69(H)	93(W) 87(H)	165(W) 175(H)	1(W) 1(H)	−170(W) −175(H)	89(W) 102(H)	−178(W) −178(H)	24
PNA·DNA (1PDT)	NMR	105(55)	−141(13)	78(16)	139(13)	35(42)	−3(3)	151(9)	−103(19)		25
αPNA·DNA (1NR8)	X-ray	−114(15) 72(7)	73(9)	67(4)	90(5)	179(10)	4(6)	−178(3)	−91(6)	−178(2)	23
γPNA·DNA[c] (3PA0)	X-ray	−106(14) −100(13)	70(12) 68(10)	60(6) 59(9)	117(20) 123(27)	−150(7) −110(24)	12(11) 13(9)	−177(6) −174(9)	87(10) 82(6)	−116(32) −155(16)	44 44
cpPNA·DNA (7KZL)	X-ray	−123(15)	86(8)	67(4)	109(7)	175(10)	0(3)	−179(3)	89(6)	−170(4)	71
PNA·RNA (176D)	NMR	150 to 172	67 to 72	79 to 86	72 to 85	64 to 105	3 to 9	−146 to −171	58 to 84		63
PNA·RNA (5EME)	X-ray	114(7) 79(3)	71(9)	70(8)	96(5)	−6 (9) 162(7)	4(4)	−172(6)	83(8)		147
PNA·RNA (5EMF)	X-ray	112(8) 76(2)	66(7)	73(7)	94(6)	−6(10) 159(8)	6(6)	−174(4)	81(5)		147

[a] Average values for all residues with SD in parentheses. Terminal residues were excluded. [b] W: The PNA strand that forms the Watson–Crick base-pairing strand; H: the PNA strand that forms Hoogsteen base-pairing. [c] Values for two different duplexes in the same asymmetric unit.

was smaller, resulting in a helix that resembles the A-type helix more,[43] but with the elongated character of the P-type helix (22 bp per turn). The γ-substituent was shown to align along the edge of the groove and it did not interfere with the duplex formation.

Three-dimensional structures of PNA·DNA[25] and PNA·RNA duplexes[63] have been studied by NMR since early dates. The first X-ray structure of the PNA·DNA duplex was published in 2003[23] and those of PNA·RNA duplexes were not available until 2016.[147] The helical parameters of PNA·DNA duplexes obtained from both NMR (1PDT)[25] and X-ray (1NR8)[23] studies are grossly similar and reveal distinctive features that are different from both typical DNA·DNA helices and P-type PNA·PNA helices. This suggests that both partners (PNA and DNA) are adjusting themselves to a mutually compromised structure that is an intermediate between the two. The displacement in PNA·DNA duplexes was in the range of −2.9 to −3.8 Å which is smaller than that of the corresponding PNA·PNA duplexes (8 Å). The number of base pairs per turn was in the range of 13–16 which was larger than that of typical DNA·DNA duplexes (10) but smaller than that of PNA·PNA duplexes (18). At the individual PNA monomer level, the X-ray and NMR structures showed considerable discrepancy especially in the torsional angle value β N(H)–Cγ–Cβ–N(CO). The NMR structure[25] reported a much larger β value of 141° (almost corresponded to the extended antiperiplanar conformation, with respect to the two backbone nitrogen atoms) compared to the β value of 73° (gauche conformation, with respect to the two backbone nitrogen atoms) in the X-ray structure.[23] The discrepancy could in part be attributed to the difference in the PNA structures (purely aegPNA in the NMR and chimeric aeg/D-Lys αPNA in the X-ray structures). However, it should be noted that the values are quite uniform (59–83°) in the latter regardless of the type of PNA monomer (aeg/α) within the X-ray structure. Due to the somewhat limited availability of three-dimensional structures of native PNA·DNA duplex in the literature, it is not clear about the origin of such discrepancy and more structural information would be helpful in guiding the designing of new PNA systems. Nevertheless, experimental results available so far indicate that the system that permanently locks the β value in the range of 70°–83° resulted in substantial stabilization of the PNA·DNA duplexes (see below). On the other hand, the duplex stability data for the system that has the β value in the larger range which corresponded to the more extended conformation are not yet available. The cyclopropyl PNA system with a native β value of 145° is the closest candidate but only T_m data of the PNA_2·DNA triplex were available, which failed to show the expected stabilization.[72]

The β value of 73° from the X-ray structure of the αPNA·DNA duplex[23] was also in good agreement with the values obtained from other PNA structures including PNA_2·DNA triplex (73°), γPNA·DNA duplex (68°), and cpPNA·DNA duplex (86°) (Table 19). Somewhat smaller torsional angle β values were found in the corresponding PNA duplexes including PNA·PNA duplex (66°) and γPNA·γPNA duplex (60°) but they were still in a similar range. Accordingly, the conformation constraint at the β and γ positions should be designed so that the β values are fixed in such range as long as the substituent does not sterically or electrostatically interfere with the binding. The remarkable stabilization of PNA·DNA duplexes derived from γPNA[42] and cpPNA[71] emphasizes the importance of this point. In both cases, the backbone substituents were located near the rim of the groove and pointed to the solvent, and thus their role was to guide the PNA to fold into the right conformation rather than providing additional stabilization. The values of the torsional angle χ_1 are close to 0° in all PNA·DNA and PNA·PNA duplexes indicating the preferred *Z*-rotamers of the amide bond connecting the nucleobase to the PNA backbone, resulting in the side-chain C=O being pointed in the C-terminus direction and interacting with the backbone C=O by the n → π* interaction. Thus, any conformation constraint should observe this requirement, and an example in the case of α-*gem*-dimethyl PNA[27,28]

© 2022 The Author(s). Published by the Royal Society of Chemistry

Open Access Article. Published on 18 Nyenyankulu 2022. Downloaded on 2026-01-28 04:18:10.
This article is licensed under a Creative Commons Attribution-NonCommercial 3.0 Unported Licence.

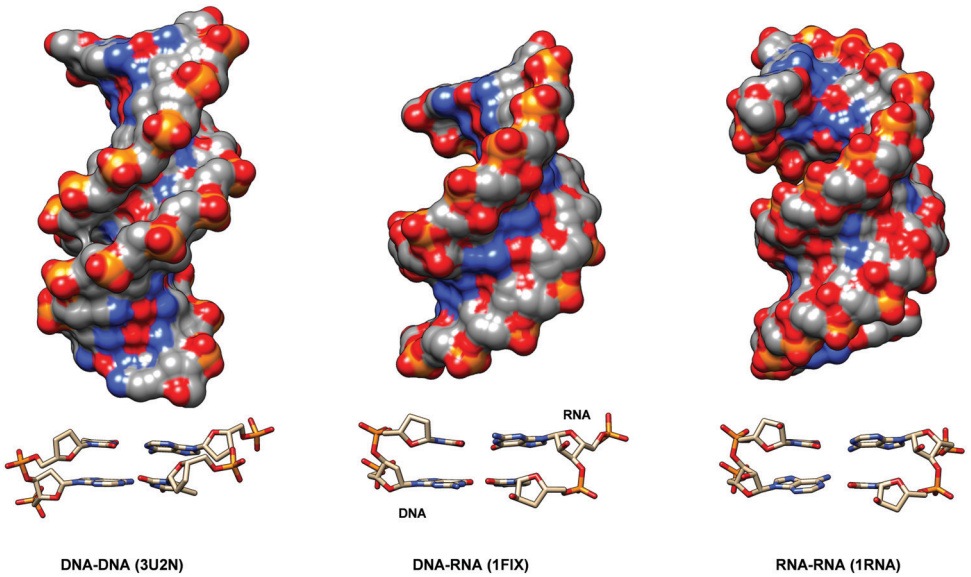

Fig. 29 Three-dimensional structures of standard DNA·DNA,[151] DNA·RNA[152] and RNA·RNA[153] duplexes, with details of the monomer conformation and base-pairing.

has illustrated the point very well. On the other hand, locking χ_1 by replacement of the tertiary amide bond with an alkene resulted in substantial destabilization regardless of the configuration of the double bond.[148] Attempts to incorporate a fluorine atom to mimic the amide carbonyl group also failed to improve the binding.[149,150] This indicates the indispensable role of the amide group in addition to the appropriate χ_1 value. The torsional angle values χ_2 are generally close to 180° to avoid clashing with the PNA backbone. The torsional angle values ω are always fixed at more or less 180° due to the *trans*-amide backbone. Other torsional angle values are also quite conserved among different structures of PNA·DNA duplexes as well as PNA·PNA duplexes as can be clearly seen in Fig. 29–31. These torsional angles could be potential points for introducing constraint in the PNA structures in addition to β and χ_1 that have already been extensively utilized. Overall, the experimental structural data indicate that the PNA requires little conformational adjustment to adopt the proper DNA-binding conformation, and the conformational constraint can help reduce the entropic penalty upon the conformational change further. However, it should be noted that it is difficult to modify just one torsional angle without affecting others, and unless an aromatic ring or a rigid bicyclic molecule was employed, the conformation lock will allow a certain degree of flexibility. In fact, such flexibility should be desirable, as in the case of the cpPNA bearing the *trans*-(*S*,*S*)-cyclopentyl PNA that formed much more stable duplexes with DNA when compared to its homolog *trans*-(*S*,*S*)-cyclohexyl PNA. This could be explained by the rigidity of the cyclohexane ring that probably locked the PNA molecule into the wrong conformation that could not be easily adjusted to accommodate the requirement for duplex formation.[58]

In most PNA·DNA structures, the sugar ring DNA can exist in both C3′-*endo* conformation, as found in A-DNA duplexes, and C2′-*endo* conformation, as found in conventional B-DNA duplexes. The two conformations can co-exist in the same structure. In the PNA·RNA structures,[63,147] the sugar ring always adopted the C3′-*endo* conformation as expected for RNA duplexes. The same is true for the sugar ring of DNA in the DNA·RNA hybrids. Early NMR structures of a PNA·DNA duplex[25] and a PNA·RNA duplex[63] might suggest two distinctive values of the torsional angle β (141 *vs* 73°) which could provide a potential basis for the design of a PNA that can differentiate between DNA and RNA. However, as mentioned earlier, subsequent studies indicated that the PNA monomers in several PNA·DNA duplexes[23,44] could also adopt torsional angles β that are more similar to those in the PNA·RNA duplexes. In view of conformational similarity of PNA in PNA·DNA and PNA·RNA duplexes, the rational design of PNA systems that can bind selectively to either RNA or DNA may not be as straightforward as designing a PNA that can bind strongly to both. In the case of γPNA, the PNA·DNA duplex was more substantially stabilized than the corresponding PNA·RNA duplex upon the introduction of the constraint. It has been suggested that the differential stabilization was the result of the less conformational flexibility of RNA to adjust itself to bind to the rigid PNA scaffold than DNA.[45] Promising DNA/RNA selectivity has been achieved in some PNA systems based on trial and error. However, mostly the data are not yet sufficient to allow a general conclusion, and the structural information is still limited. Such information will be highly valuable in guiding the design of new PNA systems with enhanced DNA binding properties.

Comparison of modified PNA·DNA and PNA·RNA hybrids' stability and specificity

For those who are interested in finding potential applications of new PNA systems, the key question is perhaps how much better they are when compared to the standard aegPNA and

Open Access Article. Published on 18 Nyenyankulu 2022. Downloaded on 2026-01-28 04:18:10.
This article is licensed under a Creative Commons Attribution-NonCommercial 3.0 Unported Licence.

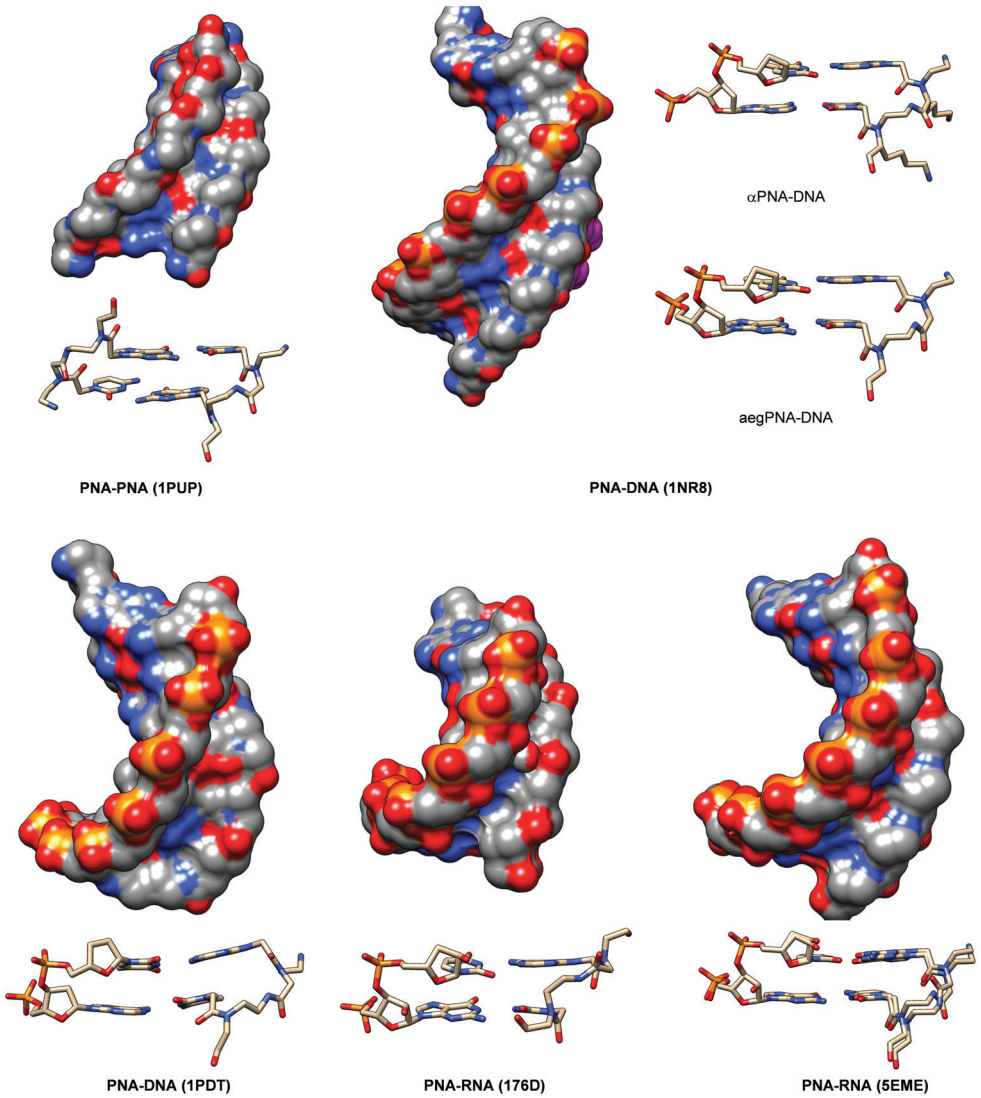

Fig. 30 Three-dimensional structures of PNA·PNA,[23,146] PNA·DNA[25] and PNA·RNA[63,147] duplexes, with details of the monomer conformation and base-pairing.

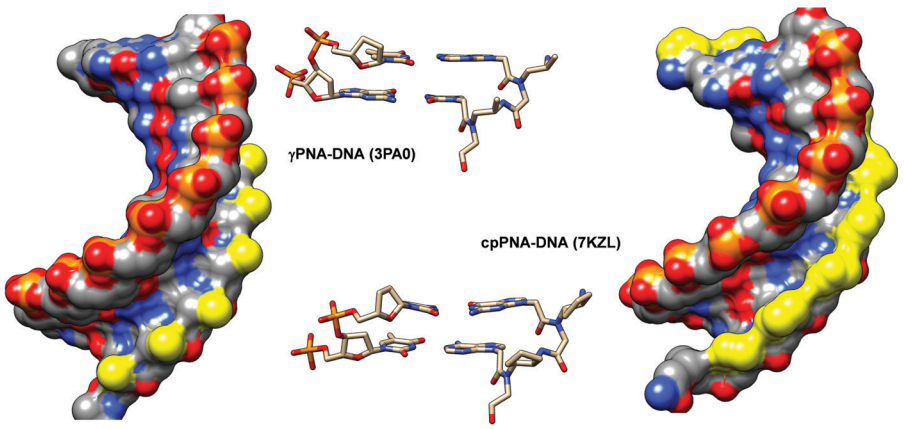

Fig. 31 Three-dimensional structures of γPNA·PNA[44] and cpPNA·DNA[71] duplexes, with details of the monomer conformation and base-pairing. The backbone substituents are highlighted in yellow.

© 2022 The Author(s). Published by the Royal Society of Chemistry

Open Access Article. Published on 18 Nyenyankulu 2022. Downloaded on 2026-01-28 04:18:10.
This article is licensed under a Creative Commons Attribution-NonCommercial 3.0 Unported Licence.

when compared among each other in terms of binding affinity and specificity. While a large data set for T_m values between PNA·DNA and PNA·RNA hybrids are available in the literature, a direct comparison among different types of PNA is not straightforward for many reasons. First, T_m values are sensitive to several parameters including the length, base sequence, salt concentration, buffer, and concentration of the PNA. Second, while PNA molecules are considered electrostatically neutral, they still carry the positively charged amino group at the *N*-terminus. Furthermore, PNA is often modified by end-capping or incorporation of one or more hydrophilic amino acid residues (typically lysine) to improve water solubility. These charged modifiers could affect the nucleic acid binding *via* the electrostatic interaction.[154] Third, the data for many modified PNA systems are available only for the homothymine sequences or chimeric mixed-sequence that carries up to a few modified monomers – typically T – along the standard aegPNA backbone. While in some instances the stabilization/destabilization effects observed in the chimeric PNA translated well to the fully modified PNA,[65,71] it is difficult to draw a general conclusion from a limited set of such data. Thus, only the T_m data that are available for fully modified, non-chimeric PNA with "average" mix base sequence with good distribution between purine and pyrimidine bases will be compared in this section (Fig. 32).

The aegPNA duplexes in Fig. 32 showed T_m values in the range of 42–44 °C for PNA·DNA hybrids and 54 °C for PNA·RNA hybrids.[53] The T_m values were decreased by 10–14 °C and 11–18 °C for the mismatched PNA·DNA and PNA·RNA hybrids, respectively. The DNA hybrids with γPNA showed considerably higher T_m values when compared to aegPNA with the same sequence (ΔT_m for the complementary γPNA·DNA duplex and the aegPNA·DNA duplex = +19 to +24 °C), and the mismatch discrimination was slightly better (ΔT_m for the mismatched γPNA·DNA duplex and the matched γPNA·DNA duplex = −16 to −21 °C).[42,45] The pyrrolidinyl acpcPNA showed an even higher T_m for the complementary DNA hybrid (ΔT_m for the complementary acpcPNA·DNA duplex and the aegPNA·DNA duplex = +28 °C) and better mismatch discrimination than both aegPNA and γPNA (ΔT_m for the mismatched acpcPNA·DNA duplex and the matched acpcPNA·DNA duplex = −28 to −41 °C).[117] The cpPNA showed the highest PNA·DNA duplex stability with a T_m value of 94 °C for a 9 nt mixed-sequence PNA·DNA duplex whereas the corresponding aegPNA·DNA duplex showed a much lower T_m at 42 °C (ΔT_m for the complementary γPNA·DNA duplex and the aegPNA·DNA duplex = +52 °C).[71] The downside of this cpPNA system is that although the T_m values were drastically decreased by 21–31 °C, the mismatched duplexes were still quite stable, with T_m values in the range of 63–73 °C. However, in practice, this may not be as bad as it sounds since only partial modifications of aegPNA can yield substantial improvement in the thermal stability of the duplex without compromising the mismatch specificity.

The aegPNA·RNA duplex was more stable than the corresponding aegPNA·DNA duplex, as shown by the increase in T_m by 10 °C for the same decameric sequence.[53] The γPNA·RNA

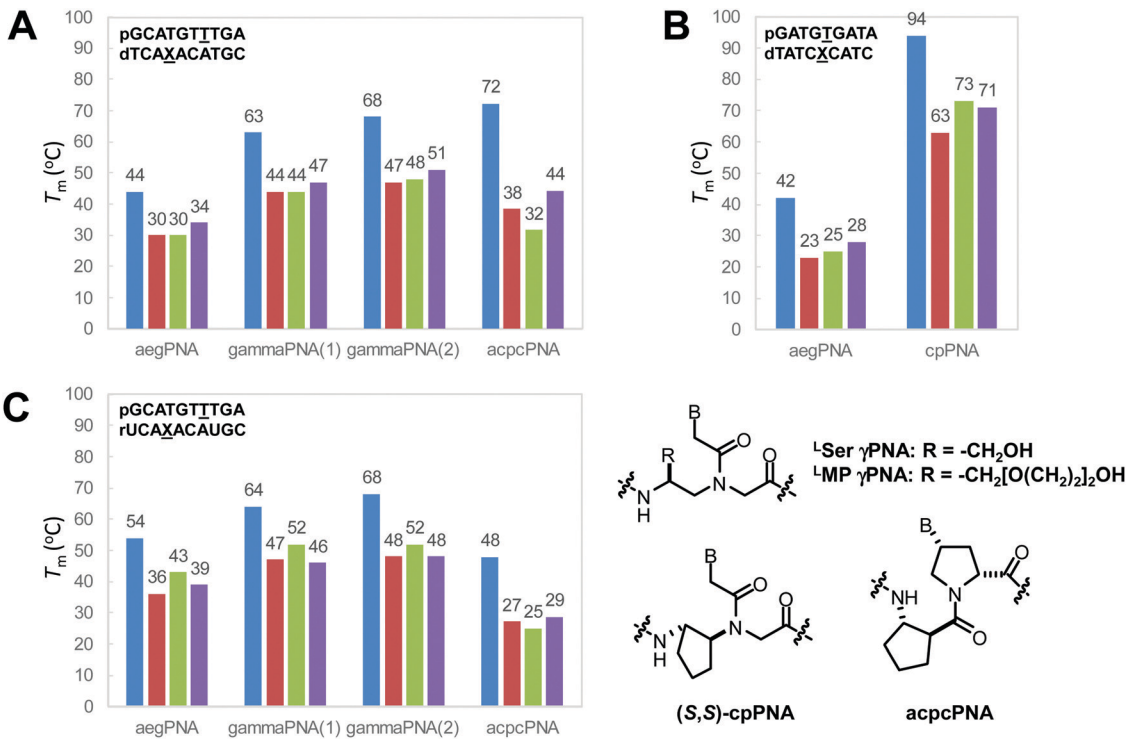

Fig. 32 Comparison of T_m values of selected PNA·DNA duplexes (A and B) and PNA·RNA duplexes (C). Color code for X in the DNA/RNA strand: A (blue), C (red), G (green), T/U (purple). γPNA(1) = LSer γPNA; γPNA(2) = LminiPEG (LMP) γPNA. T_m data were taken from ref. 42, 45, 53, 71 and 117 (adapted with permission from ref. 117. Copyright 2015 American Chemical Society).

Open Access Article. Published on 18 Nyenyankulu 2022. Downloaded on 2026-01-28 04:18:10.
This article is licensed under a Creative Commons Attribution-NonCommercial 3.0 Unported Licence.

duplexes, on the other hand, showed about the same thermal stability as the corresponding γPNA·DNA duplexes. Nevertheless, the γPNA·RNA duplexes are still more stable than the aegPNA·RNA duplexes.[42,45] In contrast, acpcPNA showed a distinctive preference for DNA over RNA, and thus the T_m of the acpcPNA·RNA hybrid was lower than that of the corresponding acpcPNA·DNA hybrid by 24 °C, making it the least stable RNA duplex of all PNAs. However, the mismatch specificity of acpcPNA was better than that of both γPNA and aegPNA (ΔT_m for mismatched and complementary PNA·RNA duplexes acpcPNA: −19 to −23 °C; γPNA: −12 to −20 °C; aegPNA: −11 to −18 °C).[117] No RNA binding data for cpPNA are available.

Applications of backbone-modified PNA in chemical biology

PNA has found widespread uses in many areas of applications that rely on the specific pairing between nucleobases.[155] The characteristic advantages of PNA over conventional oligonucleotides include the following: (1) the high binding affinity of PNA allows the design of shorter probes, which result in better discrimination; (2) the binding strength of PNA to nucleic acids is less sensitive to ionic strength; (3) PNA can interact with structured nucleic acid targets in various modes – the most common being the triplex invasion which can be reliably used for site-specific targeting of dsDNA; and (4) PNA is completely stable towards nucleases and proteases. The inability of PNA as a nuclease and polymerase substrate makes it an effective blocker of enzyme activities such as in the PCR clamping technique.[156] On the other hand, this makes PNA not compatible with several enzyme-mediated strategies for signal amplification. This also includes the inability of PNA to induce the RNAse-H mediated RNA degradation, and thus antisense PNA could only inhibit translation by steric blocking. In addition, the more hydrophobic nature of PNA can result in non-specific effects including self-aggregation, off-target binding, and adsorption to various hydrophobic surfaces such as plastic tubes that may complicate the interpretation of the results. In this section, applications of backbone-modified PNA related to the field of chemical biology and advantages over unmodified PNA, if comparison data are available, are discussed.

Targeting of DNA/RNA duplexes

PNA can interact with DNA and RNA duplexes in many ways depending on the sequence context (Fig. 33).[157] In the case of unmodified aegPNA, binding to dsDNA can occur efficiently *via* the triplex invasion mode with the formation of a highly stable PNA_2·DNA triplex. In this binding mode, two pyrimidine-rich PNA strands bind cooperatively to the purine-rich DNA strand *via* the Watson–Crick and Hoogsteen base-pairings, leaving the pyrimidine-rich DNA strand unpaired. This is in contrast to other triplex-forming oligonucleotides (TFOs) such as the locked nucleic acid (LNA) whereby the TFO strand resides in the major groove of the original dsDNA and forms only the Hoogsteen base pairs.[158,159] The formation of triplex invasion complexes was reported since the very early date of PNA discovery and their X-ray structure has been reported at atomic resolution.[24] The triplex invasion relies on the formation of T·A·T and/or C·G·C^+ base triplets (Fig. 34A); thus the DNA target sites require an extended stretch of the oligopurine tract. For the recognition of G, the protonation of C is required; otherwise an unnatural nucleobase that mimics C^+ such as pseudoisocytosine (J) or N^7-G should be used to allow efficient invasion at physiological pH. By appending to the PNA strand a tail-clamp consisting of two oligopyrimidine PNA blocks joined together by a flexible linker, duplex invasion by the remaining sequence

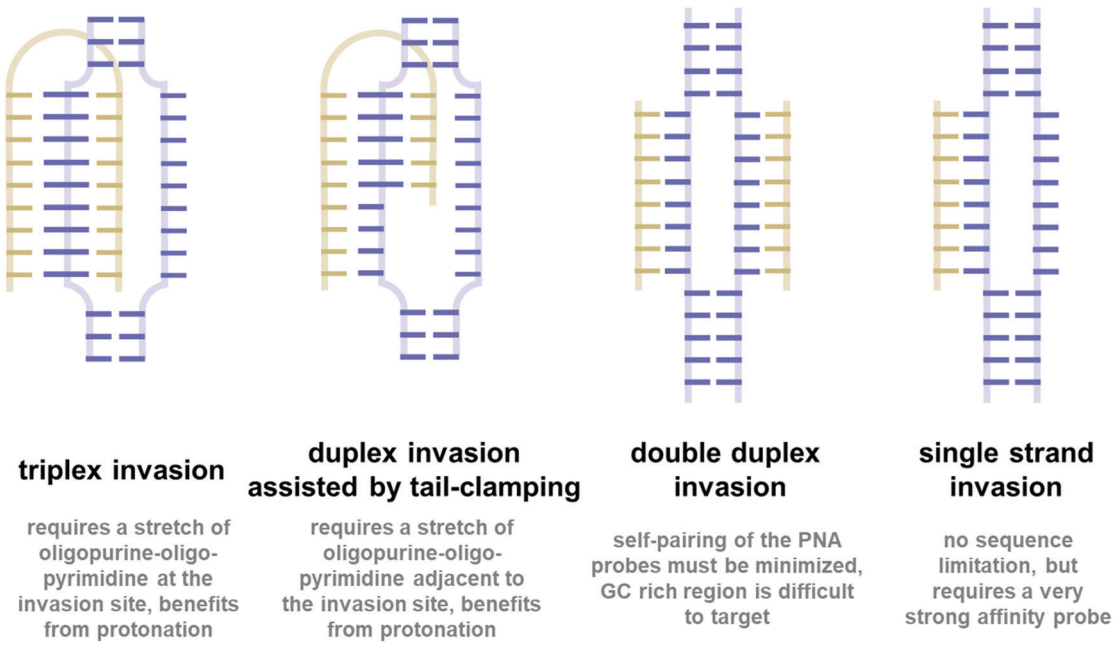

Fig. 33 Various modes of targeting DNA duplexes (blue) by PNA (gold).

© 2022 The Author(s). Published by the Royal Society of Chemistry

Open Access Article. Published on 18 Nyenyankulu 2022. Downloaded on 2026-01-28 04:18:10.
This article is licensed under a Creative Commons Attribution-NonCommercial 3.0 Unported Licence.

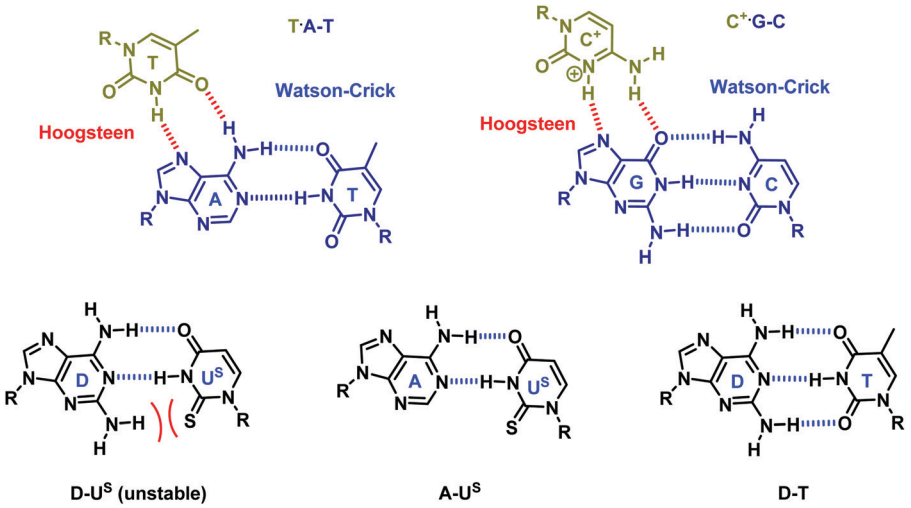

Fig. 34 (A) Watson–Crick/Hoogsteen base triplets involved in the triplex formation between PNA (gold) and DNA (blue). (B) A pseudocomplementary base-pairing scheme for A·T pairs.

on the PNA strand can be induced close to the triplex invasion site.[160,161] Nevertheless, this approach still requires the presence of a stretch of oligopurine sequence in the target. The double duplex invasion strategy (Fig. 33) whereby two PNA strands bind to each DNA strand in the same region does not suffer the same limitation. However, since the two PNA strands required to invade at the same site are necessarily complementary to each other, it was necessary to modify both PNA strands to destabilize the (usually more stable) PNA·PNA hybrid and to promote PNA·DNA hybrid formation. For aegPNA, the only option was to modify the nucleobases so that they are pseudocomplementary, *i.e.*, cannot bind to each other, but can still bind with the respective canonical complementary nucleobases. Pseudocomplementary bases are only available for the A·T pair by the replacement of T and A in the PNA strand with 2-thiouridine (U^S) and 2,6-diaminopurine (D), respectively (Fig. 34B).[162] The development of an equivalent pseudocomplementary G·C pair has yet to be achieved, but it was recently discovered that the replacement of G in the PNA strand with N^7-methylated G (G+) significantly stabilized the PNA·DNA duplexes and destabilized the PNA·PNA duplexes provided that the G+ are present on both PNA strands.[163] This strategy has been employed to improve the invasion efficiency of GC-rich dsDNA targets.

Backbone modification opens new avenues for enhancing the DNA/RNA duplex recognition. In one example, the pseudocomplementary αPNA with multiple positive charges allowed more effective double duplex invasion in GC rich dsDNA targets. Normally invasion at the GC rich target is difficult since the G·C pairs in PNA·PNA duplexes tend to be more stable than the corresponding PNA·DNA duplexes and there was no effective pseudocomplementary G·C pair available. In this case, the electrostatic repulsion between the two positively charged modified PNA strands destabilized the pseudocomplementary PNA·PNA duplex and stabilized the PNA·DNA duplex further. It was also demonstrated that incorporation of multiple positive charges along the PNA strands is more effective than placing the positive charges at both ends of the PNA strands.[154]

The cyclic acpcPNA is unique among other PNA systems in the sense that the two strands of acpcPNA with complementary sequences could not efficiently form a self-duplex. Although the stability and directionality of the self-duplex are stereochemistry dependent,[130,164] the self-duplexes are much less stable than the corresponding PNA·DNA duplexes in general. Thus, these pyrrolidinyl PNAs are inherently pseudocomplementary. Quantitative double duplex invasion of DNA duplexes by a pair of short acpcPNA sequences under low salt conditions was demonstrated by fluorescence energy transfer[165,166] and gel electrophoresis studies.[166] Invasion of a DNA duplex by a single-stranded acpcPNA was also observed, albeit with less efficiency.[165]

The strong affinity of γPNA enables efficient DNA duplex invasion by single-stranded γPNA without sequence restriction (up to 100% GC content) but longer γPNA sequences (15–20 bases) were required to invade efficiently.[167,168] The specificity was demonstrated by the absence of invasion in single mismatched DNA targets. The invasion at the designated site was further confirmed by chemical probing using diethyl pyrocarbonate (DEPC)/piperidine. However, it was still necessary to perform the invasion under low salt conditions that destabilize the DNA·DNA duplexes. When a pre-formed invasion complex was incubated in a buffer at physiological ionic strength, the DNA duplex was reconstituted with the dissociation of the PNA strand.[168] This suggests that the failure of the γPNA to invade under physiological conditions is due to thermodynamic rather than kinetic factors.[168] For shorter γPNA sequences (10 bases), additional modifications are necessary to increase the affinity to allow the invasion. These include the incorporation of a terminal acridine group[169] or a modified base (G-clamp).[170,171] The latter strategy allowed duplex invasion under physiological conditions.[172] The combination of a single-stranded γPNA invasion sequence and a DNAzyme designed to cleave a specific

Open Access Article. Published on 18 Nyenyankulu 2022. Downloaded on 2026-01-28 04:18:10.
This article is licensed under a Creative Commons Attribution-NonCommercial 3.0 Unported Licence.

region of ssDNA formed by the DNA duplex invasion allows the introduction of nicks or double-strand breaks into dsDNA with a higher sequence fidelity than the CRISPR/Cas system.[173] Recently, an efficient sequence-specific invasion of the DNA duplex by single-stranded cyclopentyl PNA (cpPNA) as short as 9 nt was reported, but the invasion failed at high salt concentrations.[71]

In the single strand invasion of the DNA duplex, the looped-out DNA strand is not stabilized by base-pairing as in the case of double duplex invasion. At high salt concentrations, the DNA duplex can thus easily re-form. To circumvent this problem, the chimeric duplex formed between γPNA and pyrene-modified DNA (''invader'' probe) was recently proposed as an alternative pseudocomplementary PNA·DNA pair that can invade the DNA duplex in a double duplex invasion mode without the complication due to the self-complementarity of the γPNA self-duplex formation. The driving force is the strong base-pairing between DNA and γPNA as well as invader DNA, as opposed to the weak binding of γPNA and invader DNA due to the inability of the pyrene to intercalate into the γPNA·DNA duplex.[175] In a different approach, γPNAs bearing a set of bifacial or Janus nucleobases were designed to recognize canonical Watson–Crick base pairs (AT, TA, CG, and GC) by inserting themselves between the base pair with a perfect shape and hydrogen bonding complementarity (Fig. 35).[174] Such bifacial PNA would bind to the DNA duplex as a central strand instead of fitting into the major groove as in the case of triplex recognition. The process is expected to be enthalpically favorable since two strong PNA·DNA base pairs are simultaneously formed at the expense of one weaker DNA·DNA base pair. In addition, there is no sequence restriction as in the triplex recognition or triplex invasion that requires an oligopurine/oligopyrimidine tract. Despite the possibilities of self-pairing by the formation of E·E and E·F base pairs and the reported high stability of γPNA·γPNA duplexes,[176] no self-pairing of the bifacial γPNA was observed both experimentally and in an MD simulation. A bifacial γPNA as short as 6 nt sequence can efficiently invade CG rich hairpin structures and longer DNA duplexes under physiological conditions with much faster kinetics than the usual duplex invasion (30 min rather than hours). A bifacial

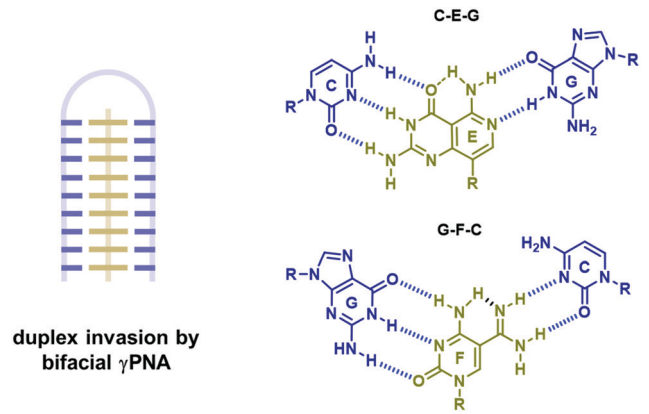

Fig. 35 Invasion of DNA duplexes by bifacial PNA.[174]

γPNA as short as 3 nt was shown to target dsRNA with r(CAG) repeats. An RNA-templated native chemical ligation of the short PNA chains was employed to enhance the binding efficiency further.[177,178]

PNA can also bind sequence specifically to double-stranded RNA (dsRNA) targets by triplex formation[181] or triplex invasion.[182] Targeting dsRNA by PNA is important since many biologically relevant RNA targets exist in structured forms.[183] For example, a short PNA probe has been used to inhibit the replication of the influenza virus by targeting the viral RNA in the region that is not accessible by conventional antisense agents.[184] In the triplex binding mode, aegPNA as short as 6 nt binds to an oligopurine/pyrimidine stretch region in dsRNA with a low nanomolar affinity. The affinity of PNA to dsRNA was better than that towards the corresponding dsDNA duplex by an order of magnitude, and attempts to adjust the PNA structure to favor the triplex formation with dsDNA over dsRNA binding by extending the PNA backbone to accommodate the B-DNA structure have been so far unsuccessful.[185] Since the triplex formation requires a Hoogsteen base-pairing, the process is benefited from the protonation of C in the PNA strand at low pH (Fig. 36).[181] Substitution of the base C with the more easily protonated 2-aminopyridine (M) promotes the triplex formation at physiological pH.[179] The requirement of the oligopurine/pyrimidine stretch was relaxed by the use of 2-pyrimidinone (P) and 3-oxo-2,3-dihydropyridazine (E) bases (Fig. 36).[180] Relatively few studies on the binding of PNA with backbone modifications to dsRNA targets have been published. When a few guanidine-modified αPNA monomers (GPNA) were incorporated into the aegPNA backbone, the binding to dsRNA occurred but with reduced affinity and specificity. In addition, depending on the sequence, the binding may occur in the triplex or duplex invasion modes instead of the expected triplex formation.[186] Only invasion by a γPNA was observed in dsRNA with r(CUG) repeats.[187] Fluorine NMR studies on the binding of PNA partially modified with ^{L}Ser γPNA monomers to the miR-215 dsRNA model indicated the ability of γPNA to form a triplex invasion complex in addition to triplex formation. The preference of either of the binding modes could be fine-tuned by the appropriate placement of the γPNA monomer.[188] Modified PNA with three consecutive γ-(*S*)-guanidinylmethyl PNA subunits showed improved affinity and selectivity for dsRNA binding *via* the triplex formation and enhanced cell internalization.[189] The dependence of the binding mode on the precise positions of the γPNA backbone modification might explain the poorer performance of γPNA when compared to unmodified aegPNA in a templated fluorogenic reaction between two PNA probes mediated by a dsRNA template.[190] Incorporation of modified bases that could not form stable Watson–Crick base pairs should offer a viable strategy to improve the selectivity of triplex binding over the triplex invasion of these modified PNAs.[191]

Targeting G-quadruplexes

Targeting G-quadruplexes in a sequence-specific fashion by forming PNA·DNA heteroquadruplexes (Fig. 37A) is less straightforward than targeting duplex DNA as it is subjected

© 2022 The Author(s). Published by the Royal Society of Chemistry

Open Access Article. Published on 18 Nyenyankulu 2022. Downloaded on 2026-01-28 04:18:10.
This article is licensed under a Creative Commons Attribution-NonCommercial 3.0 Unported Licence.

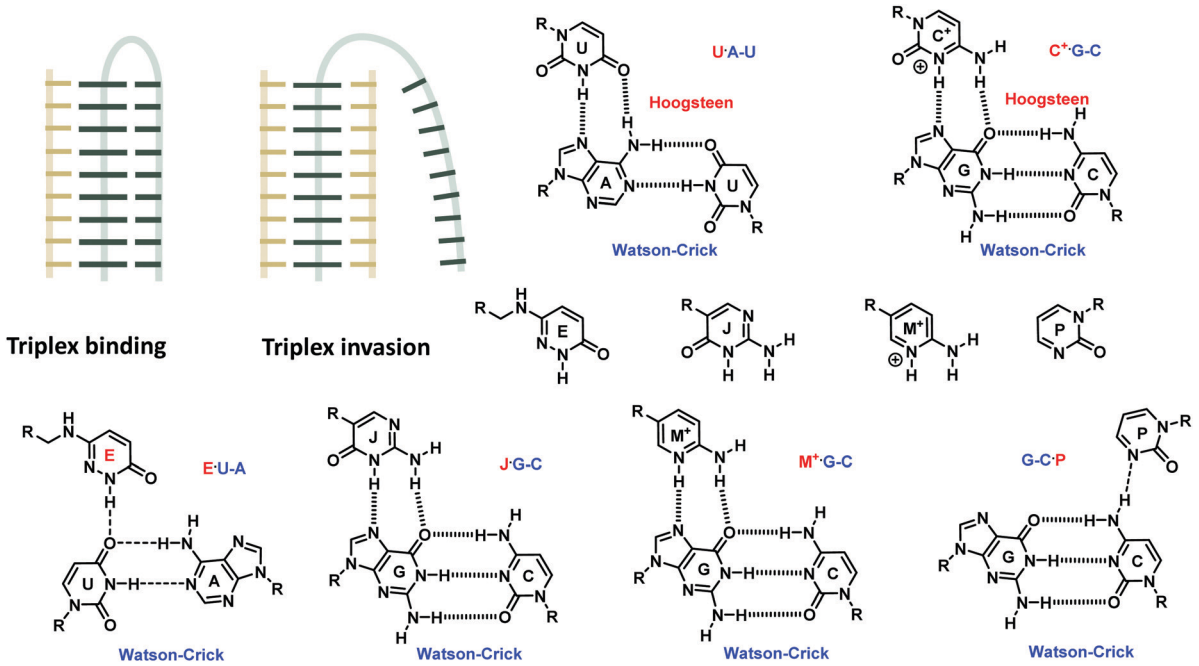

Fig. 36 Targeting RNA duplexes (gray) by PNA (gold) *via* triplex formation and invasion, and the structures of the modified base that facilitate the triplex binding mode.[179,180]

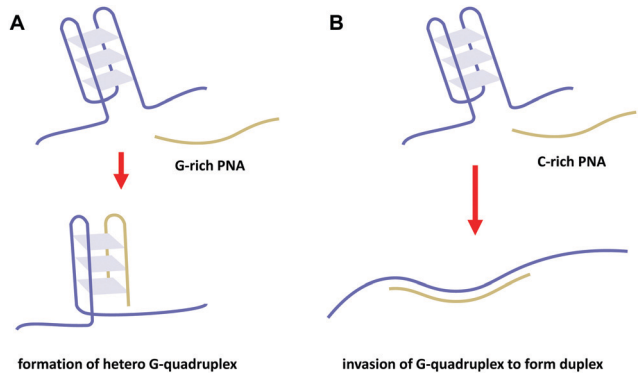

Fig. 37 Targeting DNA G-quadruplexes (blue) by PNA (gold) by hetero G-quadruplex formation (A) or duplex formation (B).

to competition with the duplex formation between the G-rich PNA and the C-rich complementary DNA strand as well as self-quadruplex formation and aggregation of G-rich PNA sequences.[192] Armitage *et al.* proposed two strategies to promote G-quadruplex formation over duplex formation[193] which involves the elimination of nucleobases in the loop region and PNA backbone modification to discourage the duplex formation without affecting the (hetero)G-quadruplex formation. The use of ^{D}Ala γPNA which pre-organizes into left-handed helical structures substantially destabilized the duplexes while the stability of the (*hetero*)-G-quadruplex was much less affected as a result of the underwound nature of the G-quadruplex structures. The combination of the two strategies allowed targeting of Myc19 DNA with low nanomolar affinities. Although the binding was weaker than that of the unmodified aegPNA or ^{L}Ala γPNA, the selectivity for hetero G-quadruplex formation over the complementary DNA strand was much improved. The G-quadruplex invasion by ^{L}Lys γPNA was employed for the multivalent display of the RGD peptide on a DNA G-quadruplex scaffold.[194] Cyclopentyl PNA with a $G_4T_4G_4$ sequence can also form self-(cpPNA·cpPNA) and hetero-(cpPNA·DNA) G-quadruplex structures. When compared to aegPNA, the self-quadruplex was destabilized and the hetero-G-quadruplex was stabilized. Thus, the use of cpPNA offers another viable strategy to modulate the preference for self- *versus* hetero-quadruplex formation.[70]

The high stability of γPNA·RNA duplexes allowed an efficient invasion of RNA G-quadruplexes by C-rich γPNA which resulted in the disruption of the G-quadruplex and concomitant formation of the γPNA·RNA duplex (Fig. 37B). The inhibition of *in vitro* translation of an artificial reporter mRNA transcript bearing the G-quadruplex-forming sequence inserted in the 5′-untranslated (UTR) region by the γPNA designed to target the G-quadruplex was reported to be more potent than 2′-OMe RNA and more specific than aegPNA.[195]

Complex structures involving backbone-modified PNA

The concept of bimodal PNA (bmPNA) that can simultaneously and independently recognize two strands of DNA has been proposed by the Ganesh group very recently. A sequence of nucleobases appended to the aegPNA backbone at the α or γ position *via* an appropriate linker can recognize an additional DNA strand *via* another set of Watson–Crick base-pairing that is independent of the first one (Fig. 38A).[196–198] In the absence of the nucleobase attached to the nitrogen atom, the α or γ nucleobase-modified PNA can also recognize its DNA

Open Access Article. Published on 18 Nyenyankulu 2022. Downloaded on 2026-01-28 04:18:10.
This article is licensed under a Creative Commons Attribution-NonCommercial 3.0 Unported Licence.

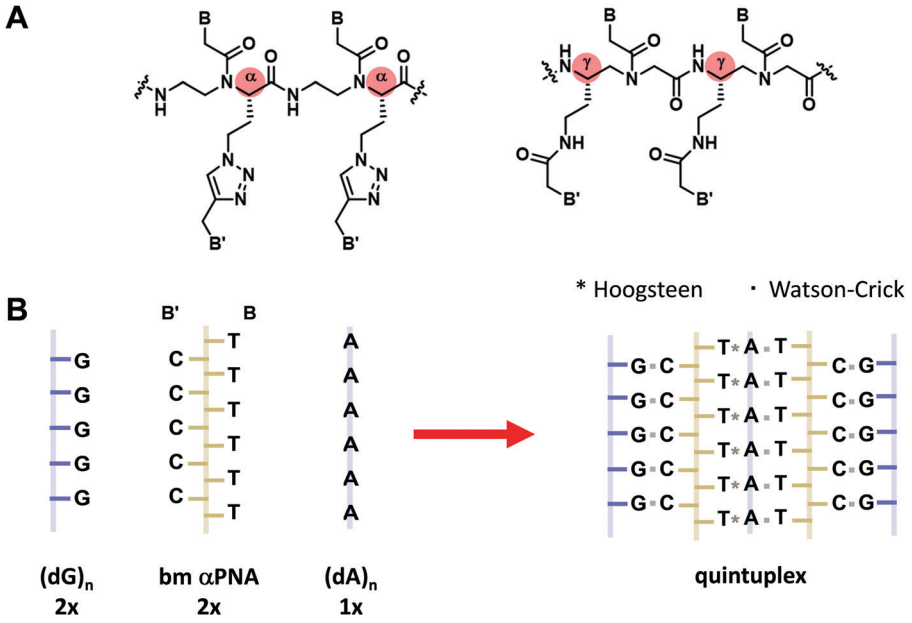

Fig. 38 (A) Structures of bimodal αPNA and γPNA. (B) Spontaneous assembly of bimodal PNA (gold) with DNA (blue) to form complex structures.[198]

complementary target, albeit with somewhat weaker affinity than the original aegPNA. When both sets of nucleobase sequences are present on the same PNA strand, each sequence binds to its specific complementary DNA target independent of one another to form a ternary complex between one PNA and two DNA strands. Thermal stability measurements indicated that the melting occurred in two steps and that the two base-pairings mutually stabilized each other as shown by the increase in T_m for both steps. This led to the proposal that the melting occurred through the re-organization of the ternary complex followed by single step dissociation of the three strands rather than sequential dissociation of each strand.[197] High-order complexes can also form when the PNA carries a homothymine sequence that can form a stable triplex structure with homoadenine DNA either at the α-face[198] or the γ-face.[199] An example is a quintuplex structure formed from two bimodal PNA, two G-rich, and one A-rich DNA strands (Fig. 38B). The central A-rich DNA strand formed a triplex with the T-rich face of the bimodal PNA strands, leaving the C-rich face available to bind to another G-rich DNA strand. The order of the hybrid formation does not affect the final composition of the ultimate complex. Such design might find new applications in the areas of nucleic acid nanotechnology or in biologically relevant systems by targeting two nucleic acid strands simultaneously.

Another bifacial PNA (bPNA) system was recently proposed by Bong *et al.* Instead of using two sets of base sequences, melamine was chosen as a Janus nucleobase that allows simultaneous recognition of two thymine/uracil bases on two DNA or RNA strands (Fig. 39).[200,201] In this work, the dipeptide derived from glutamyllysine[202] was chosen as a scaffold rather

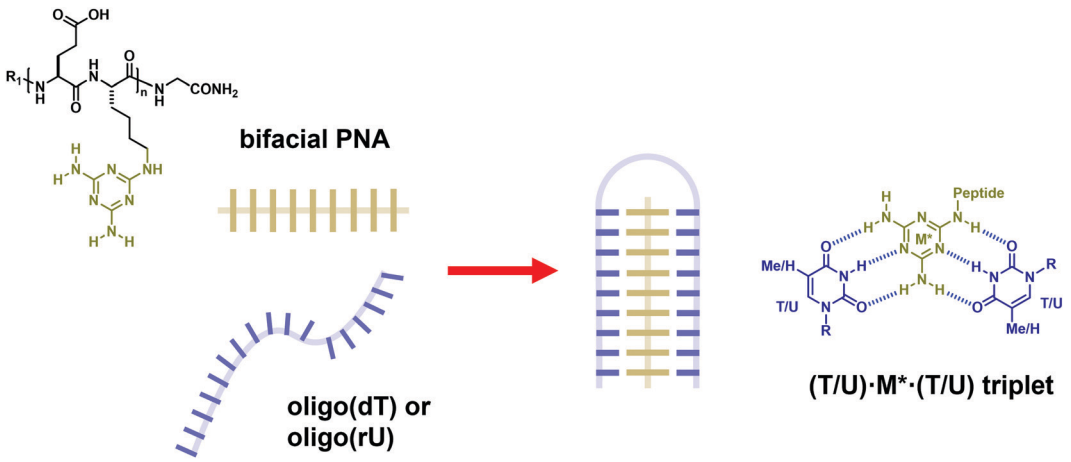

Fig. 39 Structures of bifacial PNA containing the melamine base (gold) and its interaction with thymine in DNA (blue) or uracil in RNA strands to form a stable triplex structure (adapted with permission from ref. 200. Copyright 2012 American Chemical Society).

© 2022 The Author(s). Published by the Royal Society of Chemistry

Open Access Article. Published on 18 Nyenyankulu 2022. Downloaded on 2026-01-28 04:18:10.
This article is licensed under a Creative Commons Attribution-NonCommercial 3.0 Unported Licence.

than the aegPNA for synthetic convenience. The melamine was attached to the lysine amino group. A well-defined triplex with K_d in the low nanomolar range was formed in the presence of homothymine DNA, either as two separated strands or as a hairpin. These triplexes show a sharp cooperative melting and their formation can be detected spectrophotometrically and by gel electrophoresis. The PNA with the fully or partially methylated melamine base showed no triplex formation. Remarkably, the corresponding diaminotriazine base without the extra NH group on a similar peptide scaffold only formed a duplex with poly(dT) and poly(rU).[202] The triplex formation on a single-stranded DNA/RNA target with a $(T/U)_n(A/C)_m(T/U)_n$ recognition site (n, m = 6–10) completely inhibited exonuclease activities and transcription/reverse transcription.[203] An enhanced version with two melamine groups attached to the same peptide unit allows the design of a very short peptide that selectively targets two $(U/T)_6$ domains of any DNA/RNA that can fold into the required triplex.[204] In addition, invasion of the RNA triplex carrying a U·A·U stretch – a common motif that occurs in long non-coding RNA involved in several biologically relevant processes – by bPNA occurred with concomitant displacement of the central oligo(rA) strand. Such displacement of the oligo(rA) tail accelerates the degradation of the RNA target by exonucleases, thus allowing the possibilities of using bPNA to regulate RNA functions.[205] It is conceivable that other bifacial nucleobases capable of forming similar base-triplet schemes with other combinations of nucleobases could be incorporated in the bPNA so that the recognition motif can be expanded to more diverse biologically important targets.[177]

PNA·PNA duplex formation

Due to the absence of unfavorable electrostatic repulsion, unmodified aegPNA forms highly stable PNA·PNA self-duplexes. Since aegPNA is inherently achiral, the left-handed and right-handed duplexes are formed equally well. Upon binding to DNA, the right-handed helical conformation was determined by the chirality of the DNA strand. The situation is different for modified PNA with a chiral backbone. Although most backbone-modified PNAs are chiral, they are usually not easily accessible in both enantiomers. However, the simple structure of γPNA renders both enantiomers easily accessible. It has been known since the first discovery of γPNA that single-stranded PNA with a γ-modified backbone pre-organized into a right-handed helix when the γ-substituent was in the L-configuration. It could be predicted that the opposite is true for the D-configuration and this has been experimentally verified.[176,206] Two complementary γPNA sequences with the same configuration can pair to form a highly stable duplex, and such γPNA duplex formation could be used for the regulation of gene expression in a reversible manner.[207] Only the right-handed γPNA can pair with natural DNA, and the two enantiomeric γPNAs do not cross-pair with each other. Accordingly, the two enantiomeric γPNAs are stereochemically orthogonal. Yet, both enantiomers of γPNA pair indiscriminately with the achiral aegPNA (Fig. 40). Such property has been utilized to create a hairpin structured probe from the chimeric γ/aegPNA sequence to improve its mismatch discrimination.[208] Thus, the information between the two orthogonal γPNAs and between the left-handed γPNA and natural DNA/RNA can be transmitted through the achiral aegPNA mediator. Another level of orthogonality can be introduced by including the left-handed enantiomer of natural DNA/RNA.[209,210] Several interesting applications of such orthogonal PNA systems are emerging such as in the control of nanostructure self-assemblies,[176] the improvement of signal amplification by hybridization chain reaction,[211] the design of a PNA-based beacon that incorporates a short ^{D}Ser γPNA sequence

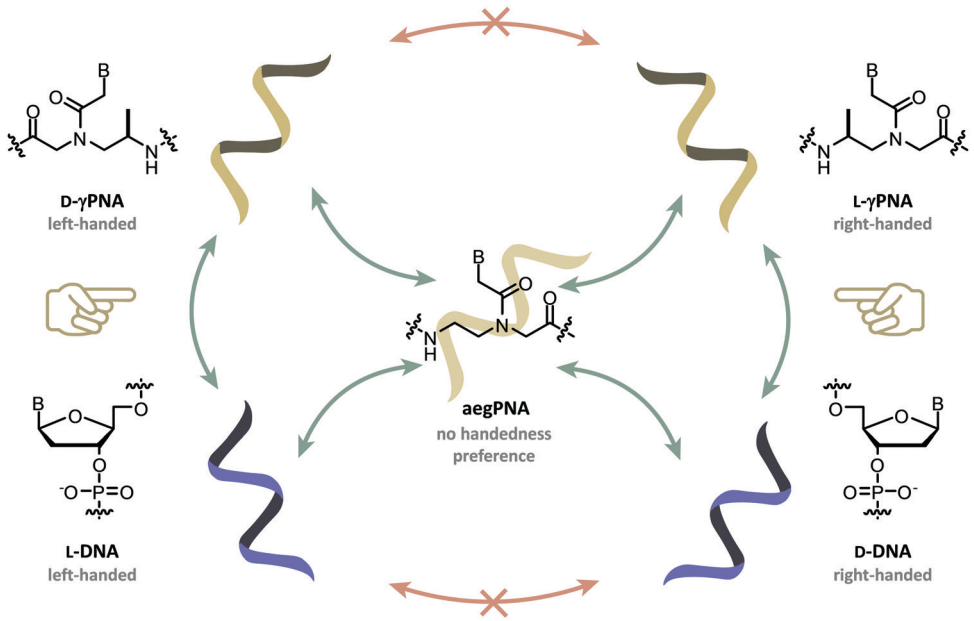

Fig. 40 Orthogonality pairing in γPNA (gold) and DNA (blue). Only γPNA and DNA with the same handedness can self-pair and cross-pair. The achiral aegPNA pairs indiscriminately with all; thus it can act as a mediator to transmit the information between these orthogonal nucleic acids.[176]

Open Access Article. Published on 18 Nyenyankulu 2022. Downloaded on 2026-01-28 04:18:10.
This article is licensed under a Creative Commons Attribution-NonCommercial 3.0 Unported Licence.

as the signaling unit to facilitate the catalytic turnover without compromising the specificity,[212] and in the supramolecular assembly of synthetic transcription factors on dsDNA without competing DNA binding.[213] Recently, the concept of orthogonal PNA pairs has been extended to cpPNA probes, in which the left-handed (*R*,*R*)-cpPNA could only pair with itself, but not with natural DNA/RNA and the right-handed (*S*,*S*)-cpPNA. Importantly, only a few modifications by the chiral cpPNA monomers were sufficient to determine the helicity and the ultimate base-pairing behavior of the resulting chimeric PNA. This orthogonal strategy was employed for the development of a microfluidic-based assay of HIV-1 RNA.[214]

Modified PNA as a supramolecular scaffold

The self-assembly of PNA, either on its own or in combination with DNA, has been exploited in creating well-defined supramolecular architectures for the construction of PNA-based nanomaterials[215] or for biological applications.[216] Short aegPNA can self-assemble into well-defined structures *via* the Watson–Crick base-pairing and base stacking to provide materials with interesting optical properties.[217,218] A programmable self-assembly of short γPNA strands that are partially complementary to each other to form well-defined 3-helix nanotubes consisting of purely γPNA[219] or γPNA and DNA[220] was demonstrated. The use of PNA instead of DNA allows the self-assembly process to occur in organic solvents and the γPNA modification carrying a hydrophilic side chain was essential as aegPNA alone tends to form aggregates.

The ability of short PNA to form a self-complementary duplex was utilized in constraining the conformation of peptides which allows enhancing and regulating their biological activities through PNA/PNA and PNA/DNA hybridization.[221,222] Three-consecutive intramolecular base-pairing of γPNA has been utilized to stabilize the cyclic peptide RTD-1 in place of disulfide bonds. The retention of potent antibacterial activities of the peptide indicated that the base-pairing perfectly mimicked the disulfide bond.[223] Armitage *et al.* also reported the use of γPNA with a hairpin construct as a staple to constrain the HIV-1 transactivator of transcription (TAT) peptide into a loop conformation which enhanced its cell penetration ability.[224] The advantage of γPNA is two-fold. First, the high stability of γPNA·γPNA duplexes enables the formation of a hairpin structure with a very short stem (only 4 nt). Second, the γPNA hairpin can be designed to have an overhang sequence that can be further conjugated to other biomolecules *via* γPNA·DNA hybridization that occurs efficiently even with a short (6 nt) overhang sequence.

Multivalent interactions play crucial roles in several biological processes. The self-assembly of PNA or its hybridization on a DNA (or PNA) scaffold enables a multivalent display of the ligand in a programmable and precisely controlled fashion (Fig. 41A). This approach offers advantages in terms of both synthetic efficiency and control of spatial arrangement as well as density of the ligand over conventional approaches whereby the ligands are connected by a flexible linker or attached to other multivalent scaffolds.[225] Winssinger pioneered the construction of multivalent oligosaccharide and peptide libraries by self-assembling two or more ligand-modified PNA on a DNA template.[226–228] This provides a powerful way to generate a large number of well-defined multivalent constructs that can be subsequently screened against the respective biological receptors in a combinatorial fashion. It should be noted that strong base pairing is not required as a result of cooperativity between the base pairing and ligand–receptor binding. Thus, dynamic assemblies of L-fucose-modified short self-complementary PNA probes that were barely stable at room temperature could effectively block the binding of bacterial lectins to epithelial cells.[229] Nonetheless, the use of aegPNA in these early approaches offers limited control of the ligand arrangement since only terminal modification was possible. In a subsequent work by Seitz, the incorporation of a Cys γPNA monomer in the PNA molecule

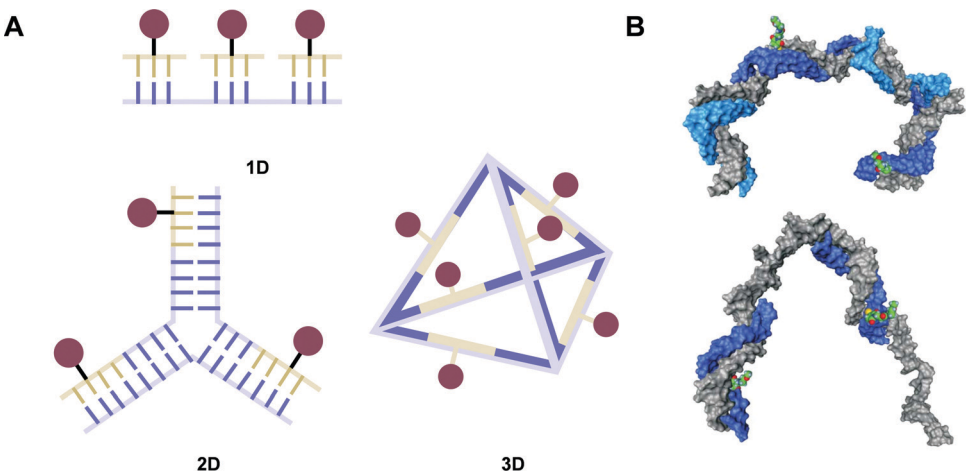

Fig. 41 (A) Schematic representation of using PNA for multivalent display of ligands on various DNA scaffolds. (B) A model showing the spatial arrangement of two *N*-acetyllactosamine (LacNAc) ligands in two different multivalent constructs derived from γPNA (blue) and DNA (gray) (reproduced from ref. 230 with permission from the Royal Society of Chemistry).

© 2022 The Author(s). Published by the Royal Society of Chemistry

Open Access Article. Published on 18 Nyenyankulu 2022. Downloaded on 2026-01-28 04:18:10.
This article is licensed under a Creative Commons Attribution-NonCommercial 3.0 Unported Licence.

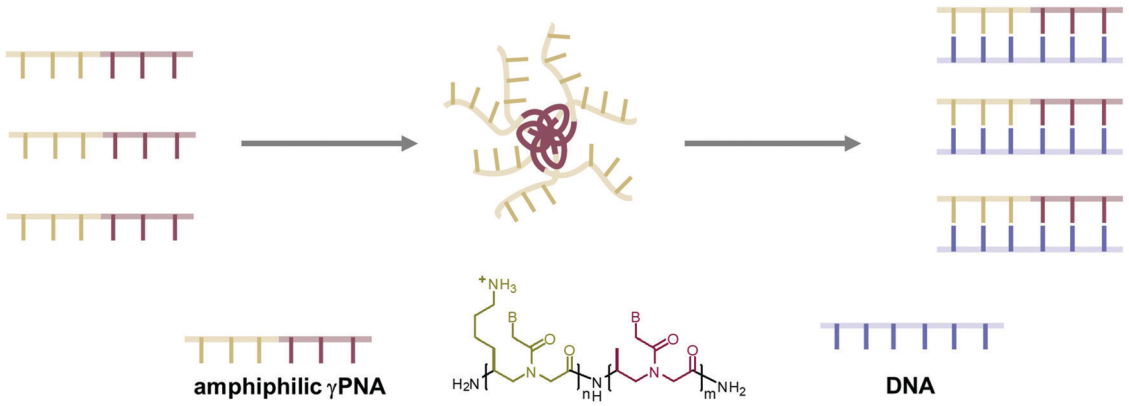

Fig. 42 The self-assembly of amphiphilic γPNA probes is modulated by γPNA·DNA/RNA duplex formation (adapted with permission from ref. 237. Copyright 2019 American Chemical Society).

allowed the introduction of the carbohydrate ligand (LacNAc) in any desired position *via* the thiol group. The results from the screening of ligands with different spatial arrangements agree with the expected structure of the receptor binding sites (*Erythrina cristagalli* lectin). In addition, the rigidity of the construct could be further fine-tuned by incorporating nick-sites or single-stranded regions (Fig. 41B).[230] Appella reported a similar strategy to construct libraries of multivalent displays of various ligands including c(RGDfK) peptide,[231] dopamine D_2 receptor (D_2R) agonist,[232] and A2A adenosine receptor antagonist[233] on DNA or PNA scaffolds employing Lys γPNA as the adapter.

In a more complex architecture design, short PNA strands were used as an adapter for the rapid assembly of protein molecules on three-dimensional DNA scaffolds.[234,235] The use of the γPNA backbone allows versatile attachment of the ligand at any required position along the PNA strand. Short bifunctional γPNA probes with a thiol group on the backbone could be site-specifically and stably attached to the DNA tetrahedron which could be used for programmed assembly of ligands or biomolecules.[236]

In the last example, the control of the supramolecular architecture of amphiphilic PNA was described by Heemstra *et al.* (Fig. 42).[237,238] The amphiphilic PNA was created by strategic placement of hydrophobic and hydrophilic side chains on a γPNA backbone. Such amphiphilic PNA spontaneously assembled to form nanoaggregates with an average diameter around 35 nm in an aqueous environment. When the target nucleic acid (miRNA-21) was added, the hybridization between the γPNA and the nucleic acid target disrupted the aggregate structures. Thus, the aggregation state of the amphiphilic PNA was modulated by the presence or absence of its nucleic acid target. In contrast to earlier designs of amphiphilic PNA whereby the hydrophobic and hydrophilic domains are conjugated to the PNA termini,[239,240] the integration of peptide side-chains directly into the PNA backbone should allow designing of more complex functional structures such as helices, sheets and their supramolecular assemblies that incorporate the base-pairing ability of PNA.

Template-directed PNA oligomerization and sequence adaptive PNA

In the previous topic, the PNA was non-covalently assembled on the DNA template *via* stable base pairings. If the PNA strand is very short, the binding will be very weak. Despite the weak interaction of individual PNA strands, the adjacent PNA strands can be chemically joined to give a ligated product with increased stability. This principle is related to the templated ligation of PNA,[241,242] but it has a more dynamic nature. Several ligation strategies have been used to join small PNA fragments on DNA or RNA templates such as native chemical ligation,[178] azide–alkyne click reaction,[243] and reductive alkylation (Fig. 43A).[244] The last strategy allows new PNA strands to be synthesized by the assembly of short PNA fragments (4–5 nt each) on a specific DNA template whereby the sequence of the product was determined by the sequence of the template similar to the natural translation process. By incorporation of γPNA or αPNA building blocks into the tetrameric/pentameric PNA aldehyde fragments, Liu has demonstrated the use of such DNA-templated oligomerization for the synthesis of PNA oligomers bearing various functional groups in a sequence-defined fashion (Fig. 43B).[244] The yield and rate of the templated reaction are related to the thermal stability of the PNA·DNA duplexes which was primarily determined by the stereochemistry and position of the side-chain attachment rather than the nature of the functional group. While similar results were observed for D-αPNA, L-αPNA, and L-γPNA building blocks, the D-γPNA showed much lower efficiency which is in good agreement with the relative stability of each modified PNA system. Such dynamic assembly of functionalized PNA on DNA templates may find application in the design and evolution of functional biopolymers by using the DNA template not only for directing the synthesis but also for facilitating identification and enrichment as well as diversification of the products.[244] In the case of triazole linkage, it was reported that the 1,4-disubstituted triazole linker with appropriate spacing can mimic the *trans*-amide bond reasonably well as demonstrated by the similar DNA binding affinity and specificity of the unmodified and modified PNAs.[243] This system should

Open Access Article. Published on 18 Nyenyankulu 2022. Downloaded on 2026-01-28 04:18:10.
This article is licensed under a Creative Commons Attribution-NonCommercial 3.0 Unported Licence.

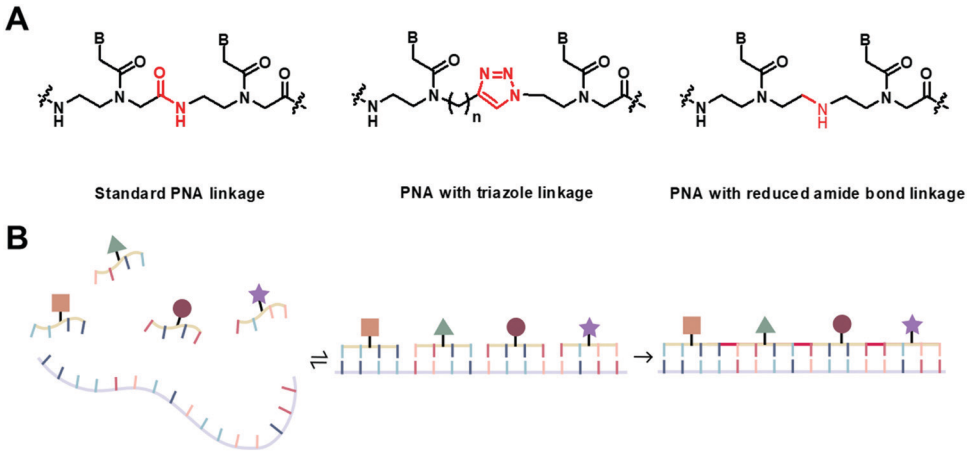

Fig. 43 (A) Some chemistry useful for template-directed PNA oligomerization. (B) The self-assembly and oligomerization of functionalized PNA probes on a DNA template.

potentially be useful in DNA templating polymerization similar to the reductive alkylation described above.

Relating to the abovementioned template-assisted oligomerization, another kind of PNA called thioester PNA (tPNA) was designed by attaching the nucleobases, *via* the thiol-thioester exchange reaction, to an oligopeptide backbone bearing alternating cysteine and another amino acid (Fig. 44).[245] The tPNA can form reasonably stable hybrids with DNA/RNA as well as self-hybrids. A broad range of amino acids can be accepted, with positively charged side chains forming more stable hybrids than negatively charged ones as would be expected from the electrostatic effects with the DNA backbone. Importantly, the thiol exchange reaction is readily reversible, thus allowing a dynamic exchange of the nucleobase in the presence of a template. A proof-of-concept experiment using a 1 : 1 mixture of adenine and deazaguanine thioester demonstrated a shift in the base ratio at equilibrium from 1 : 1 to 3 : 1 in the presence of an oligo(dT) template. The opposite results were obtained in the presence of an oligo(dC) template. Thus, this tPNA system represents an adaptive system whose sequence information can dynamically change according to the environment.

Modified PNA for nucleic acid biosensing and bioimaging

The high affinity, specificity, and biological stability of PNA suggest its obvious utility in biosensing and bioimaging applications. Accelerated by the recent discovery of many regulatory roles of RNA,[246] a particularly fast-growing area that received widespread attention and could benefit from the high performance of PNA probes is the imaging of RNA in live cells.[247] Biosensing and bioimaging applications of PNA are major topics that may be worth several separate monographs. Although many reviews on such topics exist,[248–251] they primarily focus on conventional PNA probes with only a few examples of modified PNA probes. This section will primarily focus on the advantages of conformationally constrained PNA which has the potential to offer improved nucleic acid binding affinity and sequence specificity over conventional aegPNA probes in biosensing and bioimaging applications.

The cyclopentyl-modified PNA (cpPNA) showed a substantial improvement in DNA binding affinities and mismatched specificity over aegPNA. The incorporation of only a few residues of the cpPNA monomer was sufficient to increase the stability by two orders of magnitude giving the dissociation constants in the sub-nanomolar range.[71] Hence, cpPNA offers

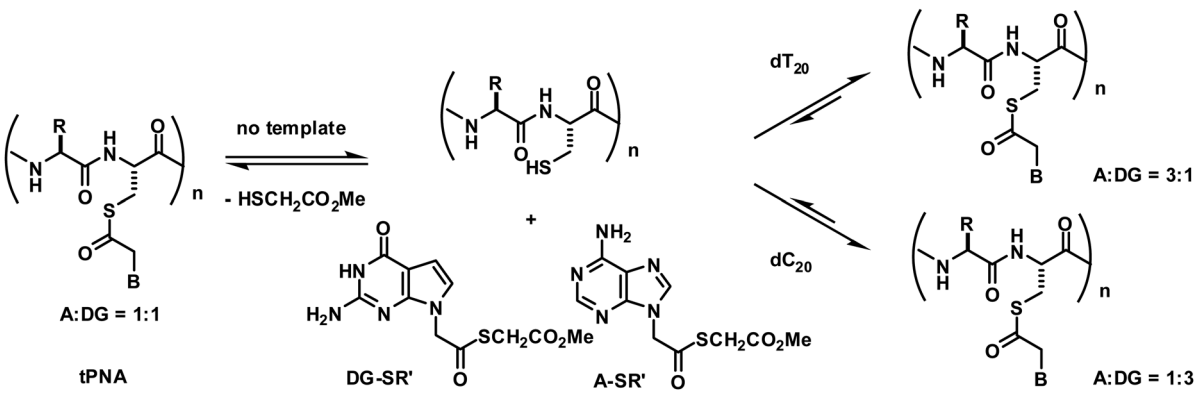

Fig. 44 Dynamic sequence adaptive behavior of thioester peptide nucleic acids (tPNA).[245]

© 2022 The Author(s). Published by the Royal Society of Chemistry

Open Access Article. Published on 18 Nyenyankulu 2022. Downloaded on 2026-01-28 04:18:10.
This article is licensed under a Creative Commons Attribution-NonCommercial 3.0 Unported Licence.

great potential to enhance the performance of PNA-based sensors. In one example, a PNA probe with single cpPNA modification was immobilized on a glass slide for the scanometric detection of anthrax lethal factor DNA in a microarray format.[252] The DNA target simultaneously hybridized with the immobilized PNA probe and another DNA-functionalized gold nanoparticles, resulting in the deposition of the gold nanoparticles on the sensor chip surface. Subsequent electroless-silver deposition to enhance the signal enabled a simple colorimetric readout by a scanner. The DNA target was detectable down to 25 aM, which was much better than the 50 fM detection limit obtained by the corresponding DNA capture probe. Interestingly, no signal was obtained when unmodified aegPNA was employed as the capture probe. Although the basis of such remarkable performance improvement was not obvious, the advantage of cpPNA over aegPNA probes was demonstrated.

In another study, the cpPNA probe was employed for the detection of anthrax protective antigen DNA in a PNA-based sandwich hybridization. The cpPNA was immobilized on a 96-well plate as a capture probe, and aegPNA modified with biotin at the C-terminus was used as the reporter probe. Subsequent binding to the avidin-HRP conjugate followed by the addition of the HRP substrate resulted in color generation that was measured spectrophotometrically. As low as 10 zmol of DNA was successfully detected while the corresponding unmodified aegPNA probe gave measurable signals down to only 10 fmol levels under the same conditions.[253] Quantitative detection of anthrax DNA was possible over the range of 10 to 10^7 copies of DNA.[254] The cpPNA version of the forced intercalation PNA (FIT) probe was also recently reported.[255] The FIT probe originally developed by Seitz consists of thiazole orange or similar dyes linked to the aegPNA backbone as an artificial nucleobase that lights up upon binding to the correct DNA/RNA target sequence that restricted the dyes' motion.[256] The introduction of two flanking cpPNA monomers significantly improved the performance of the FIT PNA probes in terms of both brightness and mismatch discrimination for the *in vitro* detection of RNA. This resulted in lowering of the limit of detection to 1.8 nM which was almost an order of magnitude better than that of conventional FIT probes based on aegPNA. However, the comparative performance in cellular RNA imaging is yet to be demonstrated.

Applications of pyrrolidinyl PNA probes with the α/β-peptide backbone (acpcPNA) for DNA sensing have already been reviewed elsewhere.[117,257] The superior mismatch discrimination ability of immobilized acpcPNA over DNA and aegPNA probes was experimentally demonstrated in a surface plasmon resonance (SPR) experiment whereby the three probes were critically compared side-by-side in capturing the same ssDNA target.[258] The experiments also revealed the faster kinetics of hybridization and confirmed the exclusive binding in the antiparallel direction of acpcPNA probes. On the other hand, the same comparative SPR experiments revealed that the binding of immobilized acpcPNA probes to dsDNA targets was less efficient than aegPNA likely due to its steric bulkiness.[259] Thus, acpcPNA probes have been extensively used as the key recognition element in paper- or chip-based electrochemical and optical nucleic acid sensing devices for point-of-care applications.[260–267] In many cases, the PNA·DNA hybridization resulted in the change of electrical properties such as capacitance and thus no labeling or other signal transduction mechanism was required.[268,269] While acpcPNA probes have been primarily used for DNA detection, satisfactory performance in the electrochemical detection of RNA was successfully demonstrated.[270] The differential electrostatic properties of PNA and DNA have been utilized for the detection of the DNA sequence. According to this principle, the negatively charged DNA was selectively captured *via* electrostatic interactions on various surfaces such as polymer beads,[271,272] magnetic beads,[273] cellulose paper,[274] or carbon electrode[275] that were coated with a positively charged polymer such as chitosan or poly(2-(dimethylamino)ethyl methacrylate) (PQDMAEMA). The neutral PNA molecule could not interact with such a surface unless it was hybridized with the captured DNA target, and the presence of the PNA probe hybridized to DNA could be detected by optical, electrochemical, or mass spectrometric detection.

The acpcPNA probes have also been used in the development of self-reporting fluorescence probes for DNA hybridization.[257] These probes are designed to carry an environment-sensitive dye such as pyrene or thiazole orange attached to the terminal, backbone, or nucleobase. The fluorescence change was induced by the hybridization between the PNA probe and the DNA target that alters the environment of the dye.[134,276,277] Alternatively, a simple fluorophore-labeled PNA probe was used in combination with a quencher which can be present on the same PNA strand[166] or as a separate entity such as another quencher labeled PNA or DNA strand,[278] oligo(dG),[279] graphene oxide (GO),[280] and metal nanoparticles.[281] In all cases, the fluorescence of the free probe could be restored after hybridization with the correct DNA/RNA target which resulted in the separation of the probe and the quencher. Faster kinetics, superior single mismatch discrimination as well as improved sensitivity in the fluorescence restoration of GO-quenched acpcPNA over aegPNA and DNA probes by DNA targets have been demonstrated and the principle had been successfully applied for both *in vitro* DNA/RNA detection and cellular RNA imaging.[281]

The high affinity of short γPNA probes towards DNA targets enabled a sandwich hybridization assay to be performed on very short DNA and RNA targets which is typically not possible with conventional DNA or even aegPNA probes. γPNA amphiphiles have been used in combination with fluorescent DNA nanotags in micelle-tagging electrophoresis.[284,285] The two short probes bound to adjacent positions on the same DNA target cooperatively stabilize each other by base stacking without compromising the specificity as generally observed when only one longer probe sequence was used. This strategy allows multiplex detection of various members of the *let-7* miRNA family at a single mismatch resolution with detection limits of 10–100 pM.[285] Likewise, the use of γPNA allows an efficient hybridization chain reaction (HCR) *via* γPNA·γPNA duplex

Open Access Article. Published on 18 Nyenyankulu 2022. Downloaded on 2026-01-28 04:18:10.
This article is licensed under a Creative Commons Attribution-NonCommercial 3.0 Unported Licence.

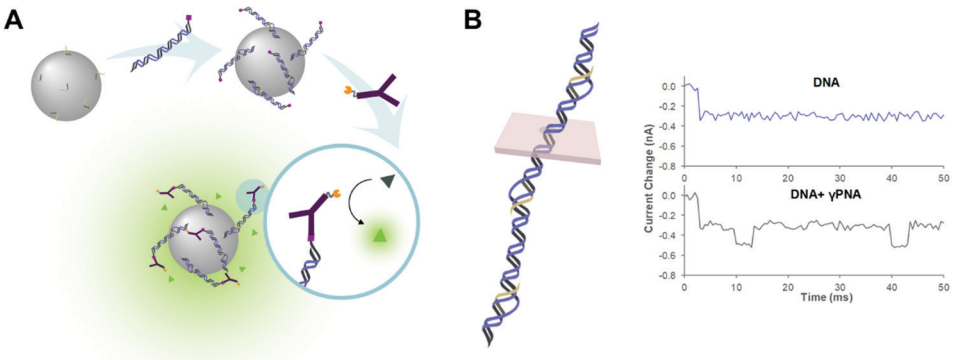

Fig. 45 Examples of biosensing strategies that took the advantages of the duplex invasion ability of modified PNA probes. (A) Chemiluminescence microbeads γPNA array for the rapid and simultaneous identification of blood pathogens.[282] (B) Nanopore-based sequencing and barcoding of long dsDNA strands by γPNA probes (adapted with permission from ref. 283. Copyright 2012 American Chemical Society).

formation to be performed using very short hairpin probes with only 5 nt stem, 5 nt loop, and 5 nt toehold making the total length of the hairpin constructs only 20 nt, far shorter than the DNA-based constructs (typically 30–40 nt). The use of miniPEG γPNA solved the problem of the limited solubility of the PNA-derived cHCR products.[286] A microarray prepared from miniPEG γPNA probes was reported to distinguish between complementary and mismatched DNA targets better than aegPNA arrays,[287] although the results may not be directly comparable due to the difference in the probe sequence and length as well as other factors. The DNA duplex invasion ability of single-stranded γPNA was utilized in the chemiluminescence microbeads array for the rapid and simultaneous identification of 21 blood pathogens without requiring denaturation (Fig. 45A).[282] It was also used in the nanopore-based sequencing and barcoding of long DNA strands without suffering the sequence limitation as in the case of triplex-forming bis-aegPNA.[288] The sequence-specific invasion of DNA duplexes by γPNA probes resulted in the change of electronic signals when the DNA strand is passing through the nanopore (Fig. 45B). This strategy allows the detection of CFTRΔF508 gene mutation[289] and classification of HIV-1 sub-types[283] that could not be directly performed by the nanopore alone due to the similarity between the viral subtype genes.

The γ-position of PNA is an ideal place for internal modification of PNA *via* amide bond formation[38,39] or click chemistry.[293] A 5-azidomethyluracil Lys γPNA monomer allows facile double functionalization at the internal positions of the PNA strand.[294] The modifying group on the γ-Lys side chain pointed in the minor groove direction while the modifying group on the C5 of uracil pointed in the major groove direction and thus the strategy allows placement of the label in a controllable fashion. Chimeric γGPNA-aegPNA probes have been used for quantitative imaging of cellular miRNA-21 and miRNA-31 in different cancer cell lines *via* a fluorogenic RNA-templated Staudinger reaction which unmasked the fluorophore on one of the PNA strands (Fig. 46A).[290] The GPNA modification facilitates the cell permeability of the probes. The short Cy5-labeled γPNA miniprobe bound cooperatively to the TTAGGG repeats in the human telomere. The binding was enhanced by the incorporation of the G-clamp into the γPNA and thus the performance of a short (6 nt) probe could approach that of longer probes (12–18 nt) without the G-clamp. The shorter probe stained faster and showed improved sensitivity due to the increasing number of labeled-probes bound to the same length of the telomere target. Its effectiveness in the staining of short telomeres in Jurkat cells that do not stain well with conventional aegPNA probes was demonstrated.[295] By a strategic design of the probe sequence, two 9 nt γPNA miniprobes with a pair of FRET dyes could bind alternately on the same DNA telomere. This allows the visualization of the telomere in the cells and tissues under wash-free conditions with minimal interference from background autofluorescence (Fig. 46B).[291] The application of miniPEG γPNA in combination with HCR for visualizing non-nucleic acid targets was demonstrated for the membrane protein carbonic anhydrase IX (CA IX, a cancer biomarker) expressed on the cell surface. It should be noted that in this example, the non-nucleic acid target was indirectly detected with the assistance of a CA IX ligand conjugated to an initiator γPNA strand (Fig. 46C).[292]

Applications of the chiral box ^{D}Lys αPNA for *in vitro* detection of DNA single point mutations in clinical diagnostic were demonstrated by capillary electrophoresis[296] and SPR.[297] The improved mismatch discrimination over DNA and aegPNA probes was explained by the strong destabilizing effects of the mismatch over the complementary hybrids as a result of limited conformational flexibility of the modified PNA.

Modified PNA for enhancement of cellular uptake and gene regulation

The conventional aegPNAs have already found tremendous applications in the areas of gene regulation and editing.[298–300] Backbone modification offers potential improvement of the performance of aegPNA not only by increasing binding affinities and specificity but also by providing opportunities for introducing various functional moieties to improve the cellular uptake and pharmacodynamic and pharmacokinetic properties, as well as reduce non-specific binding.

Various functions can be incorporated into the PNA molecule through the modification of the α-substituents. In the

© 2022 The Author(s). Published by the Royal Society of Chemistry

Open Access Article. Published on 18 Nyenyankulu 2022. Downloaded on 2026-01-28 04:18:10.
This article is licensed under a Creative Commons Attribution-NonCommercial 3.0 Unported Licence.

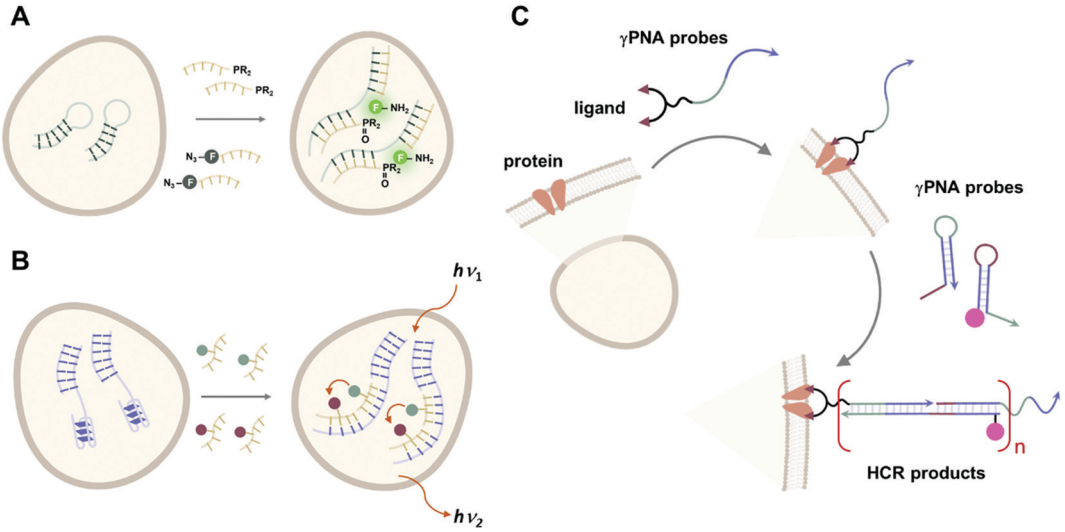

Fig. 46 Examples of strategies for cellular imaging that took the advantages of high affinity modified PNA probes. (A) RNA imaging by templated Staudinger reaction between two PNA probes.[290] (B) Visualization of telomeric DNA by PNA probes.[291] (C) Visualization of carbonic anhydrase IX with the aid of γPNA probes and HCR.[292]

simplest form, fluorophores can be incorporated at the internal positions of the PNA molecule *via* the lysine side-chain amino group.[301] More complex functional groups such as sugars have been incorporated at the α-position of PNA to modulate its pharmacokinetic properties without deteriorating the DNA binding ability.[302,303] Some glycosylated αPNAs showed improved hepatic uptake by 7–40 fold relative to unmodified PNA.[303] Another related study in *N*-acetylgalactosamine (GalNAc)-modified γPNA suggested that exact placement of the GalNAc group produced a strong effect on the uptake efficiency whereby the introduction of three-consecutive backbone GalNAc-modification was preferred over a single terminal modification with three GalNAc groups.[304] Inspired by the HIV-1 TAT transduction domain which is rich in amino acids with basic side chains, the αPNA with Arg modification ("GPNA") was proposed to improve cellular uptake by Ly *et al.*[305] The GPNA could indeed enter human cells and localize in the nucleus. GPNA with D-Arg modification was shown to offer superior binding affinity than L-Arg towards RNA targets,[306] although the duplex stability was lower than that of the unmodified PNA·RNA hybrids, especially when consecutive modified residues were present in the PNA strand. The PNA sequences with an alternating unmodified and D-Arg modified backbone showed smaller effects on the affinity towards both DNA and RNA targets and still allowed effective cell penetration.[307] At micromolar concentrations, the GPNA designed to target the 5'-UTR region of the E-cadherin mRNA transcript exerted the antisense effect by downregulating the E-cadherin expression in A549 cells as shown by immunofluorescence staining.[308] A GPNA designed to target the epidermal growth factor receptor (EGFR) mRNA was shown to inhibit EGFR expression and cancer cell growth without the aid of transfection agents. Antitumor effects at the same level as that of standard EGFR inhibitors including erlotinib and cetuximab were demonstrated in xenograft mouse models.[309] Another study by Mitra and Ganesh on the positively charged (*R*)-aminomethylene αPNA revealed similar trends in terms of DNA binding and cell permeability.[51] The latter work also revealed the superiority of γ-modifications over α-modifications.

The γPNA has been extensively used for biological applications because of the excellent binding properties and ready availability. The γ-side chain modification for biological applications usually incorporates positively charged[38,39,46–48,50,51] or hydrophilic groups[42,45,49] to improve the water solubility and cell penetration, and reduce non-specific interactions. The miniPEG γPNA with a hydrophilic diethyleneglycol side chain[45] has found widespread use in several biological applications including the control of gene expression and gene editing.

The cell-penetrable guanidine modified αGPNA and γGPNA were evaluated for anti-miRNA-210 activities in K562 chronic myelogenous leukaemic cells by Corradina *et al.* in 2012.[310] The incorporation of the arginine carrier within the GPNA backbone was shown to improve the cellular uptake and stability towards enzymatic digestion when compared to aegPNA with oligoarginine appended at the N-terminus, although the observed anti-miRNA-210 effects were similar in cell-based assays. While the enzymatic stability issue could be solved by using oligo(D-arginine), PNA-oligoarginine conjugates have been reported to be more cytotoxic than GPNA as a result of their amphipathic nature.[308] Monga *et al.* also reported an intrinsically cell-permeable antisense γ-guanidine-modified PNA (γGPNA)-aegPNA chimera designed to target either the transcription or translation start sites of the β-catenin gene in human hepatocellular cancer cells (HCC).[311] Complementary γGPNA decreased the expression level of β-catenin mRNA and protein in HepG cells while the mismatched sequence did not. Moreover, the treatment also affects the liver tumor cell biology such

Open Access Article. Published on 18 Nyenyankulu 2022. Downloaded on 2026-01-28 04:18:10.
This article is licensed under a Creative Commons Attribution-NonCommercial 3.0 Unported Licence.

as decreasing cell proliferation and survival, and expression of angiogenic factors.

Glazer *et al.*[312] reported the cellular delivery of miniPEG γPNA and γGPNA employing poly(lactide-*co*-glycolide) (PLGA) nanoparticles as a carrier. The γPNA was designed to target the CCR5 chemokine receptor mRNA transcript at the middle of the mRNA transcript. The CCR5 expression level was suppressed by a half while essentially no change in the CCR5 expression was observed with the control aegPNA and a scrambled γPNA. This suggests that the high-affinity γPNA could better inhibit the translation machinery than conventional antisense aegPNA that usually requires targeting at the 5'-UTR site. A tetra-arginine-modified tail-clamp ^{L}Ser γPNA designed to target miRNA-155 was shown to exhibit superior anticancer activities in lymphoma cell lines and in mouse models over anti-miR-155 aegPNA and a control γPNA sequence.[313] Likewise, a 22nt miniPEG γPNA designed to target miRNA-210 can suppress tumor growth in mice much better than aegPNA with the same sequence and another miniPEG γPNA with a scrambled sequence when co-delivered with PLGA nanoparticles.[314] In a more elaborated control, an antisense miniPEG γPNA conjugated with pH-low insertion peptides (pHLIP) was shown to selectively target the DNA double-strand break repair factor KU80 in tumor cells thereby making them susceptible to irradiation.[315] In most cases, it was proposed that the better biological activities of the conformationally constrained γ-modified PNA might be related to the pre-organization ability that leads to higher binding affinity. However, the increased hydrophilicity of the miniPEG γPNA could also play an important role in reducing off-target interactions that could limit the availability of the PNA to exhibit the desired biological effects.

Recently, Glazer *et al.* have reported a series of interesting studies on site-specific genome editing induced by PNA in the presence of donor DNA.[299,300,316] The genome editing in mouse bone marrow to correct the β-globin gene IVS2-654 (C → T) mutation by a miniPEG γPNA and PLGA nanoparticle platform was demonstrated *ex vivo* and *in vivo*.[317] The γPNA binds at a mixed-sequence site on the gene *via* the DNA duplex invasion, allowing the gene edit to be performed without the need of the triplex-forming sequence typically required for the aegPNA-based gene-editing.[318] Although the efficiency still requires improvement to compete with the well-developed CRISPR-Cas9 and related technologies,[319] such PNA-based gene editing appears to offer promising potential for therapeutics and beyond. However, despite the seemingly solid evidence of gene-editing by γPNA including *in vivo*[320] and *in utero*[321] studies in mouse models, a question has been raised whether the observed effects are real or just artifacts resulting from the possible aggregation of the (miniPEG) PNA onto the donor DNA.[322]

The pyrrolidinyl acpcPNA has not yet been extensively studied for biological applications. In one report, the acpcPNA designed to target the NF-κB binding site in the promoter region of the *Il6* gene was introduced to macrophage cells with the help of oxidized carbon nanoparticles and was shown to inhibit the stimulated production of *Il6* mRNA as well as IL-6 protein levels *in vitro*.[323] Enhanced cell membrane permeation of the acpcPNA was also realized by backbone modification with positively charged groups.[135]

Conclusions and outlook

This review covers the modification of PNA by introducing constraint in the aegPNA backbone. A big landscape has been provided to show what has been done and what remains to be explored. We have attempted to provide sufficient details to allow comparison of the performance and evaluation of the success of each PNA design in a systematic fashion. However, this may not be possible in all circumstances due to the availability and completeness of data issues. In many cases only data for chimeric PNA resulting from only one or two substitutions of the constrained PNA monomer along the aegPNA backbone, many of which are the homothymine or homoadenine sequences that are not typical structures, were reported. Although in some instances, the stabilization translates well into the homogeneous mixed-sequence backbone-modified PNA, the data from chimeric systems should be used with care. It is most likely that the exact stabilization/destabilization will depend on the type of nucleobase, position of modification, the extent of modification, and the nature of the nucleic acid target, among many other parameters. Destabilization upon introduction of up to a few residues may reflect the incompatibility of the modified monomer with the aegPNA duplex structure resulting in local or global distortion of the PNA structure and the modified PNA with a homogeneous backbone may show different binding profiles. Likewise, the observed stabilization should be interpreted with equal care.

There are many factors to consider in the design of conformationally constrained PNA. The purpose of the introduction of conformation constraint was to reduce the entropy loss. In order to make this strategy effective, the conformation must be locked into the right one. Many examples in this review repeatedly demonstrated that conformational constraints are more often than not have detrimental effects on the binding. The aegPNA should be regarded as a fortunate success because a balance between rigidity and flexibility (''constrained flexibility'') provides a benchmark system that already outperformed natural DNA or RNA in terms of binding affinity and specificity. The availability of several NMR and X-ray structures of PNA hybrids provides a basis for the rational design of conformationally constrained PNA. However, in reality this may not be as straightforward as it sounds. Although all the torsional angle parameters are known for each type of PNA structure, there are variations among different data sets, and even in the same structures some variations exist. In attempts to control one torsional angle, one inevitably disturbs the others. This is especially true when more than one bond in the PNA backbone is part of cyclic structures. There is an inevitable trade-off between flexibility and rigidity to find a good balance. In addition, the introduction of a cyclic structure

© 2022 The Author(s). Published by the Royal Society of Chemistry

Open Access Article. Published on 18 Nyenyankulu 2022. Downloaded on 2026-01-28 04:18:10.
This article is licensed under a Creative Commons Attribution-NonCommercial 3.0 Unported Licence.

introduces stereochemical complication which grows exponentially with the number of chiral centers incorporated thus contributing to the synthetic challenges. Stereochemistry is very important in controlling the topology of the molecule such as being in extended or helical (left-handed *vs* right-handed) conformations. Unfortunately, the effect of stereochemistry has not been fully evaluated in many PNA systems. Thus, it is likely that several promising modified PNA systems are waiting to be discovered and show their full potential.

Despite such complications, impressive progress has been made since the first discovery of aegPNA some 30 years ago. It has become clear that the introduction of conformational constraint is a viable strategy for the improvement of PNA binding affinity, base-pairing specificity, and selectivity in terms of both directional selectivity and type of target (DNA *vs* RNA). One of the best-performed strategies that also happens to be the least demanding in terms of synthetic efforts is the introduction of the γ-substitution, which pre-organizes the PNA into helical conformation to avoid an unfavorable steric clash with the PNA backbone.[42] Another successful strategy was the introduction of a cyclic structure to primarily control the β values, and the *trans*-five membered ring appeared to provide a good balance between flexibility and rigidity.[70] Alternatively, one may move beyond the aegPNA template and find an alternative scaffold as demonstrated by the acpcPNA with an α/β-peptide backbone.[117] This is akin to moving from the natural nucleic acid sugar-phosphate backbone to PNA which has already proven to be an exciting and rewarding discovery.[8] Most chiral PNAs perform well in terms of improving the directional selectivity of the achiral aegPNA, but selectivity for either DNA or RNA has not yet been fully realized. Ironically, decent selectivity for DNA over RNA and other unusual properties such as the inability to self-pair have been realized by serendipity rather than by rational design.[117]

This review also highlights the practical advantages of these modified PNAs in various applications ranging from materials science, drug discovery, cellular imaging, gene regulation, and gene editing. Although the emphasis was made on the advantages of these modified PNAs in terms of higher binding affinity and specificity, this should be regarded as the minimum requirement and not the only factor that will determine the ultimate success of the modified PNA for particular applications. Of course, many of such applications indeed rely on the high-affinity binding and take full advantage of the modified PNA that can form more stable hybrids with nucleic acid targets than aegPNA. Several other applications also clearly benefited from the higher specificity of modified PNA probes as well as the ability to incorporate functional entities directly into the PNA backbone in a precisely controlled fashion. Nevertheless, for applications in complex biological systems, other properties that should be taken into consideration include solubility, cell permeability, non-specific aggregation, off-target binding, pharmacokinetics, and pharmacodynamics, among others. In many cases, it might be difficult to judge whether the apparently better performance of modified PNA over aegPNA is due to the stronger affinity to the target as a result of the backbone modification or there are complications from indirect effects that might modulate other properties such as permeability, non-specific binding, or biological stability. Currently, little is known about such indirect effects, and more studies are still required to clarify this.

Conflicts of interest

There are no conflicts of interest to declare.

Acknowledgements

Financial support from the Thailand Research Fund through the International Research Network Grant (IRN62W0002) (to T. V.) is acknowledged. The authors also thank Miss Kotchakorn Supabowornsathit and Mr Kriangsak Faikhruea for preparing some illustrations. Molecular graphics and analyses were performed with UCSF Chimera, developed by the Resource for Biocomputing, Visualization, and Informatics at the University of California, San Francisco, with support from NIH P41-GM103311.

References

1 C. Buccitelli and M. Selbach, mRNAs, proteins and the emerging principles of gene expression control, *Nat. Rev. Genet.*, 2020, **21**, 630–644.
2 N. Chaudhary, D. Weissman and K. A. Whitehead, mRNA Vaccines for infectious diseases: Principles, delivery and clinical translation, *Nat. Rev. Drug Discovery*, 2021, **20**, 817–838.
3 K. Morihiro, Y. Kasahara and S. Obika, Biological applications of xeno nucleic acids, *Mol. Biosyst.*, 2017, **13**, 235–245.
4 K. Duffy, S. Arangundy-Franklin and P. Holliger, Modified nucleic acids: Replication, evolution, and next-generation therapeutics, *BMC Biolol.*, 2020, **18**, 112.
5 K. Ruiz-Mirazo, C. Briones and A. de la Escosura, Prebiotic systems chemistry: New perspectives for the origins of life, *Chem. Rev.*, 2014, **114**, 285–366.
6 A. Eschenmoser, Searching for nucleic acids alternatives, *Chimia*, 2005, **59**, 836–850.
7 S. Ochoa and V. T. Milam, Modified nucleic acids: Expanding the capabilities of functional oligonucleotides, *Molecules*, 2020, **25**, 4659.
8 P. E. Nielsen, M. Egholm, R. H. Berg and O. Buchardt, Sequence-selective recognition of DNA by strand displacement with a thymine-substituted polyamide, *Science*, 1991, **254**, 1497–1500.
9 M. Egholm, O. Buchardt, L. Christensen, C. Behrens, S. M. Freler, D. A. Driver, R. H. Berg, S. K. Ki, B. Norden and P. E. Nielsen, PNA hybridizes to complementary oligonucleotides obeying the Watson–Crick hydrogen-bonding rules, *Nature*, 1993, **365**, 566–568.
10 P. Muangkaew and T. Vilaivan, Modulation of DNA and RNA by PNA, *Bioorg. Med. Chem. Lett.*, 2020, **30**, 127064.

Open Access Article. Published on 18 Nyenyankulu 2022. Downloaded on 2026-01-28 04:18:10.
This article is licensed under a Creative Commons Attribution-NonCommercial 3.0 Unported Licence.

11 J. D. R. Perera, K. E. W. Carufe and P. M. Glazer, Peptide nucleic acids and their role in gene regulation and editing, *Biopolymers*, 2021, **112**, e23460.
12 V. A. Kumar and K. N. Ganesh, Conformationally constrained PNA analogs: Structural evolution toward DNA/RNA binding selectivity, *Acc. Chem. Res.*, 2005, **38**, 404–412.
13 T. Sugiyama and A. Kittaka, Chiral peptide nucleic acids with a substituent in the *N*-(2-aminoethyl)glycine backbone, *Molecules*, 2013, **18**, 287–310.
14 M. Moccia, M. F. A. Adamo and M. Saviano, Insights on chiral, backbone modified peptide nucleic acids: Properties and biological activity, *Artif. DNA: PNA & XNA*, 2014, **5**, e1107176.
15 A. Das and B. Pradhan, Evolution of peptide nucleic acid with modifications of its backbone and application in biotechnology, *Chem. Biol. Drug Des.*, 2021, **97**, 865–892.
16 N. Brodyagin, M. Katkevics, V. Kotikam, C. A. Ryan and E. Rozners, Chemical approaches to discover the full potential of peptide nucleic acids in biomedical applications, *Beilstein J. Org. Chem.*, 2021, **17**, 1641–1688.
17 K. L. Dueholm, K. H. Petersen, D. K. Jensen, M. Egholm, P. E. Nielsen and O. Buchardt, Peptide nucleic acid (PNA) with a chiral backbone based on alanine, *Bioorg. Med. Chem. Lett.*, 1994, **4**, 1077–1080.
18 G. Haaima, A. Lohse, O. Buchardt and P. E. Nielsen, Peptide nucleic acids (PNAs) containing thymine monomers derived from chiral amino acids: Hybridization and solubility properties of D-lysine pNA, *Angew. Chem., Int. Ed. Engl.*, 1996, **35**, 1939–1942.
19 A. Puschl, S. Sforza, G. Haaima, O. Dahl and P. E. Nielsen, Peptide nucleic acids (PNAs) with a functional backbone, *Tetrahedron Lett.*, 1998, **39**, 4707–4710.
20 S. Sforza, G. Haaima, R. Marchelli and P. E. Nielsen, Chiral peptide nucleic acids (PNAs): Helix handedness and DNA recognition, *Eur. J. Org. Chem.*, 1999, 197–204.
21 I. Dilek, M. Madrid, R. Singh, C. P. Urrea and B. A. Armitage, Effect of PNA backbone modifications on cyanine dye binding to PNA–DNA duplexes investigated by optical spectroscopy and molecular dynamics simulations, *J. Am. Chem. Soc.*, 2005, **127**, 3339–3345.
22 S. Sforza, R. Corradini, S. Ghirardi, A. Dossena and R. Marchelli, DNA binding of a D-lysine-based chiral PNA: Direction control and mismatch recognition, *Eur. J. Org. Chem.*, 2000, 2905–2913.
23 V. Menchise, G. De Simone, T. Tedeschi, R. Corradini, S. Sforza, R. Marchelli, D. Capasso, M. Saviano and C. Pedone, Insights into peptide nucleic acid (PNA) structural features: The crystal structure of a D-lysine-based chiral PNA–DNA duplex, *Proc. Natl. Acad. Sci. U. S. A.*, 2003, **100**, 12021–12026.
24 L. Betts, J. A. Josey, J. M. Veal and S. R. Jordan, A nucleic acid triple helix formed by a peptide nucleic acid–DNA complex, *Science*, 1995, **270**, 1838–1841.
25 M. Eriksson and P. E. Nielsen, Solution structure of a peptide nucleic acid–DNA duplex, *Nat. Struct. Biol.*, 1996, **3**, 410–413.
26 O. Almarsson and T. C. Bruice, Peptide nucleic acid (PNA) conformation and polymorphism in PNA–DNA and PNA–RNA hybrids, *Proc. Natl. Acad. Sci. U. S. A.*, 1993, **90**, 9542–9546.
27 A. Gourishankar and K. N. Ganesh, (α,α-Dimethyl)glycyl (dmg) PNAs achiral PNA analogs that form stronger hybrids with CDNA relative to isosequential RNA, *Artif. DNA: PNA & XNA*, 2012, **3**, 5–13.
28 P. Kulkarni, D. Datta, R. O. Ramabhadran and K. Ganesh, Gem-dimethyl peptide nucleic acid (α/β/γ-gdm-PNA) monomers: Synthesis and the role of gdm-substituents in preferential stabilisation of *Z*/*E*-rotamers, *Org. Biomol. Chem.*, 2021, **19**, 6534–6545.
29 K. L. Dueholm, M. Egholm, C. Behrens, L. Christensen, H. F. Hansen, T. Vulpius, K. H. Petersen, R. H. Berg, P. E. Nielsen and O. Buchardt, Synthesis of peptide nucleic acid monomers containing the four natural nucleobases: Thymine, cytosine, adenine, and guanine and their oligomerizationsynthesis of peptide nucleic acid monomers containing the four natural nucleobases: Thymine, cytosine, adenine, and guanine and their oligomerization, *J. Org. Chem.*, 1994, **59**, 5767–5773.
30 S.-M. Chen, V. Mohan, J. S. Kiely, M. C. Griffith and R. H. Griffey, Molecular dynamics and NMR studies of single-stranded PNAs, *Tetrahedron Lett*, 1994, **35**, 5105–5108.
31 M. Oleszczuk, S. Rodziewicz-Motowidlo and B. Falkiewicz, Restricted rotation in chiral peptide nucleic acid (PNA) monomers-influence of substituents studied by means of ^{1}H NMR, *Nucleos. Nucleot. Nucl.*, 2001, **20**, 1399–1402.
32 W. He, E. Hatcher, A. Balaeff, D. N. Beratan, R. R. Gil, M. Madrid and C. Achim, Solution structure of a peptide nucleic acid duplex from NMR data: Features and limitationssolution structure of a peptide nucleic acid duplex from NMR data: Features and limitations, *J. Am. Chem. Soc.*, 2008, **130**, 13264–13273.
33 W. Maison, I. Schlemminger, O. Westerhoff and J. Martens, Modified PNAs: A simple method for the synthesis of monomeric building blocks, *Bioorg. Med. Chem. Lett.*, 1999, **9**, 581–584.
34 W. Maison, I. Schlemminger, O. Westerhoff and J. Martens, Multicomponent synthesis of novel amino acid–nucleobase chimeras: A versatile approach to PNA-monomers, *Bioorg. Med. Chem.*, 2000, **8**, 1343–1360.
35 J. Martens, W. Maison, I. Schlemminger, O. Westerhoff and H. Gröger, *Precursors for PNA-monomers*, *International Patent Application*, WO 00/02864, 2000.
36 T. Sugiyama, Y. Imamura, Y. Demizu, M. Kurihara, M. Takano and A. Kittaka, β-PNA: Peptide nucleic acid (PNA) with a chiral center at the β-position of the PNA backbone, *Bioorg. Med. Chem. Lett.*, 2011, **21**, 7317–7320.
37 L. Kosynkina, W. Wang and T. C. Liang, A convenient synthesis of chiral peptide nucleic acid (PNA) monomers, *Tetrahedron Lett.*, 1994, **35**, 5173–5176.
38 E. A. Englund and D. H. Appella, Synthesis of γ-substituted peptide nucleic acids: A new place to attach fluorophores

© 2022 The Author(s). Published by the Royal Society of Chemistry

Open Access Article. Published on 18 Nyenyankulu 2022. Downloaded on 2026-01-28 04:18:10.
This article is licensed under a Creative Commons Attribution-NonCommercial 3.0 Unported Licence.

without affecting DNA binding, *Org. Lett.*, 2005, **7**, 3465–3467.

39 E. A. Englund and D. H. Appella, γ-Substituted peptide nucleic acids constructed from L-lysine are a versatile scaffold for multifunctional display, *Angew. Chem., Int. Ed.*, 2007, **46**, 1414–1418.

40 C. Dose and O. Seitz, Convergent synthesis of peptide nucleic acids by native chemical ligation, *Org. Lett.*, 2005, **7**, 4365–4368.

41 M. C. de Koning, L. Petersen, J. J. Weterings, M. Overhand, G. A. van der Marel and D. V. Filippov, Synthesis of thiol-modified peptide nucleic acids designed for post-assembly conjugation reactions, *Tetrahedron*, 2006, **62**, 3248–3258.

42 A. Dragulescu-Andrasi, S. Rapireddy, B. M. Frezza, C. Gayathri, R. R. Gil and D. H. Ly, A simple γ-backbone modification pre-organizes peptide nucleic acid into a helical structure, *J. Am. Chem. Soc.*, 2006, **128**, 10258–10267.

43 W. He, M. J. Crawford, M. Madrid, R. R. Gil, D. H. Ly and C. Achim, The structure of a γ-modified peptide nucleic acid duplexthe structure of a γ-modified peptide nucleic acid duplex, *Mol. Biosyst.*, 2010, **6**, 1619–1629.

44 J. I. Yeh, B. Shivachev, S. Rapireddy, M. J. Crawford, R. R. Gil, S. Du, M. Madrid and D. H. Ly, Crystal structure of chiral γPNA with complementary DNA strand: Insights into the stability and specificity of recognition and conformational pre-organization, *J. Am. Chem. Soc.*, 2010, **132**, 10717–10727.

45 B. Sahu, I. Sacui, S. Rapireddy, K. J. Zanotti, R. Bahal, B. A. Armitage and D. H. Ly, Synthesis and characterization of conformationally pre-organized, (*R*)-diethylene glycol-containing γ-peptide nucleic acids with superior hybridization properties and water solubility, *J. Org. Chem.*, 2011, **76**, 5614–5627.

46 D. R. Jain, L. Anandi, V. M. Lahiri and K. N. Ganesh, Influence of pendant chiral C^{γ}-(alkylideneamino/guanidino) cationic side-chains of PNA backbone on hybridization with complementary DNA/RNA and cell permeability, *J. Org. Chem.*, 2014, **79**, 9567–9577.

47 B. Sahu, V. Chenna, K. L. Lathrop, S. M. Thomas, G. Zon, K. J. Livak and D. H. Ly, Synthesis of conformationally pre-organized and cell-permeable guanidine-based γ-peptide nucleic acids (γGPNAs), *J. Org. Chem.*, 2009, **74**, 1509–1516.

48 P. Kumar and D. R. Jain, Cγ-Aminopropylene peptide nucleic acid (*amp*-PNA): Chiral cationic PNAs with superior PNA:DNA/RNA duplex stability and cellular uptake, *Tetrahedron*, 2015, **71**, 3378–3384.

49 Y. Kirillova, N. Boyarskaya, A. Dezhenkov, M. Tankevich, I. Prokhorov, A. Varizhuk, S. Eremin, D. Esipov, I. Smirnov and G. Pozmogova, Polyanionic carboxyethyl peptide nucleic acids (ce-PNAs): Synthesis and DNA binding, *PLoS One*, 2015, **10**, e0140468.

50 R. Mitra and K. N. Ganesh, PNAs grafted with (α/γ, *R*/*S*)-aminomethylene pendants: Regio and stereo specific effects on DNA binding and improved cell uptake, *Chem. Commun.*, 2011, **47**, 1198–1200.

51 R. Mitra and K. N. Ganesh, Aminomethylene peptide nucleic acid (am-PNA): Synthesis, regio-/stereospecific DNA binding, and differential cell uptake of (α/γ,*R*/*S*)am-PNA analogs, *J. Org. Chem.*, 2012, **77**, 5696–5704.

52 C. Avitabile, L. Moggio, G. Malgieri, D. Capasso, S. Di Gaetano, M. Saviano, C. Pedone and A. Romanelli, γ-Sulphate PNA (PNA S): Highly selective DNA binding molecule showing promising antigene activity, *PLoS One*, 2012, **7**, e35774.

53 N. T. S. De Costa and J. M. Heemstra, Differential DNA and RNA sequence discrimination by PNA having charged side chains, *Bioorg. Med. Chem. Lett.*, 2014, **24**, 2360–2363.

54 G. Haaima, H. Rasmussen, G. Schmidt, D. K. Jensen, J. S. Kastrup, P. W. Stafshede, B. Norden, O. Buchardt and P. E. Nielsen, Peptide nucleic acids (PNA) derived from *N*-(*N*-methylaminoethyl)glycine. Synthesis, hybridization and structural properties, *New J. Chem.*, 1999, **23**, 833–840.

55 T. Tedeschi, S. Sforza, R. Corradini and R. Marchelli, Synthesis of new chiral PNAs bearing a dipeptide-mimic monomer with two lysine-derived stereogenic centres, *Tetrahedron Lett.*, 2005, **46**, 8395–8399.

56 S. Sforza, T. Tedeschi, R. Corradini and R. Marchelli, Induction of helical handedness and DNA binding properties of peptide nucleic acids (PNAs) with two stereogenic centres, *Eur. J. Org. Chem.*, 2007, 5879–5885.

57 T. Bose, A. Banerjee, S. Nahar, S. Maiti and V. A. Kumar, β,γ-Bis-substituted PNA with configurational and conformational switch: Preferred binding to CDNA/RNA and cell-uptake studies, *Chem. Commun.*, 2015, **51**, 7693–7696.

58 P. Lagriffoule, P. Wittung, M. Eriksson, K. K. Jensen, B. Norden, O. Buchardt and P. E. Nielsen, Peptide nucleic acids with a conformationally constrained chiral cyclohexyl-derived backbone, *Chem. – Eur. J.*, 1997, **3**, 912–919.

59 T. Govindaraju, R. G. Gonnade, M. M. Bhadbhade, V. A. Kumar and K. N. Ganesh, (1*S*,2*R*/1*R*,2*S*)-Aminocyclohexyl glycyl thymine PNA: Synthesis, monomer crystal structures, and DNA/RNA hybridization studies, *Org. Lett.*, 2003, **5**, 3013–3016.

60 T. Govindaraju, V. A. Kumar and K. N. Ganesh, (1*S*,2*R*/1*R*,2*S*)-*cis*-Cyclopentyl PNAs (cpPNAs) as constrained PNA analogs: Synthesis and evaluation of aeg-cpPNA chimera and stereopreferences in hybridization with DNA/RNA, *J. Org. Chem.*, 2004, **69**, 5725–5734.

61 T. Govindaraju, V. Madhuri, V. A. Kumar and K. N. Ganesh, Cyclohexanyl peptide nucleic acids (chPNAs) for preferential RNA binding: Effective tuning of dihedral angle β in PNAs for DNA/RNA discrimination, *J. Org. Chem.*, 2006, **71**, 14–21.

62 S. Sharma, U. B. Sonavane and R. R. Joshi, Molecular dynamics simulations of cyclohexyl modified peptide nucleic acids (PNA), *J. Biomol. Struct.*, 2010, **27**, 663–676.

63 S. C. Brown, S. A. Thomson, J. M. Veal and D. G. Davis, NMR solution structure of a peptide nucleic acid complexed with RNA, *Science*, 1994, **265**, 777–780.

64 T. Govindaraju, V. A. Kumar and K. N. Ganesh, (*SR*/*RS*)-Cyclohexanyl PNAs: Conformationally pre-organized PNA

Open Access Article. Published on 18 Nyenyankulu 2022. Downloaded on 2026-01-28 04:18:10.
This article is licensed under a Creative Commons Attribution-NonCommercial 3.0 Unported Licence.

analogs with unprecedented preference for duplex formation with RNA, *J. Am. Chem. Soc.*, 2005, **127**, 4144–4145.
65 J. K. Pokorski, M. A. Witschi, B. L. Purnell and D. H. Appella, (*S*,*S*)-*trans*-Cyclopentane-constrained peptide nucleic acids. A general backbone modification that improves binding affinity and sequence specificity, *J. Am. Chem. Soc.*, 2004, **126**, 15067–15073.
66 A. Sharma, S. H. More and K. N. Ganesh, Electrostatics Favor PNA: DNA stability over stereochemistry in pyrrolidine-based cationic dual-backbone PNA analogs, *Eur. J. Org. Chem.*, 2021, 1146–1155.
67 H. Zheng, M. Saha and D. H. Appella, Synthesis of Fmoc-protected (*S*,*S*)-*trans*-cyclopentane diamine monomers enables the preparation and study of conformationally restricted peptide nucleic acids, *Org. Lett.*, 2018, **20**, 7637–7640.
68 T. Govindaraju, V. A. Kumar and K. N. Ganesh, *cis*-Cyclopentyl PNA (*cp*PNA) as constrained chiral PNA analogs: Stereochemical dependence of DNA/RNA hybridization, *Chem. Commun.*, 2004, 860–861.
69 M. C. Myers, M. A. Witschi, N. V. Larionova, J. M. Franck, R. D. Haynes, T. Hara, A. Grajkowski and D. H. Appella, A cyclopentane conformational restraint for a peptide nucleic acid: Design, asymmetric synthesis, and improved binding affinity to DNA and RNA, *Org. Lett.*, 2003, **5**, 2695–2698.
70 E. A. Englund, Q. Xu, M. A. Witschi and D. H. Appella, PNA–DNA duplexes, triplexes, and quadruplexes are stabilized with *trans*-cyclopentane units, *J. Am. Chem. Soc.*, 2006, **128**, 16456–16457.
71 H. Zheng, I. Botos, V. Clausse, H. Nikolayevskiy, E. E. Rastede, M. F. Fouz, S. J. Mazur and D. H. Appella, Conformational constraints of cyclopentane peptide nucleic acids facilitate tunable binding to DNA, *Nucleic Acids Res.*, 2021, **49**, 713–725.
72 J. K. Pokorski, M. C. Myers and D. H. Appella, Cyclopropane PNA: observable triplex melting in A PNA constrained with A 3-membered ring, *Tetrahedron Lett.*, 2005, **46**, 915–917.
73 S. Jordan, C. Schwemler, W. Kosch, A. Kretschmer, E. Schwenner, U. Stropp and B. Mielke, Synthesis of new building blocks for peptide nucleic acids containing monomers with variations in the backbone, *Bioorg. Med. Chem. Lett.*, 1997, **7**, 681–686.
74 S. Jordan, C. Schwemler, W. Kosch, A. Kretschmer, U. Stropp, E. Schwenner and B. Mielke, New heterooligomeric peptide nucleic acids with improved binding properties to complementary DNA, *Bioorg. Med. Chem. Lett.*, 1997, **7**, 687–690.
75 B. P. Gangamani, V. A. Kumar and K. N. Ganesh, Synthesis of Nα-(purinyl/pyrimidinyl acetyl)-4-aminoproline diastereomers with potential use in PNA synthesis, *Tetrahedron*, 1996, **52**, 15017–15030.
76 B. P. Gangamani, M. D'costa, V. A. Kumar and K. N. Ganesh, Conformationally restrained chiral PNA conjugates: Synthesis and DNA complementation studies, *Nucleos. Nucleot.*, 1999, **18**, 1409–1411.
77 A. Puschl, T. Boesen, G. Zuccarello, O. Dahl, S. Pitsch and P. E. Nielsen, Synthesis of pyrrolidinone PNA: A novel conformationally restricted PNA analog, *J. Org. Chem.*, 2001, **66**, 707–712.
78 A. Püschl, T. Boesen, T. Tedeschi, O. Dahl and P. E. Nielsen, Synthesis of (3*R*,6*R*)- and (3*S*,6*R*)-piperidinone PNA, *J. Chem. Soc., Perkin Trans. 1*, 2001, 2757–2763.
79 A. Puschl, T. Tedeschi and P. E. Nielsen, Pyrrolidine PNA: A novel conformationally restricted PNA analog, *Org. Lett.*, 2000, **2**, 4161–4163.
80 D. T. Hickman, P. M. King, M. A. Cooper, J. M. Slater and J. Micklefield, Unusual RNA and DNA binding properties of a novel pyrrolidine–amide oligonucleotide mimic (POM), *Chem. Commun.*, 2000, 2251–2252.
81 T. H. Samuel Tan, D. T. Hickman, J. Morral, I. G. Beadham and J. Micklefield, Nucleic acid binding properties of thyminyl and adeninyl pyrrolidine-amide oligonucleotide mimics (POM), *Chem. Commun.*, 2004, 516–517.
82 R. J. Worthington, A. P. O'Rourke, J. Morral, T. H. Samuel Tan and J. Micklefield, Mixed-sequence pyrrolidine-amide oligonucleotide mimics: Boc(Z) synthesis and DNA/RNA binding properties, *Org. Biomol. Chem.*, 2007, **5**, 249–259.
83 J. A. Hodges and R. T. Raines, Stereoelectronic effects on collagen stability: The dichotomy of 4-fluoroproline diastereomers, *J. Am. Chem. Soc.*, 2003, **125**, 9262–9263.
84 R. W. Newberry and R. T. Raines, 4-Fluoroprolines: Conformational analysis and effects on the stability and folding of peptides and proteins, *Top. Heterocycl. Chem.*, 2017, **48**, 1–25.
85 T. H. Samuel Tan, R. J. Worthington, R. G. Pritchard, J. Morral and J. Micklefield, Homopolymeric pyrrolidine-amide oligonucleotide mimics: Fmoc-synthesis and DNA/RNA binding properties, *Org. Biomol. Chem.*, 2007, **5**, 239–248.
86 Y. Li, T. Jin and K. Liu, Synthesis and binding affinity of a chiral PNA analog, *Nucleos. Nucleot. Nucl.*, 2001, **20**, 1705–1721.
87 M. D'Costa, V. A. Kumar and K. N. Ganesh, Aminoethylprolyl (*aep*) PNA: Mixed purine/pyrimidine oligomers and binding orientation preferences for PNA:DNA duplex formation, *Org. Lett.*, 2001, **3**, 1281–1284.
88 M. D'Costa, V. A. Kumar and K. N. Ganesh, Aminoethylprolyl peptide nucleic acids (aepPNA): Chiral PNA analogs that form highly stable DNA:aepPNA$_2$ triplexes, *Org. Lett.*, 1999, **1**, 1513–1516.
89 T. Vilaivan, C. Khongdeesameor, P. Harnyuttanakorn, M. S. Westwell and G. Lowe, Synthesis and properties of chiral peptide nucleic acids with a *N*-aminoethyl-D-proline backbone, *Bioorg. Med. Chem. Lett.*, 2000, **10**, 2541–2545.
90 P. Ngamwiriyawong and T. Vilaivan, Synthesis and nucleic acids binding properties of diastereomeric aminoethylprolyl peptide nucleic acids (aepPNA), *Nucleos. Nucleot. Nucl.*, 2011, **30**, 97–112.
91 P. S. Shirude, V. A. Kumar and K. N. Ganesh, (2S,5R/2R,5S)-Aminoethylpipecolyl aepip-aegPNA Chimera: Synthesis

© 2022 The Author(s). Published by the Royal Society of Chemistry

Open Access Article. Published on 18 Nyenyankulu 2022. Downloaded on 2026-01-28 04:18:10.
This article is licensed under a Creative Commons Attribution-NonCommercial 3.0 Unported Licence.

and Duplex/Triplex Stability, *Tetrahedron*, 2004, **60**, 9485–9491.

92 N. K. Sharma and K. N. Ganesh, Expanding the repertoire of pyrrolidyl PNA analogs for DNA/RNA hybridization selectivity: Aminoethylpyrrolidinone PNA (*aepone*-PNA), *Chem. Commun.*, 2003, 2484–2485.

93 N. K. Sharma and K. N. Ganesh, Base dependent pyrrolidine ring pucker in aep-PNA monomers: NMR and PSEUROT analysis, *Tetrahedron*, 2010, **66**, 9165–9170.

94 P. S. Shirude, V. A. Kumar and K. N. Ganesh, Chimeric peptide nucleic acids incorporating (2*S*,5*R*)-aminoethyl pipecolyl units: Synthesis and DNA binding studies, *Tetrahedron Lett.*, 2004, **45**, 3085–3088.

95 P. S. Lonkar and V. A. Kumar, Design and synthesis of conformationally frozen peptide nucleic acid backbone: Chiral piperidine PNA as a hexitol nucleic acid surrogate, *Bioorg. Med. Chem. Lett.*, 2004, **14**, 2147–2149.

96 S. Bregant, F. Burlina, J. Vaissermann and G. Chassaing, Synthesis and hybridization properties of thiazolidine PNAs, *Eur. J. Org. Chem.*, 2001, 3285–3294.

97 S. Bregant, F. Burlina and G. Chassaing, New thiazane and thiazolidine PNA Monomers: Synthesis, incorporation into PNAs and hybridization studies, *Bioorg. Med. Chem. Lett.*, 2002, **12**, 1047–1050.

98 A. Slaitas and E. Yeheskiely, A novel *N*-(pyrrolidinyl-2-methyl)glycine-based PNA with a strong preference for RNA over DNA, *Eur. J. Org. Chem.*, 2002, 2391–2399.

99 S. S. Gokhale and V. A. Kumar, Amino/guanidino-functionalized *N*-(pyrrolidin-2-ethyl) glycine-based pet-PNA: Design, synthesis and binding with DNA/RNA, *Org. Biomol. Chem.*, 2010, **8**, 3742–3750.

100 A. Banerjee and V. A. Kumar, $C^{3'}$-Endo-puckered pyrrolidine containing PNA has favorable geometry for RNA binding: Novel ethano locked PNA (ethano-PNA), *Bioorg. Med. Chem.*, 2013, **21**, 4092–4101.

101 R. J. Worthington, N. M. Bell, R. Wong and J. Micklefield, RNA-selective cross-pairing of backbone-extended pyrrolidine-amide oligonucleotide mimics (bePOMs), *Org. Biomol. Chem.*, 2008, **6**, 92–103.

102 T. Govindaraju and V. A. Kumar, Backbone extended pyrrolidine PNA (bepPNA): A chiral PNA for selective RNA recognition, *Tetrahedron*, 2006, **62**, 2321–2330.

103 P. S. Lonkar, V. A. Kumar and K. N. Ganesh, Constrained flexibility in PNA:DNA binding studies with bridged aminopropylglycyl PNA, *Nucleos. Nucleot. Nucl.*, 2001, **20**, 1197–1200.

104 P. S. Lonkar and V. A. Kumar, *trans*-5-Aminopipecolyl-*aeg*PNA chimera: Design, synthesis, and study of binding preferences with DNA/RNA in duplex/triplex mode, *J. Org. Chem.*, 2005, **70**, 6956–6959.

105 L. D. Fader, M. Boyd and Y. S. Tsantrizos, Backbone modifications of aromatic peptide nucleic acid (APNA) monomers and their hybridization properties with DNA and RNA, *J. Org. Chem.*, 2001, **66**, 3372–3379.

106 L. D. Fader and Y. S. Tsantrizos, Hybridization properties of aromatic peptide nucleic acids: A novel class of oligonucleotide analogs, *Org. Lett.*, 2002, **4**, 63–66.

107 L. D. Fader, E. L. Myersa and Y. S. Tsantrizos, Synthesis of novel analogs of aromatic peptide nucleic acids (APNAs) with modified conformational and electrostatic properties, *Tetrahedron*, 2004, **60**, 2235–2246.

108 M. Kuwahara, M. Arimitsu and M. Sisido, Novel peptide nucleic acid that shows high sequence specificity and all-or-none-type hybridization with the complementary DNA, *J. Am. Chem. Soc.*, 1999, **121**, 256–257.

109 M. Kuwahara, M. Arimitsu, M. Shigeyasu, N. Saeki and M. Sisido, Hybridization between oxy-peptide nucleic acids and DNAs: Dependence of hybrid stabilities on the chain-lengths, types of base pairs, and the chain directions, *J. Am. Chem. Soc.*, 2001, **123**, 4653–4658.

110 M. Kitamatsu, M. Shigeyasu, M. Saitoh and M. Sisido, Configurational preference of pyrrolidine-based oxy-peptide nucleic acids as hybridization counterparts with DNA and RNA, *Biopolymers*, 2006, **84**, 267–273.

111 M. Kitamatsu, M. Shigeyasu, T. Okada and M. Sisido, Oxy-peptide nucleic acid with a pyrrolidine ring that is configurationally optimized for hybridization with DNA, *Chem. Commun.*, 2004, 1208–1209.

112 M. Kitamatsu, T. Kashiwagi, R. Matsuzaki and M. Sisido, Synthesis of a novel pyrrolidine-based peptide nucleic acid that contains tertiary amines in the main chain and its internalization into cells, *Chem. Lett.*, 2006, **35**, 300–301.

113 K. Gogoi and V. A. Kumar, Chimeric (α-amino acid + nucleoside-β-amino acid)$_n$ peptide oligomers show sequence specific DNA/RNA recognition, *Chem. Commun.*, 2008, 706–708.

114 A. Banerjee, S. Bagmare, M. Varada and V. A. Kumar, Glycine-linked nucleoside-β-amino acids: Polyamide analogs of nucleic acids, *Bioconjugate Chem.*, 2015, **26**, 1737–1742.

115 R. Threlfall, A. Davies, N. M. Howarth, J. Fisher and R. Cosstick, Peptides derived from nucleoside β-amino acids form an unusual 8-helix, *Chem. Commun.*, 2008, 585–587.

116 S. Bagmare, M. D'Costa and V. A. Kumar, Effect of chirality of L/D-proline and prochiral glycine as the linker amino acid in five-atom linked thymidinyl-(α-amino acid)-thymidine dimers, *Chem. Commun.*, 2009, 6646–6648.

117 T. Vilaivan, Pyrrolidinyl PNA with α/β-dipeptide backbone: From development to applications, *Acc. Chem. Res.*, 2015, **48**, 1645–1656.

118 G. Lowe, T. Vilaivan and M. S. Westwell, Hybridization studies with chiral peptide nucleic acids, *Bioorg. Chem.*, 1997, **25**, 321–329.

119 D. H. Appella, L. A. Christianson, D. A. Klein, M. R. Richards, D. R. Powell and S. H. Gellman, Synthesis and structural characterization of helix-forming β-peptides: *trans*-2-Aminocyclopentanecarboxylic acid oligomers, *J. Am. Chem. Soc.*, 1999, **121**, 6206–6212.

120 T. Vilaivan, C. Suparpprom, P. Harnyuttanakorn and G. Lowe, Synthesis and properties of novel pyrrolidinyl PNA carrying β-amino acid spacers, *Tetrahedron Lett.*, 2001, **42**, 5533–5536.

© 2022 The Author(s). Published by the Royal Society of Chemistry

Open Access Article. Published on 18 Nyenyankulu 2022. Downloaded on 2026-01-28 04:18:10.
This article is licensed under a Creative Commons Attribution-NonCommercial 3.0 Unported Licence.

121 T. Vilaivan and G. Lowe, A novel pyrrolidinyl PNA showing high sequence specificity and preferential binding to DNA over RNA, *J. Am. Chem. Soc.*, 2002, **124**, 9326–9327.

122 T. Vilaivan, C. Suparpprom, P. Duanglaor, P. Harnyuttanakorn and G. Lowe, Synthesis and nucleic acid binding studies of novel pyrrolidinyl PNA carrying an *N*-amino-*N*-methylglycine spacer, *Tetrahedron Lett.*, 2003, **44**, 1663–1666.

123 C. Suparpprom, C. Srisuwannaket, P. Sangvanich and T. Vilaivan, Synthesis and oligo- deoxynucleotide binding properties of pyrrolidinyl peptide nucleic acids bearing prolyl-2-aminocyclopentanecarboxylic acid (ACPC) backbones, *Tetrahedron Lett.*, 2005, **46**, 2833–2837.

124 T. Vilaivan and C. Srisuwannaket, Hybridization of pyrrolidinyl peptide nucleic acids and DNA: Selectivity, base-pairing specificity, and direction of binding, *Org. Lett.*, 2006, **8**, 1897–1900.

125 C. Vilaivan, C. Srisuwannaket, C. Ananthanawat, C. Suparpprom, J. Kawakami, Y. Yamaguchi, Y. Tanaka and T. Vilaivan, Pyrrolidinyl peptide nucleic acid with α/β-peptide backbone a conformationally constrained PNA with unusual hybridization properties, *Artif. DNA: PNA & XNA*, 2011, **2**, 50–59.

126 K. Siriwong, P. Chuichay, S. Saen-oon, C. Suparpprom, T. Vilaivan and S. Hannongbua, Insight into why pyrrolidinyl peptide nucleic acid binding to DNA is more stable than the DNA·DNA duplex, *Biochem. Biophys. Res. Commun.*, 2008, **372**, 765–771.

127 N. Poomsuk, T. Remsungnen, T. Vilaivan, A. J. Hunt and K. Siriwong, Conformational and energetic properties of pyrrolidinyl PNA–DNA duplexes: A molecular dynamics simulation, *Comput. Theor. Chem.*, 2017, **1122**, 27–33.

128 N. Poomsook, T. Vilaivan and K. Siriwong, Insights into the structural features and stability of peptide nucleic acid with a D-prolyl-2-aminocyclopentane carboxylic acid backbone that binds to DNA and RNA, *J. Mol. Graph. Modell.*, 2018, **84**, 36–42.

129 A. Maitarad, N. Poomsuk, C. Vilaivan, T. Vilaivan and K. Siriwong, Insight into a conformation of the PNA–PNA duplex with (2'*R*,4'*R*)- and (2'*R*,4'*S*)-prolyl-(1*S*,2*S*)-2-aminocyclopentanecarboxylic acid backbones, *Chem. Phys. Lett.*, 2018, **698**, 132–137.

130 J. Taechalertpaisarn, P. Sriwarom, C. Boonlua, N. Yotapan, C. Vilaivan and T. Vilaivan, DNA-, RNA- and self-pairing properties of a pyrrolidinyl peptide nucleic acid with a (2'*R*,4'*S*)-Prolyl-(1*S*,2*S*)-2-aminocyclopentanecarboxylic acid backbone, *Tetrahedron Lett.*, 2010, **51**, 5822–5826.

131 N. Reenabthue, C. Boonlua, C. Vilaivan, T. Vilaivan and C. Suparpprom, 3-Aminopyrrolidine-4-carboxylic acid as versatile handle for internal labeling of pyrrolidinyl PNA, *Bioorg. Med. Chem. Lett.*, 2011, **21**, 6465–6469.

132 P. Sriwarom, P. Padungros and T. Vilaivan, Synthesis and DNA/RNA binding properties of conformationally constrained pyrrolidinyl PNA with a tetrahydrofuran backbone deriving from deoxyribose, *J. Org. Chem.*, 2015, **80**, 7058–7065.

133 C. Boonlua, B. Ditmangklo, N. Reenabthue, C. Suparpprom, N. Poomsuk, K. Siriwong and T. Vilaivan, Pyrene-labeled pyrrolidinyl peptide nucleic acid as a hybridization-responsive DNA Probe: Comparison between internal and terminal labeling, *RSC Adv.*, 2014, **4**, 8817–8827.

134 B. Ditmangklo, C. Boonlua, C. Suparpprom and T. Vilaivan, Reductive alkylation and sequential reductive alkylation-click chemistry for on-solid-support modification of pyrrolidinyl peptide nucleic acid, *Bioconjugate Chem.*, 2013, **24**, 614–625.

135 H. PansuwanH. Pansuwan, B. Ditmangklo, C. Vilaivan, B. Jiangchareon, P. Pan-In, S. Wanichwecha, T. Palaga, T. Nuanyai, C. Suparpprom and T. Vilaivan, Hydrophilic and cell-penetrable pyrrolidinyl peptide nucleic acid via post-synthetic modification with hydrophilic side chains, *Bioconjugate Chem.*, 2017, **28**, 2284–2292.

136 P. Seankongsuk, V. Vchirawongkwin, R. W. Bates, P. Padungros and T. Vilaivan, Enantioselective synthesis of (2*S*,3*S*)-*Epi*-oxetin and its incorporation into conformationally constrained pyrrolidinyl PNA with an oxetane backbone, *Asian J. Org. Chem.*, 2017, **6**, 551–560.

137 W. Mansawat, C. Vilaivan, A. Balazs, D. J. Aitken and T. Vilaivan, Pyrrolidinyl peptide nucleic acid homologues: Effect of ring size on hybridization properties, *Org. Lett.*, 2012, **14**, 1440–1443.

138 D. H. Appella, L. A. Christianson, I. L. Karle, D. R. Powell and S. H. Gellman, Synthesis and characterization of *trans*-2-aminocyclohexanecarboxylic acid oligomers: An unnatural helical secondary structure and implications for β-peptide tertiary structure, *J. Am. Chem. Soc.*, 1999, **121**, 6206–6212.

139 D. H. Appella, L. A. Christianson, D. A. Klein, M. R. Richards, D. R. Powell and S. H. Gellman, Synthesis and structural characterization of helix-forming β-peptides: trans-2-Aminocyclopentanecarboxylic acid oligomerssynthesis and structural characterization of helix-forming β-peptides: trans-2-Aminocyclopentanecarboxylic acid oligomers, *J. Am. Chem. Soc.*, 1999, **121**, 7574–7581.

140 C. Fernandes, S. Faure, E. Pereira, V. Théry, V. Declerck, R. Guillot and D. J. Aitken, 12-Helix folding of cyclobutane β-amino acid oligomers, *Org. Lett.*, 2010, **12**, 3606–3609.

141 B. Ditmangklo, W. Sittiwong, T. Boddaert, T. Vilaivan and D. J. Aitken, Pyrrolidinyl peptide nucleic acids bearing hydroxy-modified cyclobutane building blocks: Synthesis and binding properties, *Biopolymers*, 2021, **112**, e23459.

142 H. Kashida, K. Murayama, T. Toda and H. Asanuma, Control of the chirality and helicity of oligomers of serinol nucleic acid (SNA) by sequence design, *Angew. Chem., Int. Ed.*, 2011, **50**, 1285–1288.

143 H. Asanuma, T. Toda, K. Murayama, X. Liang and H. Kashida, Unexpectedly stable artificial duplex from flexible acyclic threoninol, *J. Am. Chem. Soc.*, 2010, **132**, 14702–14703.

144 K. Murayama, Y. Tanaka, T. Toda, H. Kashida and H. Asanuma, Highly stable duplex formation by artificial nucleic acids acyclic threoninol nucleic acid (aTNA) and

 © 2022 The Author(s). Published by the Royal Society of Chemistry

Open Access Article. Published on 18 Nyenyankulu 2022. Downloaded on 2026-01-28 04:18:10.
This article is licensed under a Creative Commons Attribution-NonCommercial 3.0 Unported Licence.

serinol nucleic acid (SNA) with acyclic scaffolds, *Chem. – Eur. J.*, 2013, **19**, 14151–14158.

145 K. Murayama, H. Kashida and H. Asanuma, Acyclic L-threoninol nucleic acid (L-aTNA) with suitable structural rigidity cross-pairs with DNA and RNA, *Chem. Commun.*, 2015, **51**, 6500–6503.

146 H. Rasmussen, J. S. Kastrup, J. N. Nielsen, J. M. Nielsen and P. E. Nielsen, Crystal structure of a peptide nucleic acid (PNA) duplex at 1.7 Å resolution, *Nat. Struct. Biol*, 1997, **4**, 98–101.

147 A. Kiliszek, K. Banaszak, Z. Dauter and W. Rypniewski, The First crystal structures of RNA–PNA duplexes and a PNA–PNA duplex containing mismatches–toward anti-sense therapy against TREDs, *Nucleic Acids Res.*, 2016, **44**, 1937–1943.

148 R. Schütz, M. Cantin, C. Roberts, B. Greiner, E. Uhlmann and C. Leumann, Olefinic peptide nucleic acids (OPAs): New aspects of the molecular recognition of DNA by PNA, *Angew. Chem., Int. Ed.*, 2000, **39**, 1250–1253.

149 M. Hollenstein and C. J. Leumann, Synthesis and incorporation into PNA of fluorinated olefinic PNA (F-OPA) monomers, *Org. Lett.*, 2003, **5**, 1987–1990.

150 M. Hollenstein and C. J. Leumann, Fluorinated olefinic peptide nucleic acid: Synthesis and pairing properties with complementary DNA, *J. Org. Chem.*, 2005, **70**, 3205–3217.

151 D. Wei, W. D. Wilson and S. Neidle, Small-molecule binding to the DNA minor groove is mediated by a conserved water cluster, *J. Am. Chem. Soc.*, 2013, **135**, 1369–1377.

152 N. C. Horton and B. C. Finzel, The structure of an RNA/DNA hybrid: A substrate of the ribonuclease activity of HIV-1 reverse transcriptase, *J. Mol. Biol.*, 1996, **264**, 521–533.

153 B. B. Chevrier, A. Podjarny, J. Johnson, J. S. de Bear, G. R. Gough, P. T. Gilham and D. Moras, Crystallographic structure of an RNA Helix: $[U(UA)_6A]_2$, *J. Mol. Biol.*, 1989, **209**, 459–474.

154 T. Ishizuka, J. Yoshida, Y. Yamamoto, J. Sumaoka, T. Tedeschi, R. Corradini, S. Sforza and M. Komiyama, Chiral introduction of positive charges to PNA for double-duplex invasion to versatile sequences, *Nucleic Acids Res.*, 2008, **36**, 1464–1471.

155 J. Saarbach, P. M. Sabale and N. Winssinger, Peptide nucleic acid (PNA) and its applications in chemical biology, diagnostics, and therapeutics, *Curr. Opin. Chem. Biol.*, 2019, **52**, 112–124.

156 H. Ørum, P. E. Nielsen, M. Egholm, R. H. Berg, O. Buchardt and C. Stanley, Single base pair mutation analysis by PNA directed PCR clamping, *Nucleic Acids Res.*, 1993, **21**, 5332–5336.

157 X. Liang, M. Liu and M. Komiyama, Recognition of target site in various forms of DNA and RNA by peptide nucleic acid (PNA): From fundamentals to practical applications, *Bull. Chem. Soc. Jpn.*, 2021, **94**, 1737–1756.

158 S. Buchini and C. Leumann, Recent improvements in antigene technology, *Curr. Opin. Chem. Biol.*, 2003, **3**, 717–746.

159 B. Vester and J. Wengel, LNA (locked nucleic acid): High-affinity targeting of complementary RNA and DNA, *Biochemistry*, 2004, **43**, 13233–13241.

160 T. Bentin, H. J. Larsen and P. E. Nielsen, Combined triplex/duplex invasion of double-stranded DNA by ''Tail-Clamp'' peptide nucleic acid, *Biochemistry*, 2003, **42**, 13987–13995.

161 K. Kaihatsu, R. H. Shah, X. Zhao and D. R. Corey, Extending recognition by peptide nucleic acids (PNAs): Binding to duplex DNA and inhibition of transcription by tail-clamp PNA-peptide conjugates, *Biochemistry*, 2003, **42**, 13996–14003.

162 J. Lohse, O. Dahl and P. E. Nielsen, Double duplex invasion by peptide nucleic acid: A general principle for sequence-specific targeting of double-stranded DNA, *Proc. Natl. Acad. Sci. U. S. A.*, 1999, **96**, 11804–11808.

163 M. Hibino, Y. Aiba and O. Shoji, Cationic guanine: Positively charged nucleobase with improved DNA affinity inhibits self-duplex formation, *Chem. Commun.*, 2020, **56**, 2546–2549.

164 A. Maitarad, N. Poomsuk, C. Vilaivan, T. Vilaivan and K. Siriwong, Insight into a conformation of the PNA–PNA duplex with (2'*R*,4'*R*)- and (2'*R*,4'*S*)-prolyl-(1*S*,2*S*)-2-aminocyclopentanecarboxylic acid backbones, *Chem. Phys. Lett.*, 2018, **698**, 132–137.

165 P. R. Bohländer, T. Vilaivan and H.-A. Wagenknecht, Strand displacement and duplex invasion into double-stranded DNA by pyrrolidinyl peptide nucleic acids, *Org. Biomol. Chem.*, 2015, **13**, 9223–9230.

166 N. Yotapan, D. Nim-anussornkul and T. Vilaivan, Pyrrolidinyl peptide nucleic acid terminally labeled with fluorophore and end-stacking quencher as a probe for highly specific DNA sequence discrimination, *Tetrahedron*, 2016, **72**, 7992–7999.

167 G. He, S. Rapireddy, R. Bahal, B. Sahu and D. H. Ly, Strand invasion of extended, mixed-sequence B-DNA by γPNAs, *J. Am. Chem. Soc.*, 2009, **131**, 12088–12090.

168 R. Bahal, B. Sahu, S. Rapireddy, C.-M. Lee and D. H. Ly, Sequence-unrestricted, Watson–Crick recognition of double helical B-DNA by (*R*)-MiniPEG-γPNAs, *ChemBioChem*, 2012, **13**, 56–60.

169 S. Rapireddy, G. He, S. Roy, B. A. Armitage and D. H. Ly, Strand invasion of mixed-sequence B-DNA by acridine-linked, γ-peptide nucleic acid (γ-PNA), *J. Am. Chem. Soc.*, 2007, **129**, 15596–15600.

170 V. Chenna, S. Rapireddy, B. Sahu, C. Ausin, E. Pedroso and D. H. Ly, A simple cytosine to G-clamp nucleobase substitution enables chiral γ-PNAs to invade mixed-sequence double-helical B-form DNA, *ChemBioChem*, 2008, **9**, 2388–2391.

171 H. Kuhn, B. Sahu, S. Rapireddy, D. H. Ly and M. D. Frank-Kamenetskii, Sequence specificity at targeting double-stranded DNA with A γ-PNA oligomer modified with guanidinium G-clamp nucleobases, *Artif. DNA: PNA & XNA*, 2010, **1**, 45–53.

172 S. Rapireddy, R. Bahal and D. H. Ly, Strand invasion of mixed-sequence, double-helical B-DNA by γ-peptide

Open Access Article. Published on 18 Nyenyankulu 2022. Downloaded on 2026-01-28 04:18:10.
This article is licensed under a Creative Commons Attribution-NonCommercial 3.0 Unported Licence.

nucleic acids containing G-clamp nucleobases under physiological conditions, *Biochemistry*, 2011, **50**, 3913–3918.

173 M. Lyu, L. Kong, Z. Yang, Y. Wu, C. E. McGhee and Y. Lu, PNA-assisted DNAzymes to cleave double-stranded DNA for genetic engineering with high sequence fidelity, *J. Am. Chem. Soc.*, 2021, **143**, 9724–9728.

174 S. A. Thadke, V. M. Hridya, J. D. R. Perera, R. R. Gil, A. Mukherjee and D. H. Ly, Shape selective bifacial recognition of double helical DNA, *Commun. Chem.*, 2018, **1**, 79.

175 R. G. Emehiser and P. J. Hrdlicka, Chimeric γPNA–invader probes: Using intercalator-functionalized oligonucleotides to enhance the DNA-targeting properties of γPNA, *Org. Biomol. Chem.*, 2020, **18**, 1359–1368.

176 I. Sacui, W.-C. Hsieh, A. Manna, B. Sahu and D. H. Ly, Gamma peptide nucleic acids: As orthogonal nucleic acid recognition codes for organizing molecular self-assembly, *J. Am. Chem. Soc.*, 2015, **137**, 8603–8610.

177 S. A. Thadke, J. D. R. Perera, V. M. Hridya, K. Bhatt, A. Y. Shaikh, W.-C. Hsieh, M. Chen, C. Gayathri, R. R. Gil, G. S. Rule, A. Mukherjee, C. A. Thornton and D. H. Ly, Design of bivalent nucleic acid ligands for recognition of RNA repeated expansion associated with Huntington's disease, *Biochemistry*, 2018, **57**, 2094–2108.

178 R. Bahal, A. Manna, W.-C. Hsieh, S. A. Thadke, G. Sureshkumar and D. H. Ly, RNA-Templated concatenation of triplet nucleic-acid probe, *ChemBioChem*, 2018, **19**, 674–678.

179 T. Zengeya, P. Gupta and E. Rozners, Triple-helical recognition of RNA using 2-aminopyridine-modified PNA at physiologically relevant conditions, *Angew. Chem., Int. Ed.*, 2012, **51**, 12593–12596.

180 P. Gupta, T. Zengeyaz and E. Rozners, Triple helical recognition of pyrimidine inversions in polypurine tracts of RNA By nucleobase-modified PNA, *Chem. Commun.*, 2011, **47**, 11125–11127.

181 M. Li, T. Zengeya and E. Rozners, Short peptide nucleic acids bind strongly to homopurine tract of double helical RNA at pH 5.5, *J. Am. Chem. Soc.*, 2010, **132**, 8676–8681.

182 N. Dias, C. Senamaud-Beaufort, E. le Forestier, C. Auvin, C. Helene and T. E. Saison-Behmoaras, RNA hairpin invasion and ribosome elongation arrest by mixed base PNA oligomer, *J. Mol. Biol.*, 2002, **320**, 489–501.

183 X. Zhan, L. Deng and G. Chen, Mechanisms and applications of peptide nucleic acids selectively binding to double-stranded RNA, *Biopolymers*, 2021, e23476.

184 J. Kesy, K. M. Patil, S. R. Kumar, Z. Shu, H. Y. Yong, L. Zimmermann, A. A. L. Ong, D.-F. K. Toh, M. S. Krishna, L. Yang, J.-L. Decout, D. Luo, M. Prabakaran, G. Chen and E. Kierzek, A short chemically modified dsRNA-binding PNA (dbPNA) inhibits influenza viral replication by targeting viral RNA panhandle structure, *Bioconjugate Chem.*, 2019, **30**, 931–943.

185 V. Kumar, N. Brodyagin and E. Rozners, Triplex-forming peptide nucleic acids with extended backbones, *ChemBioChem*, 2020, **21**, 3410–3416.

186 P. Gupta, O. Muse and E. Rozners, Recognition of double-stranded RNA by guanidine-modified peptide nucleic acids, *Biochemistry*, 2012, **51**, 63–73.

187 W.-C. Hsieh, R. Bahal, S. A. Thadke, K. Bhatt, K. Sobczak, C. Thornton and D. H. Ly, Design of a ''Mini'' nucleic acid probe for cooperative binding of an RNA-repeated transcript associated with myotonic dystrophy type 1, *Biochemistry*, 2018, **57**, 907–911.

188 V. Tahtinen, L. Granqvist, M. Murtola, R. Stromberg and P. Virta, ^{19}F NMR spectroscopic analysis of the binding modes in triple-helical peptide nucleic acid (PNA)/MicroRNA complexes, *Chem. – Eur. J.*, 2017, **23**, 7113–7124.

189 V. Tahtinen, A. Verhassel, J. Tuomela and P. Virta, γ-(*S*)-Guanidinylmethyl-modified triplex-forming peptide nucleic acids increase Hoogsteen-face affinity for a MicroRNA and enhance cellular uptake, *ChemBioChem*, 2019, **20**, 3041–3051.

190 K. T. Kim, D. Chang and N. Winssinger, Double-stranded RNA-specific templated reaction with triplex forming PNA, *Helv. Chim. Acta*, 2018, **101**, e1700295.

191 G. Devi, Z. Yuan, Y. Lu, Y. Zhao and G. Chen, Incorporation of thio-pseudoisocytosine into triplex-forming peptide nucleic acids for enhanced recognition of RNA duplexes, *Nucleic Acids Res.*, 2014, **42**, 4008–4018.

192 I. G. Panyutin, M. I. Onyshchenko, E. A. Englund, D. H. Appella and R. D. Neumann, Targeting DNA G-quadruplex structures with peptide nucleic acids, *Curr. Pharm. Des.*, 2012, **18**, 1984–1991.

193 S. Lusvarghi, C. T. Murphy, S. Roy, F. A. Tanious, I. Sacui, W. D. Wilson, D. H. Ly and B. A. Armitage, Loop and backbone modifications of PNA improve G-quadruplex binding selectivity, *J. Am. Chem. Soc.*, 2009, **131**, 18415–18424.

194 P. Gupta, E. E. Rastede and D. H. Appella, Multivalent ^{L}Kγ-PNA oligomers bind to a human telomere DNA G-rich sequence to form quadruplexes, *Bioorg. Med. Chem. Lett.*, 2015, **25**, 4757–4760.

195 S. N. Oyaghire, C. J. Cherubim, C. A. Telmer, J. A. Martinez, M. P. Bruchez and B. A. Armitage, RNA G-quadruplex invasion and translation inhibition by antisense γ-peptide nucleic acid oligomers, *Biochemistry*, 2016, **55**, 1977–1988.

196 M. K. Gupta, B. R. Madhanagopal, D. Datta and K. N. Ganesh, Structural design and synthesis of bimodal PNA that simultaneously binds two complementary DNAs to form fused double duplexes, *Org. Lett.*, 2020, **22**, 5255–5260.

197 P. Bhingardeve, B. R. Madhanagopal and K. N. Ganesh, Cγ(*S*/*R*)-Bimodal peptide nucleic acids (Cγ-bm-PNA) form coupled double duplexes by synchronous binding to two complementary DNA strands, *J. Org. Chem.*, 2020, **85**, 13680–13693.

198 M. K. Gupta, B. R. Madhanagopal and K. N. Ganesh, Peptide nucleic acid with double face: Homothymine–homocytosine bimodal Cα-PNA (bm-Cα-PNA) forms a double duplex of the bm-PNA$_2$:DNA triplex, *J. Org. Chem*, 2021, **86**, 414–428.

199 P. Bhingardeve, P. Jain and K. N. Ganesh, Molecular assembly of triplex of duplexes from homothyminyl-

© 2022 The Author(s). Published by the Royal Society of Chemistry

Open Access Article. Published on 18 Nyenyankulu 2022. Downloaded on 2026-01-28 04:18:10.
This article is licensed under a Creative Commons Attribution-NonCommercial 3.0 Unported Licence.

homocytosinyl Cγ(*S*/*R*)-bimodal peptide nucleic acids with dA_8/dG_6 and the cell permeability of bimodal peptide nucleic acids, *ACS Omega*, 2021, **6**, 19757–19770.

200 Y. Zeng, Y. Pratumyot, X. Piao and D. Bong, Discrete assembly of synthetic peptide-DNA triplex structures from polyvalent melamine-thymine bifacial recognition, *J. Am. Chem. Soc.*, 2012, **134**, 832–835.

201 X. Piao, X. Xia and D. Bong, Bifacial peptide nucleic acid directs cooperative folding and assembly of binary, ternary, and quaternary DNA complexes, *Biochemistry*, 2013, **52**, 6313–6323.

202 G. K. Mittapalli, K. R. Reddy, H. Xong, O. Munoz, B. Han, F. De Riccardis, R. Krishnamurthy and A. Eschenmoser, Mapping the landscape of potentially primordial informational oligomers: Oligodipeptides and oligopetoids tagged with triazines as recognition elements, *Angew. Chem., Int. Ed.*, 2007, **46**, 2470–2477.

203 X. Xia, X. Piao and D. Bong, Bifacial PNA complexation inhibits enzymatic access to DNA and RNA, *ChemBioChem*, 2014, **15**, 31–36.

204 S. Miao, Y. Liang, I. Marathe, J. Mao, C. DeSantis and D. Bong, Duplex stem replacement with bPNA+ triplex hybrid stems enables reporting on tertiary interactions of internal RNA domains, *J. Am. Chem. Soc.*, 2019, **141**, 9365–9372.

205 S. Miao, D. Bhunia, S. Devari, Y. Liang, O. Munyaradzi, S. Rundell and D. Bong, Bifacial PNAs destabilize MALAT1 by 3′ A-tail displacement from the U-rich internal loop, *ACS Chem. Biol.*, 2021, **16**, 1600–1609.

206 A. Manicardi and R. Corradini, Effect of chirality in gamma-PNA: PNA interaction, another piece in the picture, *Artif. DNA: PNA & XNA*, 2014, **5**, e1131801.

207 T. D. Canady, C. A. Telmer, S. N. Oyaghire, B. A. Armitage and M. P. Bruchez, *In vitro* reversible translation control using γPNA probes, *J. Am. Chem. Soc.*, 2015, **137**, 10268–10275.

208 T. D. Canady, A. S. Berlyoung, J. A. Martinez, C. Emanuelson, C. A. Telmer, M. P. Bruchez and B. A. Armitage, Enhanced hybridization selectivity using structured GammaPNA probes, *Molecules*, 2020, **25**, 970.

209 B. E. Young, N. Kundu and J. T. Sczepanski, Mirror-image oligonucleotides: History and emerging applications, *Chem. – Eur. J.*, 2019, **25**, 7981–7990.

210 B. E. Young and J. T. Sczepanski, Heterochiral DNA strand-displacement based on chimeric D/L-oligonucleotides, *ACS Synth. Biol.*, 2019, **8**, 2756–2759.

211 W.-C. Hsieh, G. R. Martinez, A. Wang, S. F. Wu, R. Chamdia and D. H. Ly, Stereochemical conversion of nucleic acid circuits *via* strand displacement, *Commun. Chem.*, 2018, **1**, 89.

212 D. Chang, E. Lindberg and N. Winssinger, Critical analysis of rate constants and turnover frequency in nucleic acid-templated reactions: Reaching terminal velocity, *J. Am. Chem. Soc.*, 2017, **139**, 1444–1447.

213 Z. Yu, W.-C. Hsieh, S. Asamitsu, K. Hashiya, T. Bando, D. H. Ly and H. Sugiyama, Orthogonal γPNA dimerization domains empower DNA binders with cooperativity and versatility mimicking that of transcription factor pairs, *Chem. – Eur. J.*, 2018, **24**, 14183–14188.

214 H. Amarasekara, K. M. Oshaben, K. B. Jeans, P. R. Sangsari, N. Y. Morgan, B. O'Farrell and D. H. Appella, Cyclopentane peptide nucleic acid: Gold nanoparticle conjugates for the detection of nucleic acids in a microfluidic format, *Biopolymers*, 2021, e23481.

215 D. Bonifazi, L.-E. Carloni, V. Corvaglia and A. Delforge, Peptide nucleic acids in materials science, *Artif. DNA: PNA & XNA*, 2012, **3**, 112–122.

216 S. Barluenga and N. Winssinger, PNA as a biosupramolecular tag for programmable assemblies and reactions, *Acc. Chem. Res.*, 2015, **48**, 1319–1331.

217 O. Berger, L. Adler-Abramovich, M. Levy-Sakin, A. Grunwald, Y. Liebes-Peer, M. Bachar, L. Buzhansky, E. Mossou, V. T. Forsyth, T. Schwartz, Y. Ebenstein, F. Frolow, L. J. W. Shimon, F. Patolsky and E. Gazit, Light-emitting self-assembled peptide nucleic acids exhibit both stacking interactions and Watson–Crick base-pairing, *Nat. Nanotechnol.*, 2015, **10**, 353–360.

218 C. Avitabile, C. Diaferia, B. D. Ventura, F. A. Mercurio, M. Leone, V. Roviello, M. Saviano, R. Velotta, G. Morelli, A. Accardo and A. Romanelli, Self-assembling of Fmoc-GC peptide nucleic acid dimers into highly fluorescent aggregates, *Chem. – Eur. J.*, 2018, **24**, 4729–4735.

219 S. Kumar, A. Pearse, Y. Liu and R. E. Taylor, Modular self-assembly of gamma-modified peptide nucleic acids in organic solvent mixtures, *Nat. Commun.*, 2020, **11**, 2960.

220 S. Kumar, I. Dhami, S. A. Thadke, D. H. Ly and R. E. Taylor, Rapid self-assembly of γPNA nanofibers at constant temperature, *Biopolymers*, 2021, **112**, e23463.

221 T. Machida, S. Dutt and N. Winssinger, Allosterically regulated phosphatase activity from peptide–PNA conjugates folded through hybridization, *Angew. Chem., Int. Ed.*, 2016, **55**, 8595–8598.

222 L. Röglin, M. R. Ahmadian and O. Seitz, DNA-Controlled reversible switching of peptide conformation and bioactivity, *Angew. Chem., Int. Ed.*, 2007, **46**, 2704–2707.

223 S. Rapireddy, L. Nhon, R. E. Meehan, J. Franks, D. B. Stolz, D. Tran, M. E. Selsted and D. H. Ly, RTD-1 mimic containing γPNA scaffold exhibits broad-spectrum antibacterial activities, *J. Am. Chem. Soc.*, 2012, **134**, 4041–4044.

224 X. Tan, M. P. Bruchez and B. A. Armitage, Closing the loop: constraining TAT peptide by γPNA hairpin for enhanced cellular delivery of biomolecules, *Bioconjugate Chem.*, 2018, **29**, 2892–2898.

225 N. Jayaraman, Multivalent ligand presentation as a central concept to study intricate carbohydrate–protein interactions, *Chem. Soc. Rev.*, 2009, **38**, 3463–3483.

226 K. Gorska, K.-T. Huang, O. Chaloin and N. Winssinger, DNA-templated homo- and heterodimerization of peptide nucleic acid encoded oligosaccharides that mimick the carbohydrate epitope of HIV, *Angew. Chem., Int. Ed.*, 2009, **48**, 7695–7700.

227 M. Ciobanu, K.-T. Huang, J.-P. Daguer, S. Barluenga, O. Chaloin, E. Schaeffer, C. G. Mueller, D. A. Mitchell

Open Access Article. Published on 18 Nyenyankulu 2022. Downloaded on 2026-01-28 04:18:10.
This article is licensed under a Creative Commons Attribution-NonCommercial 3.0 Unported Licence.

and N. Winssinger, Selection of a synthetic glycan oligomer from a library of DNA-templated fragments against DC-SIGN and inhibition of HIV gp120 binding to dendritic cells, *Chem. Commun.*, 2011, **47**, 9321–9323.

228 K. Gorska, J. Beyrath, S. Fournel, G. Guichard and N. Winssinger, Ligand dimerization programmed by hybridization to study multimeric ligand–receptor interactions, *Chem. Commun.*, 2010, **46**, 7742–7744.

229 T. Machida, A. Novoa, P. Gillon, S. Zheng, J. Claudinon, T. Eierhoff, A. Imberty, W. Rçmer and N. Winssinger, Dynamic cooperative glycan assembly blocks the binding of bacterial lectins to epithelial cells, *Angew. Chem., Int. Ed.*, 2017, **56**, 6762–6766.

230 C. Scheibe, A. Bujotzek, J. Dernedde, M. Weberb and O. Seitz, DNA-Programmed spatial screening of carbohydrate–lectin interactions, *Chem. Sci.*, 2011, **2**, 770–775.

231 E. A. Englund, D. Wang, H. Fujigaki, H. Sakai, C. M. Micklitsch, R. Ghirlando, G. Martin-Manso, M. L. Pendrak, D. D. Roberts, S. R. Durell and D. H. Appella, Programmable multivalent display of receptor ligands using peptide nucleic acid nanoscaffolds, *Nat. Commun.*, 2012, **3**, 614.

232 A. V. Dix, J. L. Conroy, K. M. G. Rosenker, D. R. Sibley and D. H. Appella, PNA-Based multivalent scaffolds activate the dopamine D_2 receptor, *ACS Med. Chem. Lett.*, 2015, **6**, 425–429.

233 A. V. Dix, S. M. Moss, K. Phan, T. Hoppe, S. Paoletta, E. Kozma, Z.-G. Gao, S. R. Durell, K. A. Jacobson and D. H. Appella, Programmable nanoscaffolds that control ligand display to a G-protein-coupled receptor in membranes to allow dissection of multivalent effects, *J. Am. Chem. Soc.*, 2014, **136**, 12296–12303.

234 J. D. Flory, C. R. Simmons, S. Lin, T. Johnson, A. Andreoni, J. Zook, G. Ghirlanda, Y. Liu, H. Yan and P. Fromme, Low temperature assembly of functional 3D DNA-PNA-protein complexes, *J. Am. Chem. Soc.*, 2014, **136**, 8283–8295.

235 J. D. Flory, S. Shinde, S. Lin, Y. Liu, H. Yan, G. Ghirlanda and P. Fromme, PNA-peptide assembly in a 3D DNA nanocage at room temperature, *J. Am. Chem. Soc.*, 2013, **135**, 6985–6993.

236 J. D. Flory, T. Johnson, C. D. Simmons, S. Lin, G. Ghirlanda and P. Fromme, Purification and assembly of thermostable Cy5 labeled γ-PNAs into a 3D DNA nanocage, *Artif. DNA: PNA & XNA*, 2014, **5**, e992181.

237 C. S. Swenson, A. Velusamy, H. S. Argueta-Gonzalez and J. M. Heemstra, Bilingual peptide nucleic acids: Encoding the languages of nucleic acids and proteins in a single self-assembling biopolymer, *J. Am. Chem. Soc.*, 2019, **141**, 19038–19047.

238 C. S. Swenson and J. M. Heemstra, Peptide nucleic acids harness dual information codes in a single molecule, *Chem. Commun.*, 2020, **56**, 1926–1935.

239 J. P. Vernille, L. C. Kovell and J. W. Schneider, Peptide nucleic acid (PNA) amphiphiles: Synthesis, self-assembly, and duplex stability, *Bioconjugate Chem.*, 2004, **15**, 1314–1321.

240 L.-H. Liu, Z.-Y. Li, L. Rong, S.-Y. Qin, Q. Lei, H. Cheng, X. Zhou, R.-X. Zhuo and X.-Z. Zhang, *ACS Macro Lett.*, 2014, **3**, 467–471.

241 S. Ficht, A. Mattes and O. Seitz, Single-nucleotide-specific PNA-peptide ligation on synthetic and PCR DNA templates, *J. Am. Chem. Soc.*, 2004, **126**, 9970–9981.

242 X. Peng, H. Li and M. Seidman, A template-mediated click–click reaction: PNA–DNA, PNA–PNA (or peptide) ligation, and single nucleotide discrimination, *Eur. J. Org. Chem.*, 2010, 4194–4197.

243 D. Chouikhi, S. Barluenga and N. Winssinger, Clickable peptide nucleic acids (cPNA) with tunable affinity, *Chem. Commun.*, 2010, **46**, 5476–5478.

244 R. E. Kleiner, Y. Brudno, M. E. Birnbaum and D. R. Liu, DNA-templated polymerization of side-chain-functionalized peptide nucleic acid aldehydes, *J. Am. Chem. Soc.*, 2008, **130**, 4646–4659.

245 Y. Ura, J. M. Beierle, L. J. Leman, L. E. Orgel and M. R. Ghadiri, Self-assembling sequence-adaptive peptide nucleic acids, *Science*, 2009, **325**, 73–77.

246 K. V. Morris and J. S. Mattick, The rise of regulatory RNA, *Nat. Rev. Genet.*, 2014, **15**, 423–437.

247 B. A. Armitage, Imaging of RNA in Live Cells, *Curr. Opin. Chem. Biol.*, 2011, **15**, 806–812.

248 C. Briones and M. Moreno, Applications of peptide nucleic acids (PNAs) and locked nucleic acids (LNAs) in biosensor development, *Anal. Bioanal. Chem.*, 2012, **402**, 3071–3089.

249 A. Saadati, S. Hassanpour, M. de la Guardia, J. Mosafer, M. Hashemzaei, A. Mokhtarzadeh and B. Baradaran, Recent advances on application of peptide nucleic acids as a bioreceptor in biosensors development, *Trends Anal. Chem.*, 2019, **114**, 56–68.

250 M. Moccia, A. Antonacci, M. Saviano, V. Caratelli, F. Arduini and V. Scognamiglio, Emerging technologies in the design of peptide nucleic acids (PNAs) based biosensors, *Trends Anal. Chem.*, 2020, **132**, 116062.

251 Q. Lai, W. Chen, Y. Zhang and Z. Liu, Application strategies of peptide nucleic acids toward electrochemical nucleic acid sensors, *Analyst*, 2021, **146**, 5822–5835.

252 J. K. Pokorski, J.-M. Nam, R. A. Vega, C. A. Mirkin and D. H. Appella, Cyclopentane-modified PNA improves the sensitivity of nanoparticle-based scanometric DNA detection, *Chem. Commun.*, 2005, 2101–2103.

253 N. Zhang and D. H. Appella, Colorimetric detection of anthrax DNA with a peptide nucleic acid sandwich-hybridization assay, *J. Am. Chem. Soc.*, 2007, **129**, 8424–8425.

254 C. M. Micklitsch, B. Y. Oquare, C. Zhao and D. H. Appella, Cyclopentane-peptide nucleic acids for qualitative, quantitative, and repetitive detection of nucleic acids, *Anal. Chem.*, 2013, **85**, 251–257.

255 O. Tepper, H. Zheng, D. H. Appella and E. Yavin, Cyclopentane FIT-PNAs: Bright RNA sensors, *Chem. Commun.*, 2021, **57**, 540–543.

256 O. Kohler, D. V. Jarikote and O. Seitz, Forced intercalation probes (FIT Probes): Thiazole orange as a fluorescent base

 © 2022 The Author(s). Published by the Royal Society of Chemistry

Open Access Article. Published on 18 Nyenyankulu 2022. Downloaded on 2026-01-28 04:18:10.
This article is licensed under a Creative Commons Attribution-NonCommercial 3.0 Unported Licence.

in peptide nucleic acids for homogeneous single-nucleotide-polymorphism detection, *ChemBioChem*, 2005, **6**, 69–77.

257 T. Vilaivan, Fluoreogenic PNA probes, *Beilstein J. Org. Chem.*, 2018, **14**, 253–281.

258 C. Ananthanawat, T. Vilaivan, V. P. Hoven and X. Su, Comparison of DNA, aminoethylglycyl PNA and pyrrolidinyl PNA as probes for detection of DNA hybridization using surface plasmon resonance technique, *Biosens. Bioelectron.*, 2010, **25**, 1064–1069.

259 C. Ananthanawat, V. P. Hoven, T. Vilaivan and X. Su, Surface Plasmon resonance study of PNA interactions with double-stranded DNA, *Biosens. Bioelectron.*, 2011, **26**, 1918–1923.

260 P. Teengam, W. Siangproh, A. Tuantranont, T. Vilaivan, O. Chailapakul and C. S. Henry, Multiplex paper-based colorimetric DNA sensor using pyrrolidinyl peptide nucleic acid-induced AgNPs aggregation for detecting MERS-Cov, MTB, and HPV oligonucleotides, *Anal. Chem.*, 2017, **89**, 5428–5435.

261 M. Leekrajang, P. Sae-ung, T. Vilaivan and V. P. Hoven, Filter paper grafted with epoxide-based copolymer brushes for activation-free peptide nucleic acid conjugation and its application for colorimetric DNA detection, *Colloids Surf., B.*, 2019, **173**, 851–859.

262 N. Jirakittiwut, T. Munkongdee, K. Wongravee, O. Sripichai, S. Fucharoen, T. Praneenararat and T. Vilaivan, Visual genotyping of thalassemia by using pyrrolidinyl peptide nucleic acid probes immobilized on carboxymethylcellulose-modified paper and enzyme-induced pigmentation, *Microchim. Acta*, 2020, **187**, 238.

263 C. Srisomwat, A. Yakoh, N. Chuaypen, P. Tangkijvanich, T. Vilaivan and O. Chailapakul, Amplification-free DNA sensor for the one-step detection of the hepatitis b virus using an automated paper-based lateral flow electrochemical device, *Anal. Chem.*, 2021, **93**, 2879–2887.

264 S. Naorungroj, P. Teengam, T. Vilaivan and O. Chailapakul, Paper-Based DNA sensor enabling colorimetric assay integrated with smartphone for human papillomavirus detection, *New J. Chem.*, 2021, **45**, 6960–6967.

265 P. Teengam, N. Nisab, N. Chuaypen, P. Tangkijvanich, T. Vilaivan and O. Chailapakul, Fluorescent paper-based DNA sensor using pyrrolidinyl peptide nucleic acids for hepatitis C virus detection, *Biosens. Bioelectron.*, 2021, **189**, 113381.

266 N. Jirakittiwut, T. Patipong, T. Cheiwchanchamnangij, R. Waditee-Sirisattha, T. Vilaivan and T. Praneenararat, Paper-based sensor from pyrrolidinyl peptide nucleic acid for the efficient detection of *Bacillus cereus*, *Anal. Bioanal. Chem.*, 2021, **413**, 6661–6669.

267 C. Srisomwat, A. Yakoh, A. Avihingsanon, N. Chuaypen, P. Tangkijvanich, T. Vilaivan and O. Chailapakul, An alternative label-free DNA sensor based on the alternating-current electroluminescent device for simultaneous detection of human immunodeficiency virus and hepatitis C Co-infection, *Biosens. Bioelectron.*, 2022, **196**, 113719.

268 O. Thipmanee, A. Numnuam, W. Limbut, C. Buranachai, P. Kanatharana, T. Vilaivan, N. Hirankarn and P. Thavarungkul, Enhancing capacitive DNA biosensor performance by target overhang with application on screening test of HLA-B*58:01 and HLA-B*57:01 genes, *Biosens. Bioelectron.*, 2016, **82**, 99–104.

269 O. Thipmanee, S. Samanman, S. Sankoh, A. Numnuam, W. Limbut, P. Kanatharana, T. Vilaivan and P. Thavarungkul, Label-free capacitive DNA sensor using immobilized pyrrolidinyl PNA Probe: Effect of the length and terminating head group of the blocking thiols, *Biosens. Bioelectron.*, 2012, **38**, 430–435.

270 T. Kangkamano, A. Numnuam, W. Limbut, P. Kanatharana, T. Vilaivan and P. Thavarungkul, Pyrrolidinyl PNA polypyrrole/silver nanofoam electrode as a novel label-free electrochemical miRNA-21 biosensor, *Biosens. Bioelectron.*, 2018, **102**, 217–225.

271 B. Boontha, J. Nakkuntod, N. Hirankarn, P. Chaumpluk and T. Vilaivan, Multiplex mass spectrometric genotyping of single nucleotide polymorphisms employing pyrrolidinyl peptide nucleic acid in combination with ion-exchange capture, *Anal. Chem.*, 2008, **80**, 8178–8186.

272 J. Meebungprawa, O. Wiarachai, T. Vilaivan, S. Kiatkamjornwonge and V. P. Hoven, Quaternized chitosan particles as ion exchange supports for label-freedna detection using PNA probe and MALDI-TOF mass spectrometry, *Carbohydr. Polym.*, 2015, **131**, 80–89.

273 B. Rutnakornpituk, T. Theppaleak, M. Rutnakornpituk and T. Vilaivan, Recyclable magnetite nanoparticle coated with cationic polymers for adsorption of DNA, *J. Biomater. Sci. Polym. Ed.*, 2016, **27**, 1200–1210.

274 P. S. Laopa, T. Vilaivan and V. P. Hoven, Positively charged polymer brushes-functionalized filter paper for DNA Sequence determination following dot blot hybridization employing pyrrolidinyl peptide nucleic acid probe, *Analyst*, 2013, **138**, 269–277.

275 J. Kongpeth, S. Jampasa, P. Chaumpluk, O. Chailapakul and T. Vilaivan, Immobilization-free electrochemical DNA detection with anthraquinone-labeled pyrrolidinyl peptide nucleic acid probe, *Talanta*, 2016, **146**, 318–325.

276 C. Boonlua, C. Vilaivan, H.-A. Wagenknecht and T. Vilaivan, 5-(Pyren-1-yl)uracil as a base-discriminating fluorescent nucleobase in pyrrolidinyl peptide nucleic acids, *Chem. Asian J.*, 2011, **6**, 3251–3259.

277 B. Ditmangklo, J. Taechalertpaisarn, K. Siriwong and T. Vilaivan, Clickable styryl dyes for fluorescence labeling of pyrrolidinyl PNA probes for the detection of base mutations in DNA, *Org. Biomol. Chem.*, 2019, **17**, 9712–9725.

278 C. Boonlua, C. Charoenpakdee, T. Vilaivan and T. Praneenararat, Preparation and performance evaluation of a pyrrolidinyl peptide nucleic-acid-based displacement probe as a DNA sensor, *ChemistrySelect*, 2016, **1**, 5691–5697.

279 C. Charoenpakdee and T. Vilaivan, Quenching of fluorescently labeled pyrrolidinyl peptide nucleic acid by oligodeoxyguanosine and its application in DNA sensing, *Org. Biomol. Chem.*, 2020, **18**, 5951–5962.

Open Access Article. Published on 18 Nyenyankulu 2022. Downloaded on 2026-01-28 04:18:10.
This article is licensed under a Creative Commons Attribution-NonCommercial 3.0 Unported Licence.

280 P. Yukhet, K. Buddhachat, T. Vilaivan and C. Suparpprom, Isothermal detection of canine blood parasite (*Ehrlichia canis*) utilizing recombinase polymerase amplification coupled with graphene oxide quenching-based pyrrolidinyl peptide nucleic acid, *Bioconjugate Chem.*, 2021, **32**, 523–532.

281 K. Faikhruea, I. Choopara, N. Somboonna, W. Assavalapsakul, B. H. Kim and T. Vilaivan, Enhancing peptide nucleic acid–nanomaterial interaction and performance improvement of peptide nucleic acid-based nucleic acid detection by using electrostatic effects, *ACS Appl. Bio Mater.*, 2022, **5**, 789–800.

282 J. Nölling, S. Rapireddy, J. I. Amburg, E. M. Crawford, R. A. Prakash, A. R. Rabson, Y.-W. Tang and A. Singer, Duplex DNA-invading γ-modified peptide nucleic acids enable rapid identification of bloodstream infections in whole blood, *mBio*, 2016, **7**, e00345.

283 A. Singer, S. Rapireddy, D. H. Ly and A. Meller, Electronic barcoding of a viral gene at the single-molecule level, *Nano Lett.*, 2012, **12**, 1722–1728.

284 J. M. Goldman, L. A. Zhang, A. Manna, B. A. Armitage, D. H. Ly and J. W. Schneider, High affinity γPNA sandwich hybridization assay for rapid detection of short nucleic acid targets with single mismatch discrimination, *Biomacromolecules*, 2013, **14**, 2253–2261.

285 J. M. Goldman, S. Kim, S. Narburgh, B. A. Armitage and J. W. Schneider, Rapid, multiplexed detection of the let-7 miRNA family using γPNA amphiphiles in micelle-tagging electrophoresis, *Biopolymers*, 2021, e23479.

286 K. T. Kim, S. Angerani and N. Winssinger, A minimal hybridization chain reaction (HCR) system using peptide nucleic acids, *Chem. Sci.*, 2021, **12**, 8218–8223.

287 B. Dong, K. Nie, H. Shi, L. Chao, M. Ma, F. Gao, B. Liang, W. Chen, M. Longa and Z. Liu, Film-spotting chiral mini-PEG-γPNA array for BRCA1 gene mutation detection, *Biosens. Bioelectron.*, 2019, **136**, 1–7.

288 A. Singer, M. Wanunu, W. Morrison, H. Kuhn, M. Frank-Kamenetskii and A. Meller, Nanopore based sequence specific detection of duplex DNA for genomic profiling, *Nano Lett.*, 2010, **2**, 738–742.

289 T. J. Morin, T. Shropshire, X. Liu, K. Briggs, C. Huynh, V. Tabard-Cossa, H. Wang and W. B. Dunbar, Nanopore-based target sequence detection, *PLoS One*, 2016, **11**, e0154426.

290 K. Gorska, I. Keklikoglou, U. Tschulenab and N. Winssinger, Rapid fluorescence imaging of miRNAs in human cells using templated staudinger reaction, *Chem. Sci.*, 2011, **2**, 1969–1975.

291 A. Orenstein, A. S. Berlyoung, E. E. Rastede, H. H. Pham, E. Fouquerel, C. T. Murphy, B. J. Leibowitz, J. Yu, T. Srivastava, B. A. Armitage and P. L. Opresko, γPNA FRET pair miniprobes for quantitative fluorescent *in situ* hybridization to telomeric DNA in cells and tissue, *Molecules*, 2017, **22**, 2117.

292 K. T. Kim, S. Angerani and N. Winssinger, A minimal hybridization chain reaction (HCR) system using peptide nucleic acids, *Chem. Sci.*, 2021, **12**, 8218–8223.

293 D. R. Jain and K. N. Ganesh, Clickable Cγ-azido(methylene/butylene) peptide nucleic acids and their clicked fluorescent derivatives: Synthesis, DNA hybridization properties, and cell penetration studies, *J. Org. Chem.*, 2014, **79**, 6708–6714.

294 A. Manicardi, A. Bertucci, A. Rozzi and R. Corradini, A bifunctional monomer for on-resin synthesis of polyfunctional PNAs and tailored induced-fit switching probes, *Org. Lett.*, 2016, **18**, 5452–5455.

295 H. H. Pham, C. T. Murphy, G. Sureshkumar, D. H. Ly, P. L. Opreskob and B. A. Armitage, Cooperative hybridization of γPNA miniprobes to a repeating sequence motif and application to telomere analysis, *Org. Biomol. Chem.*, 2014, **12**, 7345–7354.

296 T. Tedeschi, M. Chiari, G. Galaverna, S. Sforza, M. Cretich, R. Corradini and R. Marchelli, Detection of the R553X DNA single point mutation related to cystic fibrosis by a ''chiral box'' d-lysine-peptide nucleic acid probe by capillary electrophoresis, *Electrophoresis*, 2005, **26**, 4310–4316.

297 R. Corradini, G. Feriotto, S. Sforza, R. Marchelli and R. Gambari, Enhanced recognition of cystic fibrosis W1282X DNA point mutation by chiral peptide nucleic acid probes by a surface plasmon resonance biosensor, *J. Mol. Recognit.*, 2004, **17**, 76–84.

298 J. D. R. Perera, K. E. W. Carufe and P. M. Glazer, Peptide nucleic acids and their role in gene regulation and editing, *Biopolymers*, 2021, **112**, e23460.

299 E. Quijano, R. Bahal, A. Ricciardi, W. M. Saltzman and P. M. Glazer, Therapeutic peptide nucleic acids: Principles, limitations, and opportunities, *Yale J. Biol. Med.*, 2017, **90**, 583–598.

300 N. G. Economos, S. Oyaghire, E. Quijano, A. S. Ricciardi, W. M. Saltzman and P. M. Glazer, Peptide nucleic acids and gene editing: Perspectives on structure and repair, *Molecules*, 2020, **25**, 735.

301 C. Dose and O. Seitz, Single nucleotide specific detection of DNA by native chemical ligation of fluorescence labeled PNA-probes, *Bioorg. Med. Chem.*, 2008, **16**, 65–77.

302 R. Hamzavi, C. Meyer and N. Metzler-Nolte, Synthesis of a C-linked glycosylated thymine-based PNA monomer and its incorporation into a PNA oligomer, *Org. Biomol. Chem.*, 2005, **4**, 3648–3651.

303 R. Hamzavi, F. Dolle, B. Tavitian, O. Dahl and P. E. Nielsen, Modulation of the pharmacokinetic properties of PNA: Preparation of galactosyl, mannosyl, fucosyl, *N*-acetylgalactosaminyl, and *N*-acetylglucosaminyl derivatives of aminoethylglycine peptide nucleic acid monomers and their incorporation into PNA oligomers, *Bioconjugate Chem.*, 2003, **14**, 941–954.

304 P. Bhingardeve, B. R. Madhanagopal, H. Naick, P. Jain, M. Manoharan and K. Ganesh, Receptor-specific delivery of peptide nucleic acids conjugated to three sequentially linked *N*-acetyl galactosamine moieties into hepatocytes, *J. Org. Chem.*, 2020, **85**, 8812–8824.

305 P. Zhou, M. Wang, L. Du, G. W. Fisher, A. Waggoner and D. H. Ly, Novel binding and efficient cellular uptake of

© 2022 The Author(s). Published by the Royal Society of Chemistry

Open Access Article. Published on 18 Nyenyankulu 2022. Downloaded on 2026-01-28 04:18:10.
This article is licensed under a Creative Commons Attribution-NonCommercial 3.0 Unported Licence.

guanidine-based peptide nucleic acids (GPNA), *J. Am. Chem. Soc.*, 2003, **125**, 6878–6879.

306 A. Dragulescu-Andrasi, P. Zhou, G. He and D. H. Ly, Cell-permeable GPNA with appropriate backbone stereochemistry and spacing binds sequence-specifically to RNA, *Chem. Commun.*, 2005, 244–246.

307 P. Zhou, A. Dragulescu-Andrasi, B. Bhattacharya, H. O'Keefe, P. Vatta, J. J. Hyldig-Nielsen and D. H. Ly, Synthesis of cell-permeable peptide nucleic acids and characterization of their hybridization and uptake properties, *Bioorg. Med. Chem. Lett.*, 2006, **16**, 4931–4935.

308 A. Dragulescu-Andrasi, S. Rapireddy, G. He, B. Bhattacharya, J. J. Hyldig-Nielsen, G. Zon and D. H. Ly, Cell-permeable peptide nucleic acid designed to bind to the 5′-untranslated region of E-cadherin transcript induces potent and sequence-specific antisense effects, *J. Am. Chem. Soc.*, 2006, **128**, 16104–16112.

309 S. M. Thomas, B. Sahu, S. Rapireddy, R. Bahal, S. E. Wheeler, E. M. Procopio, J. Kim, S. C. Joyce, S. Contrucci, Y. Wang, S. I. Chiosea, K. L. Lathrop, S. Watkins, J. R. Grandis, B. A. Armitage and D. H. Ly, Antitumor effects of EGFR antisense guanidine-based peptide nucleic acids in cancer models, *ACS Chem Biol.*, 2013, **8**, 345–352.

310 A. Manicardi, E. Fabbri, T. Tedeschi, S. Sforza, N. Bianchi, E. Brognara, R. Gambari, R. Marchelli and R. Corradini, Cellular uptakes, biostabilities and anti-miR-210 activities of chiral arginine-PNAs in leukaemic K562 Cells, *ChemBioChem*, 2012, **13**, 1327–1337.

311 E. Delgado, R. Bahal, J. Yang, J. M. Lee, D. H. Ly and S. P. S. Monga, β-Catenin knockdown in liver tumor cells by a cell permeable gamma guanidine-based peptide nucleic acid, *Curr. Cancer Drug Targets*, 2013, **13**, 867–878.

312 R. Bahal, N. A. McNeer, D. H. Ly, W. M. Saltzman and P. M. Glazer, Nanoparticle for delivery of antisense γPNA oligomers targeting CCR5, *Artif. DNA: PNA & XNA*, 2013, **4**, 49–57.

313 K. Dhuri, R. R. Gaddam, A. Vikram, F. J. Slack and R. Bahal, Therapeutic potential of chemically modified, synthetic, triplex peptide nucleic acid–based oncomir inhibitors for cancer therapy, *Cancer Res.*, 2021, **81**, 5613–5624.

314 A. Gupta, E. Quijano, Y. Liu, R. Bahal, S. E. Scanlon, E. Song, W.-C. Hsieh, D. E. Braddock, D. H. Ly, W. M. Saltzman and P. M. Glazer, Anti-tumor activity of miniPEG-γ-modified PNAs to inhibit microRNA-210 for cancer therapy, *Mol. Ther. Nucleic Acids*, 2017, **9**, 111–119.

315 A. R. Kaplan, H. Pham, Y. Liu, S. Oyaghire, R. Bahal, D. M. Engelman and P. M. Glazer, Ku80-Targeted pH-sensitive peptide–PNA conjugates are tumor selective and sensitize cancer cells to ionizing radiation, *Mol. Cancer Res.*, 2020, **18**, 873–882.

316 A. S. Ricciardi, E. Quijano, R. Putman, W. M. Saltzman and P. M. Glazer, Peptide nucleic acids as a tool for site-specific gene editing, *Molecules*, 2018, **23**, 632.

317 R. Bahal, E. Quijano, N. A. McNeer, Y. Liu, D. C. Bhunia, F. López-Giráldez, R. J. Fields, W. M. Saltzman, D. H. Ly and P. M. Glazer, Single-stranded γPNAs for *in vivo* site-specific genome editing *via* Watson–Crick recognition, *Curr. Gene Ther.*, 2014, **14**, 331–342.

318 J. Y. Chin, J. Y. Kuan, P. S. Lonkar, D. S. Krause, M. M. Seidman, K. R. Peterson, P. E. Nielsen, R. Kole and P. M. Glazer, Correction of a splice-site mutation in the beta-globin gene stimulated by triplex-forming peptide nucleic acids, *Proc. Natl. Acad. Sci. U. S. A.*, 2008, **105**, 13514–13519.

319 M. Adli, The CRISPR tool kit for genome editing and beyond, *Nat. Commun.*, 2018, **9**, 1911.

320 R. Bahal, N. A. McNeer, E. Quijano, Y. Liu, P. Sulkowski, A. Turchick, Y.-C. Lu, D. C. Bhunia, A. Manna, D. L. Greiner, M. A. Brehm, C. J. Cheng, F. López-Giráldez, A. Ricciardi, J. Beloor, D. S. Krause, P. Kumar, P. G. Gallagher, D. T. Braddock, W. M. Saltzman, D. H. Ly and P. M. Glazer, *In vivo* correction of anaemia in β-thalassemic mice by γPNA-mediated gene editing with nanoparticle delivery, *Nat. Commun.*, 2016, **7**, 13304.

321 A. S. Ricciardi, R. Bahal, J. S. Farrelly, E. Quijano, A. H. Bianchi, V. L. Luks, R. Putman, F. López-Giráldez, S. Coşkun, E. Song, Y. Liu, W.-C. Hsieh, D. H. Ly, D. H. Stitelman, P. M. Glazer and W. M. Saltzman, In utero nanoparticle delivery for site-specific genome editing, *Nat. Commun.*, 2018, **9**, 2481.

322 P. Y. Ho, Z. Zhang, M. E. Hayes, A. Curd, C. Dib, M. Rayburna, S. N. Tam, T. Srivastava, B. Hriniak, X.-J. Li, S. Leonard, L. Wang, S. Tarighat, D. S. Sim, M. Fiandaca, J. M. Coull, A. Ebens, M. Fordyce and A. Czechowicz, Peptide nucleic acid–dependent artifact can lead to false-positive triplex gene editing signals, *Proc. Natl. Acad. Sci. U. S. A.*, 2021, **118**, e2109175118.

323 S. Arayachukiat, J. Seemork, P. Pan-In, K. Amornwachirabodee, N. Sangphech, T. Sansureerungsikul, K. Sathornsantikun, C. Vilaivan, K. Shigyou, P. Pienpinijtham, T. Vilaivan, T. Palaga, W. Banlunara, T. Hamada and S. Wanichwecharungruang, Bringing macromolecules into cells and evading endosomes by oxidized carbon nanoparticles, *Nano Lett.*, 2015, **15**, 3370–3376.

© 2022 The Author(s). Published by the Royal Society of Chemistry